UNIVERSIDADE ESTADUAL PAULISTA
"JÚLIO DE MESQUITA FILHO"
Instituto de Biociências – Câmpus de Botucatu/Rio Claro
Seção Técnica de Pós-Graduação

PROGRAMA DE PÓS-GRADUAÇÃO EM BIOLOGIA VEGETAL (INTERUNIDADES)

VARIAÇÃO INTRAESPECÍFICA, AUTOFAGIA E AUTOCITOTOXICIDADE EM CANAIS SECRETORES DE *Anacardium humile* A. ST.-HIL. (ANACARDIACEAE)

SHELLY FAVORITO DE CARVALHO

Tese apresentada ao Instituto de Biociências, Câmpus de (Botucatu), UNESP, para obtenção do título de Doutor no Programa de Pós-Graduação em Biologia Vegetal, Interunidades entre o Instituto de Biociências do campus de Botucatu e Instituto de Biociências do campus de Rio Claro.

BOTUCATU – SP
2023

UNIVERSIDADE ESTADUAL PAULISTA
"JÚLIO DE MESQUITA FILHO"
Instituto de Biociências – Câmpus de Botucatu/Rio Claro
Seção Técnica de Pós-Graduação

PROGRAMA DE PÓS-GRADUAÇÃO EM BIOLOGIA VEGETAL (INTERUNIDADES)

VARIAÇÃO INTRAESPECÍFICA, AUTOFAGIA E AUTOCITOTOXICIDADE EM CANAIS SECRETORES DE *Anacardium humile* A. ST.-HIL. (ANACARDIACEAE)

SHELLY FAVORITO DE CARVALHO

PROF. DR. SILVIA RODRIGUES MACHADO

Tese apresentada ao Instituto de Biociências, Câmpus de (Botucatu), UNESP, para obtenção do título de Doutor no Programa de Pós-Graduação em Biologia Vegetal, Interunidades entre o Instituto de Biociências do campus de Botucatu e Instituto de Biociências do campus de Rio Claro.

BOTUCATU – SP
2023

FICHA CATALOGRÁFICA ELABORADA PELA SEÇÃO TÉC. AQUIS. TRATAMENTO DA INFORM.
DIVISÃO TÉCNICA DE BIBLIOTECA E DOCUMENTAÇÃO - CÂMPUS DE BOTUCATU - UNESP
BIBLIOTECÁRIA RESPONSÁVEL: MARIA CAROLINA ANDRADE CRUZ E SANTOS-CRB 8/10188

Carvalho, Shelly Favorito de.
Variação intraespecífica, autofagia e autocitotoxicidade em canais secretores de *Anacardium humile* A. ST.-HIL. (*Anacardiaceae*) / Shelly Favorito de Carvalho. - Botucatu, 2023

Tese (doutorado) - Universidade Estadual Paulista "Júlio de Mesquita Filho", Instituto de Biociências de Botucatu
Orientador: Silvia Rodrigues Machado
Capes: 20300000

1. *Anacardiaceae*. 2. Autofagia. 3. Células epiteliais. 4. Citotoxicidade. 5. Citologia. 6. Botânica.

Palavras-chave: Anacardium humile; Autofagia; Canais secretores; Citotoxicidade; Variação intraespecífica.

Dedico
À minha mãe (in memorian) que dedicou
sua vida para que fôssemos felizes.

Agradecimentos

À Coordenação de Aperfeiçoamento de Pessoal de Nível Superior (CAPES), pelo auxílio financeiro.

À Fundação de Amparo à Pesquisa do Estado de São Paulo (FAPESP), pelo auxílio financeiro desse estudo (Proc. FAPESP 2019/19916-1).

À Profa. Dra. Silvia Rodrigues Machado, a quem devo toda minha vida profissional. Me ensinou não só o entusiasmo e o amor à pesquisa, mas também a levar a vida com leveza e com pessoas do bem ao seu lado.

À Profa. Dra. Daniela Carvalho dos Santos, que me permitiu concluir esse doutorado. Sempre doce, humana e com muita empatia, me apoiou em tudo que precisei. Obrigada pelas contribuições nesse estudo.

Ao meu amigo, Prof. Dr. Elton Luiz Scudeler, pela parceria, pelos muitos ensinamentos e ajuda nesse trabalho.

Às professoras Simone de Pádua Teixeira, Tatiane Maria Rodrigues e Yve Canaveze pelas importantes considerações no exame de qualificação.

Às professoras Simone de Pádua Teixeira, Elza Maria Guimarães Santos e Yve Canaveze e ao professor Luiz Ricardo dos Santos Tozin pelas contribuições na defesa dessa tese.

À Luciana, amiga que o CME me deu, que me incentivou a começar o doutorado.

Aos meus amigos do CME, Claudetinha, Maria Helena e Tiago, pelas conversas, conselhos, e inúmeras vezes que me apoiaram, seja cortando e cortando novamente minhas amostras até dar certo, seja por fazerem meu trabalho para que eu pudesse terminar o doutorado. Sou imensamente grata pelo apoio.

À Hannelise, menina doce e parceira, pelas conversas e conselhos.

Aos colegas Yve, Thunder, Fernanda, Tayeme, Juan, Stefany, Karla, Zoraide, Karise e Paulo pela ajuda em diferentes etapas desse trabalho.

À minha amiga-irmã Mari, que mesmo distante, foi meu ouvido para minhas aflições durante esse processo, sempre me incentivando.

Ao meu companheiro, Márcio, que não mediu esforços para que eu terminasse esse projeto. Muito obrigada por tudo o que faz por mim. Te amo.

Aos meus filhos, Gabriel e Pedro, que são a força que me movem.

À minha família (pai, irmãs, cunhados, cunhadas, sogra e sobrinhos) que sempre me incentivam em minhas conquistas.

SUMÁRIO

RESUMO: Por meio da combinação de diversos métodos em botânica estrutural e biologia celular, neste estudo analisamos comparativamente os canais secretores no caule em sua porção aérea e subterrânea de *Anacardium humile* A. St-Hil. a fim de acessar variações intraindividuais relacionadas ao ambiente aéreo e subterrâneo; investigar a ocorrência de autofagia e seus tipos, bem como, a ocorrência de autocitotoxicidade e de mecanismos citoprotetores em células epiteliais secretoras de resina. Os resultados mostraram diferenças significativas na distribuição, histoquímica e ultraestrutura das células epiteliais dos canais secretores no caule em sua porção aérea e subterrânea. As células epiteliais dos canais na porção aérea, no pico da secreção, apresentaram formatos e tamanhos variáveis, com núcleo volumoso e citoplasma denso com ribossomos livres, polirribossomos, mitocôndrias com cristas desenvolvidas e plastídios elipsóides com inclusões elétron-opacas circundados por retículo periplastidial. Já na porção subterrânea, as células epiteliais no pico da secreção apresentaram formato e tamanho regulares, um grande vacúolo central, citoplasma reduzido a uma fina camada na periferia da célula e população reduzida de organelas. Dois mecanismos de autofagia foram detectados nas células epiteliais, sendo a macroautofagia encontrada em células ativas em secreção e a microautofagia em células em estágio final de secreção. As mudanças observadas na morfologia das células epiteliais durante o ciclo secretor tais como dilatação acentuada do retículo endoplasmático liso, degradação das cristas mitocondriais e a formação de corpos multilamelares na matriz mitocondrial são fortes indícios de autocitotoxicidade da secreção, enquanto que a presença de HSP70 (*heat shock proteins*) e o aparecimento de figuras típicas de processo autofágico (fagóforos, autofagossomos e vacúolos autofágicos) foram associadas com mecanismos citoprotetores em resposta aos danos causados pela presença de substâncias tóxicas. O padrão de danos celulares e respostas citotóxicas das células epiteliais dos canais secretores é comum a outras estruturas secretoras de terpenos. A combinação de métodos imunohistoquímicos com análises convencionais e ultracitoquímicas em microscopia eletrônica de transmissão foi eficiente para mostrar que nesta espécie o ambiente abaixo e acima do solo exerce certa influência na organização subcelular e no funcionamento dos canais secretores; que os canais secretores apresentam tipos distintos de autofagia durante o ciclo secretor; que os componentes da secreções terpênicas são tóxicas às próprias células que os produzem, as quais, em reposta aos danos desenvolvem mecanismos citoprotetores. Os resultados obtidos neste estudo incentivam a aplicação de diferentes técnicas de microscopia de luz e eletrônica, incluindo imunolocalização e citoquímica ultraestrutural na área da botânica estrutural e abrem novas perspectivas no estudo da célula secretora em espécies nativas.

ABSTRACT: Through the combination of several methods in structural botany and cell biology, in this study we comparatively analyze the secretory canals in the stem in its above- and belowground portions of *Anacardium humile* A. St-Hil. in order to access intra-individual variations related to the above- and belowground environment; to investigate the occurrence of autophagy and its types, as well as the occurrence of autocytotoxicity and cytoprotective changes in resin-secreting epithelial cells. The results of the differentiation in the distribution, histochemistry and ultrastructure of the epithelial cells of the secretory canals in the stem in its above- and belowground portion. The epithelial cells of the canals in the aboveground portion, at the peak of secretion, reached variable formats and patterns, with a voluminous nucleus and dense cytoplasm with free ribosomes, polyribosomes, mitochondria with developed cristae and ellipsoid plastids with electron-opaque inclusions surrounded by periplastid reticulum. In the belowground portion, the epithelial cells at the apex showed regular shape and size, a large central vacuole, cytoplasm reduced to a thin layer at the periphery of the cell, and suppression of organelles. Two mechanisms of autophagy were detected in epithelial cells, macroautophagy being found in active cells in secretion and microautophagy in cells in the final stage of secretion. The changes observed in the morphology of epithelial cells during the secretory cycle such as marked dilation of the smooth endoplasmic reticulum, degradation of mitochondrial crests and the formation of multilamellar bodies in the mitochondrial matrix are strong indications of autocytotoxicity of secretion, while the presence of HSP70 (heat shock proteins) and the appearance of typical figures of autophagic process (phagophores, autophagosomes and autophagic vacuoles) were associated with cytoprotective mechanisms in response to the damage caused by the presence of toxic substances. The pattern of cellular damage and cytotoxic responses of the epithelial cells of the secretory canals is common to other terpene-secreting structures. The combination of immunohistochemical methods with conventional and ultracytochemical analyses in transmission electron microscopy was efficient to show that in this species the environment below and above ground exerts a certain influence on the subcellular organization and functioning of the secretory canals; that secretory canals have distinct types of autophagy during the secretory cycle; that the components of terpene secretions are toxic to the very cells that produce them, which, in response to damage, develop cytoprotective mechanisms. The results obtained in this study encourage the application of different techniques of light and electron microscopy, including immunolocalization and ultrastructural cytochemistry in the area of structural botany and open new perspectives in the study of the secretory cell in native species.

Introdução Geral

Anacardiaceae é uma família de angiospermas lenhosas distribuídas principalmente em regiões tropicais e subtropicais (Pell et al. 2011; Royo et al. 2015). No Brasil, Anacardiaceae é representada por 55 espécies distribuídas em 14 gêneros, sendo *Schinus* L. e *Anacardium* L. os mais diversos (BFG 2015).

A ocorrência de canais secretores de resina é uma característica marcante da família. Várias espécies de Anacardicaceae são exploradas *in loco* ou cultivadas devido à produção de frutos comestíveis (manga, caju, pistache e outros), madeiras de boa qualidade e resinas com importância medicinal, industrial e alergênica (Pickel 2008). A composição química da secreção produzida em Anacardiaceae é diversa, podendo conter goma, uma mistura de goma e resina ou apenas resina (Tolke et al. 2021). Terpenos e compostos fenólicos são compostos predominantes na secreção de Anacardiaceae, (Carmello et al. 1995; Pinto et al. 2000; Langenheim 2003; Martínez et al. 2003, 2008; Sant'Anna-Santos et al. 2006; Tolke et al. 2017; Prado e Demarco 2018; Tolke et al. 2021), porém estudos mais detalhados são necessários para identificar variações entre órgãos e espécies (Tolke et al. 2021).

Canal secretor é um tipo de estrutura secretora interna constituída por um epitélio de células especializadas organizadas ao redor de um espaço intercelular denominado lúmen, onde a secreção produzida por essas células fica armazenada e só atinge o meio externo em caso de injúrias mecânicas (Fahn 1979). A secreção produzida pelos canais secretores tem natureza química diversa e inclui óleos essenciais, resinas, gomas e mucilagens, compostos fenólicos, dentre outros, cuja importância na defesa das plantas contra herbívoros e patógenos, na manutenção do potencial hídrico de tecidos adjacentes, na dispersão de frutos e sementes, além de reconhecida importância econômica e medicinal tem sido destacada (Fahn 1979; Langenheim 2003; Evert 2006).

Estudos microscópicos das últimas décadas têm contribuído consideravelmente para o conhecimento do modo de formação, desenvolvimento e funcionamento dos canais/cavidades resiníferos em espécies de Anacardiaceae. O modo de formação dos canais secretores nos representantes desta família pode variar entre indivíduos da mesma espécie e até mesmo entre órgãos do mesmo indivíduo, sendo reportados os mecanismos esquizógeno, lisígeno e esquizo-lisígeno (Fahn 1979). Os estudos citológicos dos canais resiníferos de espécies de Anacardiaceae são limitados, em sua maioria, aos estágios iniciais da formação do lúmen (Fahn e Evert 1974; Nair et al. 1983; Machado e Carmello Guerreiro 2001; Lacchia e Carmello Guerreiro 2009), sendo que muitos aspectos dos

canais secretores de resina tais como variação intraespecífica, ocorrência de autofagia e autocitotoxicidade da secreção ainda são pouco explorados. Pesquisas com este foco são imprescindíveis para alavancar a compreensão das bases celulares da secreção em plantas e explorar a versatilidade funcional das células secretoras.

A espécie objeto de estudo

Anacardium humile A.St.-Hil., conhecida popularmente como cajuzinho-do-cerrado, cajuí e cajuzinho-do-campo é um subarbusto nativo do Cerrado brasileiro pertencente à família Anacardiaceae (Almeida et al. 1998). Pode atingir cerca de 80cm de altura e se caracteriza por apresentar vários ramos aéreos eretos e um caule subterrâneo muito desenvolvido (Cota et al. 2017).

Figura 1. Espécimes de *Anacardium humile* vegetando na região de Botucatu – SP.

A alta variabilidade morfológica de *A. humile* tem sido ressaltada em diversos estudos, e devido ao seu potencial comercial, esta espécie tem sido objeto de estudos em programas de melhoramento visando à determinação da variabilidade genética, buscando identificar procedências ou ambientes que apresentam acessos com divergências de alta magnitude (Carvalho et al. 2012). A relevância ecológica desta espécie no Cerrado tem sido enfatizada (Carvalho 2020) devido a importância de seus frutos e sementes como fonte de alimentos para a fauna, principalmente as aves e também mamíferos como a raposa (*Lycalopex vetulus*), que atuam como agentes dispersores das sementes. Os pequenos frutos quando fermentados, fornecem uma espécie de aguardente conhecida

pelos indígenas como cauim. As nozes são ricas em vitaminas B1 e B2, proteínas, lipídios, niacina, fósforo e ferro. Todos os órgãos de *A. humile* são usados na medicina popular. A infusão de suas folhas e da casca do caule subterrâneo é usada medicinalmente para curar a diarreia. O óleo encontrado nas nozes tem efeito antisséptico e cicatrizante, sendo também utilizado na indústria para a produção de plásticos, revestimentos e materiais isolantes. O pedúnculo de *A. humile* é rico em vitamina C, fibras e antioxidantes. Esta composição biológica está associada à prevenção de doenças crônico-degenerativas, como doenças cardiovasculares, câncer e diabetes. A infusão das flores é usada para combater a tosse e baixar o nível de glicose em diabéticos (Carvalho 2020). É uma espécie suscetível à intensa exploração pelo homem e à ação do fogo, e está competindo com outras espécies pelo título de espécie ameaçada de extinção (Carvalho 2020).

A ampla distribuição desta espécie em áreas de cerrado *sensu stricto* da região centro-oeste paulista, a presença de um caule aéreo e caule subterrâneo e de canais secretores de resina fazem desta espécie um bom modelo para os propósitos deste estudo.

O ambiente abaixo e acima do solo e sua provável influência no funcionamento das estruturas secretoras

Estruturas secretoras são características constitutivas e, devido a isso, são utilizadas como um caráter taxonômico em diferentes grupos de plantas (Evert 2006). No entanto, alguns aspectos das estruturas secretoras são passiveis de influência do ambiente, com relatos de variações no grau de desenvolvimento, composição da secreção e na organização ultraestrutural das células secretoras.

Estudando plântulas de *Copaifera langsdorffii* cultivadas em diferentes condições de luz e temperatura, Rodrigues et al. (2014) demonstraram que canais e cavidades secretores de óleo-resina foram mais abundantes e com características ultraestruturais de células ativas em secreção quando expostas a 25°C enquanto que se apresentaram reduzidos e com danos celulares quando expostas a 15 e 35°C.

As características ultraestruturais e a composição da secreção de coléteres mostraram-se variáveis em espécies de Rubiaceae crescendo em floresta e cerrado demonstrando a plasticidade associada ao ambiente nas células secretoras dos coléteres (Tresmondi et al. 2015, 2017). Enquanto que nas espécies de floresta a secreção era predominantemente hidrofílica, nas espécies de cerrado a secreção era lipofílica ou mista (Tresmondi et al. 2015). Esses autores atribuíram as diferenças na secreção às diferenças nas taxas de radiação solar, que foram mais elevadas no cerrado. A morfologia ultraestrutural das células secretoras foi condizente com o tipo de secreção (Tresmondi et

al. 2017). Nas espécies do cerrado, os coléteres apresentaram numerosos leucoplastos, mitocôndrias bem desenvolvidas, abundante retículo endoplasmático liso e numerosas inclusões lipídicas. Já nas espécies de floresta, dictiossomos com cisternas dilatadas e muitas vesículas, mitocôndrias volumosas, plastídeos com inclusões proteicas e um extenso retículo endoplasmático rugoso foram predominantes.

Devemos considerar que a organização tridimensional do corpo da planta é plástica (Tumber-Davila et al. 2022) havendo modificações na morfologia externa, nos tecidos e células ou especializações fisiológicas em resposta ao ambiente (Dickson 2000). Assim, aspectos bioquímicos, morfológicos e fisiológicos dos órgãos vegetais podem ser modificados em resposta aos diferentes fatores ambientais a que as plantas estão expostas durante o seu desenvolvimento (Del Valle et al. 2018). Quando se considera os ambientes aéreo e subterrâneo, as diferentes condições de temperatura, disponibilidade de água, radiação, ataque de fitofágos, além das restrições mecânicas impostas pelo ambiente em que um determinado órgão se desenvolve podem resultar em modificações histológicas e citológicas que culminam em especializações fisiológicas relevantes (Dickison 2000). Embora haja uma óbvia integração entra a parte aérea e a subterrânea da planta, há de se considerar que a diferença no microambiente nesses dois meios exerce uma influência significativa nos órgãos que ali se desenvolvem. Enquanto que no ambiente acima do solo os órgãos aéreos estão expostos a luz, no ambiente abaixo do solo, os órgãos subterrâneos serão influenciados pela água e nutrientes (McPhee e Aarssen 2001). Além dos fatores abióticos, também os organismos que habitam o solo e acima dele são diversos (van Dam e Martin Heil 2011).

Nesse contexto, a produção dos compostos do metabolismo primário e especializado também é influenciada pelo ambiente. Compostos do metabolismo especializado são essenciais para que a planta se ajuste ao ambiente em que está inserida (Casano et al. 2011). Os terpenos são uma classe de substâncias químicas do metabolismo especializado com estrutura e função biológica diversas. Nas plantas, diferentes tipos de terpenos são produzidos em diferentes compartimentos, sendo importantes na interação da planta com o ambiente e com os organismos que coabitam com a mesma. Estudos têm demonstrado que diferentes tipos de terpenos são produzidos em órgãos acima e abaixo do solo (Huang e Osbourn 2019). A secreção de terpenos nas plantas se origina da síntese de moléculas a partir do metabolismo do mevalonato ou não mevalonato (também conhecido como 2-C-metil-D-eritritol 4-fosfato (MEP) ou desoxixilulose 5-fosfato (DXP) (Huang e Osbourn 2019), do estoque existente na planta ou dos dois (Nagalingam

et al. 2023). A nova síntese de terpenos está associada à luz e à temperatura, enquanto que a estocagem deles está somente associada à temperatura (Staudt et al. 2017).

De modo geral, a literatura mostra que pouco se conhece sobre a influência do ambiente no desenvolvimento e funcionamento de canais secretores de resina em condições naturais.

Assim, neste estudo comparamos a distribuição, estrutura, histoquímica, citologia e dinâmica de secreção em canais secretores no caule em sua porção aérea e subterrânea de *Anacardium humile* A. St-Hil., uma espécie subarbustiva de Anacardiaceae, a fim de verificar a existência de plasticidade estrutural, histoquímica e funcional das células secretoras entre porções de órgãos em diferentes ambientes.

Autofagia e suas implicações no desenvolvimento de estruturas secretoras

A autofagia é um dos principais processos catabólicos em células eucarióticas, no qual constituintes citoplasmáticos são degradados e posteriormente reutilizados no metabolismo celular (Contento et al. 2005; Bassham 2007; Avin-Wittenberg et al. 2012; Bozhkov 2018; Soto-Burgos et al. 2018). Inicialmente descrita em fungos, autofagia é um processo conservado em animais e plantas onde foi durante muito tempo considerada restrita aos estágios finais do desenvolvimento de determinadas células e tecidos, tais como a diferenciação de elementos traqueais e a senescência das folhas (Kwon et al. 2010).

Dois tipos principais de autofagia foram inicialmente reportados em plantas (Mitou et al. 2009; Van Doorn e Papini 2013): microautofagia e macroautofagia.

Na microautofagia, uma pequena vesícula, com membrana única, é formada pela invaginação da membrana vacuolar englobando componentes citosólicos (Bassham et al. 2006; Soto-Burgos et al. 2018; Wang et al. 2018). Esse tipo é ainda pouco estudado em plantas e tem sido observado principalmente na senescência de folhas; desenvolvimento e germinação de sementes; acúmulo de antocianinas nos vacúolos (Chanoca et al. 2015) e em células epidérmicas de nectários em estágio pré-secretor (Machado e Rodrigues 2019).

A macroautofagia, referida simplesmente como autofagia, é a forma melhor estudada em plantas. É caracterizada pelo englobamento de conteúdo citoplasmático e organelas em vesículas de dupla membrana chamadas autofagossomos ou vesículas autofágicas (Yoshimoto et al. 2014; Soto-Burgos et al. 2018; Zhang et al. 2018). A macroautofagia envolve várias etapas, incluindo a formação e expansão de fagóforos e o fechamento dos mesmos direcionados para a formação de autofagossomos, e, finalmente,

a fusão com o vacúolo (Wojciechowska et al. 2021). Durante este processo, o autofagossomo engloba e transporta material citoplasmático até o vacúolo. Então, a membrana externa do autofagossomo funde-se com o tonoplasto e a membrana interna e o material nela contido são liberados no lúmen do vacúolo onde ocorre a degradação por hidrolases residentes (Yoshimoto et al. 2009; Zhuang et al. 2013). Os produtos degradados são transportados de volta ao citoplasma onde são reutilizados (Yang e Bassham 2015). A origem do autofagossomo ainda não é bem entendida, mas sabe-se que em células de mamíferos, a membrana do autofagossomo se origina do retículo endoplasmático e de vários compartimentos celulares, como complexo de Golgi, membrana plasmática e mitocôndria, contribuindo para sua expansão (Lamb et al. 2013). Em plantas, trabalhos recentes sugerem que o retículo endoplasmático seja a fonte de membranas e sinalização para a biogênese autofagossomal (Zhuang et al. 2018). ATG8 é uma proteína central na maquinaria autofágica relacionado à formação de autofagossomos e está presente tanto na membrana interna como na externa no início da formação do autofagossomo (quando ainda é tido como fagóforo) e permanece na membrana interna até a degradação no vacúolo. Por essas características, é um bom marcador para rastrear a autofagia desde os estágios iniciais até a degradação no vacúolo (Bassham 2007; Bassham 2015; Klionsky et al. 2021; Wojciechowska et al. 2021).

Tipos adicionais de autofagia foram descritos em plantas (Van Doorn e Papini 2013): autofagia seletiva, quando ocorre a degradação parcial do citoplasma e/ou de organelas específicas (plastídios, mitocôndrias) ainda no citoplasma, e mega-autofagia, quando a membrana do vacúolo se rompe e libera hidrolases no citoplasma, degradando-o completamente e resultando na morte da célula, comumente interpretada como sendo um tipo de morte celular programada (MCP).

Estudos recentes mostraram que a autofagia contribui para vários processos de desenvolvimento de plantas e respostas ao estresse, como restrição de nutrientes e infecções, e está claro que a autofagia é essencial para manter a homeostase celular (Mahood 2021; Sienko et al. 2020). Múltiplos estresses podem induzir autofagia nas plantas e esta é regulada por distintas vias de expressão gênica durante diferentes condições de estresse (Bassham 2007). A participação da autofagia em processos normais de desenvolvimento das plantas, como a diferenciação de estruturas reprodutivas (Haddad et al. 2019), laticíferos (Zhang et al. 2018) e nectários (Machado e Rodrigues 2019) tem sido recentemente confirmada com o uso de técnicas de biologia celular e diferentes microscopias. Neste contexto, merece destaque o estudo de Zhang et al. (2018) que identificaram e descreveram em detalhe o processo autofágico durante o desenvolvimento

de laticíferos não-articulados de *Euphorbia kansui* em nível ultraestrutural, além de descrever a presença de autofagossomos, autolisossomos e estruturas semelhantes a lisossomos. Machado e Rodrigues (2019) identificaram e descreveram três tipos de autofagia no nectário extrafloral de *Citharexylum myrianthum*, sendo dois deles (macroautofagia e microautofagia) associados com a biogênese de vacúolos no estágio pré-secretor, enquanto a mega-autofagia foi associada com a morte celular e restrita ao estágio pós-secretor. Wojciechowska et al (2021) reportaram que a autofagia participa nos processos de formação do vacúolo central no desenvolvimento do tecido cortical, bem como na diferenciação do tecido vascular e senescência da raiz.

Autocitotoxicidade das secreções vegetais e mecanismos citoprotetores

Embora os efeitos farmacológicos e a toxicidade dos terpenos e terpenoides em vários sistemas biológicos sejam bem conhecidos (Masyita et al. 2022), a toxicidade desses compostos às próprias células que os produzem, bem como, os mecanismos citoprotetores desenvolvidos pelas células em presença desses compostos ainda são pouco conhecidos e, portanto, constituem importantes alvos de pesquisa em biologia vegetal.

Os componentes da secreção dos canais secretores de Anacardiaceae incluem principalmente terpenos e compostos fenólicos (Carmello et al. 1995; Pinto et al. 2000; Langenheim 2003; Martínez et al. 2003, 2008; Sant'Anna-Santos et al. 2006; Tolke et al. 2017; Prado e Demarco 2018; Tolke et al. 2021). As secreções terpênicas contém substâncias biologicamente ativas (terpenos e terpenoides) que danificam irreversivelmente a célula culminando com a sua autólise (Fahn 1979; Roshchina e Roshchina 1993). O isolamento das substâncias tóxicas em compartimentos intracelulares específicos ou a sua modificação química em substâncias inativas tem sido considerados mecanismos que protegem o citoplasma dos efeitos tóxicos das secreções (Roshchina e Roshchina 1993; Huang e Osbourn 2019). No entanto, os danos celulares e reações de sinalização ligada às próprias secreções dessas células são ainda pouco conhecidos (Canaveze et al. 2021).

Em uma análise detalhada das células de óleo de nim (*Azadirachta indica* A. Juss (Meliaceae) durante o ciclo secretor Canaveze et al. (2021) observaram acentuada hipertrofia celular, aumento da vesiculação das membranas celulares, dilatação das cisternas do retículo endoplasmático, hipertrofia mitocondrial em processo de cristólise, vacúolos autolíticos e degeneração vacuolar culminando na autólise do protoplasto, além de depósitos citoplasmáticos de cálcio e expressão da HSP70 (*heat shock protein 70*). Tais alterações morfológicas na topografia e morfologia das organelas seguiram um

padrão semelhante ao reportado em tecidos animais expostos ao óleo de nim, um dos biopesticidas mais amplamente utilizados na atualidade (Scudeler et al. 2016). Ao examinar os estudos ultraestruturais realizados com estruturas secretoras de terpenos disponíveis em literatura, geralmente observamos alterações morfológicas ao longo do processo secretor similares às reportadas por Scudeler et al. (2016) e Canaveze et al. (2021); no entanto, tais alterações têm sido negligenciadas ou associadas com senescência ou morte celular programada. A combinação de métodos em imunohistoquímica e ultraestrutura celular convencional e citoquímica é fundamental para compreender as repostas das células secretoras às próprias secreções que produzem.

É importante salientar que os resultados de Canaveze et al. (2021) se referem a idioblasto secretor com secreção endógena. Tais estudos devem ser ampliados a fim de verificar se o padrão observado é comum a outras estruturas secretoras de terpenos mais complexas e com secreção exógena, como é o caso dos canais secretores.

Objetivos

Com o objetivo de aprofundar o conhecimento sobre aspectos celulares do desenvolvimento e funcionamento de canais secretores de resina, nesse estudo, analisamos comparativamente os canais secretores no caule aéreo e subterrâneo de *Anacardium humile* A.St.-Hil. a fim de acessar variações intraindividuais relacionadas ao ambiente aéreo e subterrâneo; investigar a ocorrência e caracterizar morfologicamente os tipos de autofagia, e pesquisar a ocorrência de autocitotoxicidade e de mecanismos citoprotetores em células epiteliais secretoras de resina. Com o desenvolvimento deste estudo, pretendemos responder as seguintes questões:

i) Há variações intraindividuais nos canais secretores do caule na porção aérea e subterrânea?

ii) Ocorre autofagia nas células epiteliais durante o processo de secreção de resina? Em caso afirmativo, em quais etapas da secreção ocorre autofagia?

iii) Existem diferentes tipos de autofagia durante o ciclo secretor? Em caso afirmativo, o tipo de autofagia é estágio-dependente?

iv) Os componentes da resina seriam tóxicos às próprias células que os produzem? Em caso afirmativo, quais organelas são mais susceptíveis? Existem mecanismos de citoproteção?

Referências Bibliográficas

Almeida S P, Proença C E B, Sano S M, Ribeiro J F (1998) Cerrado: espécies vegetais úteis.

Avin-Wittenberg T, Honig A, Galili G (2012) Variations on a theme: plant autophagy in comparison to yeast and mammals. Protoplasma 249:285–299. DOI 10.1007/s00709-011-0296-z

Bassham DC (2007) Plant autophagy - more than a starvation response. Current opinion in plant biology 10: 1–7.

Bassham DC (2015) Methods for analysis of autophagy in plants. Methods 75: 181–188.

Bassham DC, Laporte M, Marty F, Moriyasu Y, Ohsumi Y, Olsen LJ, Yoshimoto K (2006) Autophagy in development and stress responses of plants. Autophagy 2: 2–11.

BFG (2015) Growing knowledge: an overview of Seed Plant diversity in Brazil. Rodriguésia 66(4): 1085-1113. http://rodriguesia.jbrj.gov.br DOI: 10.1590/2175-7860201566411.

Bozhkov PV (2018) Plant autophagy: Mechanisms and functions. Journal of Experimental Botany 69: 1281–1285.

Canaveze Y, Scudeler EL, Machado SR (2021) Neem secretory cells: developmental cytology and indications of cell autotoxicity. Protoplasma 258:415–429. https://doi.org/10.1007/s00709-020-01580-3.

Carvalho RS, Pinto JFN, Reis EF, Santos SC, Dias LAS (2012) Variabilidade genética de cajuzinho-do-cerrado (*Anacardium humile* st. Hil.) por meio de marcadores RAPD1. Rv. Bras. Frutic. 34 (1): 227-233.

Chanoca A, Kovinich N, Burkel B, Stecha S, Bohorquez-Restrepo A, Ueda T, Eliceiri KW, Grotewold E, Otegui MS (2015) Anthocyanin Vacuolar Inclusions Form by a Microautophagy Mechanism. The Plant Cell, Vol. 27: 2545–2559.

Contento AL, Xiong Y, Bassham DC (2005) Visualization of autophagy in *Arabidopsis* using the fluorescent dye monodansylcadaverine and a GFP-AtATG8e fusion protein. Plant Journal 42: 598–608.

Cota LG, Moreira PA, Brandão MM, Royo VA, Melo Junior AF, Menezes EV, Oliveira DA (2017) Structure and genetic diversity of *Anacardium humile* (Anacardiaceae): a tropical shrub. Genet. mol. res. (Online) 16 (3): gmr16039778.

Dickison, W. C. Integrative plant anatomy New York: Harcourt/Academic, 2000. 533 p.

Evert RF (2006) Meristems, cells and tissues of the plant body their structure, function and development.

Fahn A (1979) Secretory tissues in plants.

Fahn A, Evert RF (1974) Ultrastructure of secretory ducts of *Rhus glabra* L. Am. j. bot. 61: 1–14.

Ganesan D, Cai Q (2021) Understanding amphisomes. Biochemical Journal 478: 1959–1976. https://doi.org/10.1042/BCJ20200917.

Haddad IVN, Sá-Haiad B, Santiago-Fernandes LDR, Machado SR (2019) Pollen grain development and male sterility in the perfect Flowers of *Maytenus obtusifolia* Mart. (Celastraceae) Protoplasma. 256:745–761. https://doi.org/10.1007/s00709-018-01336-0.

Kliosnky et al. (2021) Guidelines for the use and interpretation of assays for monitoring autophagy (4th edition) Autophagy 17(1):1-382. doi: 10.1080/15548627.2020.1797280.

Kwon SI, Cho HJ, Jung JH, Yoshimoto K, Shirasu K, Park OK (2010) The Rab GTPase RabG3b functions in autophagy and contributes to tracheary element differentiation in *Arabidopsis*. The Plant Journal 64: 151–164. doi: 10.1111/j.1365-313X.2010.04315.x.

Lacchia APS, Carmello-Guerreiro SM (2009) Aspectos ultra-estruturais dos canais secretores em órgãos vegetativos e reprodutivos de Anacardiaceae. Acta bot. bras. 23: 376–388.

Lamb CA, Yoshimori T, Tooze AS (2013) The autophagosome: origins unknown, biogenesis complex. Nature Reviews Molecular cell biology. 14: 759-774.

Langenheim JH (2003) Plant resins: chemistry, evolution, ecology and ethnobotany. Timber Press, Portland, Cambridge.

Machado SR, Carmello-Guerreiro SM (2001) Estrutura e desenvolvimento de canais secretores em frutos de *Schinus terebinthifolius* Raddi (Anacardiaceae). Acta bot. bras. 15: 189–195.

Machado SR, Rodrigues TM (2019) Autophagy and vacuolar biogenesis during the nectary development. Planta 250: 519–533. https://doi.org/10.1007/s00425-019-03190-7.

Mahood HE (2021) Autophagy in Plants during Nutrient Starvation, Osmotic and Heat Stresses. Annals of R.S.C.B 25(3):7933 – 7944.

Masyita A, Sari RM, Astuti RD, Yasir B, Rumata NR, Emran TB, Nainu F, Simal-Gandara J (2022) Terpenes and terpenoids as main bioactive compounds of essential oils, their roles in human health and potential application as natural food preservatives. Food Chemistry: X 13. https://doi.org/10.1016/j.fochx.2022.100217.

Mitou G, Budak H, Gozuacik D (2009) Techniques to study autophagy in plants. International Journal of Plant Genomics. doi:10.1155/2009/451357.

Nair GM, Venkaiah K, Shah JJ (1983) Ultrastructure of gumresin ducts in cashew (*Anacardium occidentale*). Ann. bot. 51: 297–305.

Palermo FH, Rodrigues MIA, de Nicolai J, Machado SR, Rodrigues TM (2018) Resin secretory canals in *Protium heptaphyllum* (Aubl.) Marchand. (Burseraceae): a tridimensional branched and anastomosed system. Protoplasma 255: 899–910.

Pell SK, Mitchell JD, Miller AJ, Lobova TA (2001) Anacardiaceae. In: Kubitzki, K. (Ed.), The Families and Genera of Vascular Plants: Flowering Plants. Eudicots: Sapindales, Cucurbitales, Myrtales: Vol. 10. Springer, Berlin/Heidelberg, pp 7–50.

Pickel DBJ (2008) Flora do Nordeste do Brasil segundo Piso e Marcgrave: no século XVII.

Roshchina VV, RoshchinaVD (1993) The excretory function of higher plants. Springer, Berlin.

Royo VA, Mercadante-Simões MO, Ribeiro LM, Oliveira DA, Aguiar MMR, Costa ER, Ferreira PRB (2015) Anatomy, histochemistry, and antifungal activity of *Anacardium humile* (Anacardiaceae) leaf. Microsc. Microanal. Microstruct. 21: 1549–1561.

Scudeler E, Garcia A, Padovani C, Pinheiro P, Santos D (2016) Cytotoxic effects of neem oil in the midgut of the predator *Ceraeochrysa claveri*. Micron 80: 96–111.

Siénko K, Poormassalehgoo A, Yamada K, Goto-Yamada S (2020) Microautophagy in Plants: Consideration of Its Molecular Mechanism. Cells 9: 887. doi:10.3390/cells9040887.

Soto-Burgos J, Zhuang X, Jiang L, Bassham DC (2018) Dynamics of autophagosome formation. Plant Physiology 176: 219–229.

Van Doorn WG, Papini A (2013) Ultrastructure of autophagy in plant cells: A review. Autophagy 9: 1922–1936.

Wang P, Mugume Y, Bassham DC (2018) New advances in autophagy in plants: Regulation, selectivity and function. Seminars in Cell and Developmental Biology 80: 113–122.

Wojciechowska N, Michalak KM, Bagniewska-Zadworna A (2021) Autophagy—an underestimated coordinator of construction and destruction during plant root ontogeny. Planta 254:15. https://doi.org/10.1007/s00425-021-03668-3.

Yang X, Bassham DC (2015) New Insight into the Mechanism and Function of Autophagy in Plant Cells. International Review of Cell and Molecular Biology 320: 1–40.

Yoshimoto K, Jikumaru Y, Kamiya Y, Kusano M, Consonni C, Panstruga R, Ohsumi Y, ShirasuK (2009) Autophagy Negatively Regulates Cell Death by Controlling NPR1-Dependent Salicylic Acid Signaling during Senescence and the Innate Immune Response in *Arabidopsis*. The Plant Cell Online 21: 2914–2927.

Yoshimoto K, Shibata M, Kondo M, Oikawa K, Sato M, Toyooka K, Shirasu K, Nishimura M, Ohsumi Y (2014) Organ-specific quality control of plant peroxisomes is mediated by autophagy. Journal of Cell Science 127: 1161–1168.

Zeng Y, Li B, Lin Y, Jiang L (2019) The interplay between endomembranes and autophagy in plants Current Opinion in Plant Biology 52:14–22.

Zhang Q, Wang D, Zhang H, Wang M, Li P, Fang X, Cai X (2018) Detection of autophagy processes during the development of nonarticulated laticifers in *Euphorbia kansui* Liou. Planta 247: 845– 861.

Zhuang X, Wang H, Lam SK, Gao C, Wang X, Cai Y, Jiang L (2013) A BAR-Domain Protein SH3P2, Which Binds to Phosphatidylinositol 3-Phosphate and ATG8, Regulates Autophagosome Formation in *Arabidopsis*. The Plant Cell 25: 4596–4615.

Zhuang X, Chung KP, Luo M, Jiang L (2018) Autophagosome Biogenesis and the Endoplasmic Reticulum: A Plant Perspective. Trends in Plant Science 23(8). https://doi.org/10.1016/j.tplants.2018.05.002.

Conforme estabelecido pelo Programa de Pós-Graduação em Biologia Vegetal Interunidades, UNESP, os resultados obtidos durante a execução deste projeto de doutorado estão sendo apresentados na forma de capítulos já organizados para publicação, os quais foram redigidos de acordo com as normas de periódicos relevantes da área (Comitê de Biodiversidade da Capes).

São apresentados três capítulos na forma de artigos, sendo:

Artigo 1: Intraspecific variation in ultrastructure and secretion of the resin-secreting canals in *Anacardium humile* (Anacardiaceae) – Publicado no periódico "Protoplasma" (A1 - Comitê de Biodiversidade da Capes)

Artigo 2: Identification and characterization of autophagy in resin secretory canals – submetido para publicação no periódico científico "Planta"

Artigo 3: Evidências ultraestruturais e imunohistoquímicas de autocitotoxicidade em canais secretores de resina

Protoplasma
https://doi.org/10.1007/s00709-022-01823-5

ORIGINAL ARTICLE

Intraspecific variation in ultrastructure and secretion of the resin canals in *Anacardium humile* (Anacardiaceae)

Shelly Favorito de Carvalho[1,2] · Elton Luiz Scudeler[3] · Daniela Carvalho dos Santos[1,3] · Silvia Rodrigues Machado[1,2]

Received: 2 August 2022 / Accepted: 17 November 2022

Abstract

The study combines a range of light and electron microscopy methods to access variation in secretion and ultrastructure in the secretory canals in the above- and belowground stems of *Anacardium humile*, which here serves as a model system. The aboveground stem canals show epithelial cells with ultrastructural characteristics typical of cells active in secretion, while in the belowground stems, the subcellular characteristics are typical of cells with low rates of metabolism. The secretory canals of the belowground stems show uniformity in size and shape, a large central vacuole, a cytoplasm reduced to a thin layer at the cell periphery, and a reduced population of organelles. The aboveground stem canals had voluminous nuclei with evident nucleoli, a very dense cytoplasm with free ribosomes, polyribosomes, mitochondria with developed cristae, and ellipsoid plastids with electron-opaque droplets surrounded by a periplastid reticulum. The vacuoles were of different sizes and often had membranous contents and the dictyosomes were very developed with dilated ends to the cisternae, rough endoplasmic reticulum, and numerous vesicles. The results show that particularities in above- and belowground environment have significant implications for ultrastructural morphology and functioning of secretory canals in the stems of *A. humile*.

Keywords Anacardiaceae · Cytology · Histochemistry · Secretory canals · Ultrastructural cytochemistry

Introduction

Plant organs are reported to be able to adjust many of their biochemical, morphological, and physiological characteristics in response to the environmental signals to which they are exposed during development (Del Valle et al. 2018). Thus, the above- and belowground organs of a plant are exposed to quite different environmental conditions of temperature, water availability, and radiation. They are also exposed to attack by quite different ranges of predators and to quite different kinds of mechanical constraint. The concept of aboveground-belowground ecology assumes that plants, aboveground biota, and soil biota are all part of one system, in which aboveground and belowground organs, individuals, populations, and communities influence each other (van der Putten et al. 2009; Bardgett and van der Putten 2014). The consequences of aboveground-belowground interactions during organ development and its histological, cytological, and physiological specializations are still poorly understood (Dickison 2000).

Secretory structures are constitutive features, having taxonomic relevance in many plant groups (Evert 2006). Nevertheless, some aspects of these are also susceptible to environmental influences, with reports of variations in their degree of development, in their secretion composition, and in the ultrastructural organization of their secretory cells. Such have been reported for the oil-resin secretory canals of *Copaifera langsdorffii* when grown under different conditions of light and temperature (Rodrigues et al. 2014) and for the colleters in Rubiaceae species growing in forests or cerrado (Tresmondi et al. 2015, 2017). Little is known of the influences

Handling Editor: Dorota Kwiatkowska

✉ Silvia Rodrigues Machado
silvia.machado@unesp.br

[1] Electron Microscopy Center (CME), Institute of Biosciences of Botucatu (IBB), São Paulo State University (UNESP), Botucatu, SP 18618-689, Brazil

[2] Department of Biostatistics, Plant Biology, Parasitology and Zoology, Institute of Biosciences of Botucatu (IBB), São Paulo State University (UNESP), Botucatu, SP, Brazil

[3] Department of Structural and Functional Biology, Botucatu Institute of Biosciences (IBB), São Paulo State University (UNESP), Botucatu, SP, Brazil

Published online: 30 November 2022

of the environment on the development, histochemistry, cytology, and secretion dynamics of secretory structures. This dearth is due to a lack of comparative studies between species and between organs of the same species, which also report on the structural and functional plasticity of secretory cells. In this context, our study sets out to access the intraspecific variation in the secretions of the secretory canals in the above- and belowground axes of *Anacardium humile* (Anacardiaceae).

The occurrence of resin canals is a common feature of the Anacardiaceae (Metcalfe and Chalk 1950), a family of woody plants distributed mainly in tropical and subtropical regions (Judd et al. 2007; Pell et al. 2011; Royo et al. 2015). Several species of the Anacardiaceae are exploited in loco or cultivated for their edible fruits, including mango (*Mangifera indica*), cajá (*Spondias* spp.), and siriguela (*Spondias purpurea*). The cashew fruit (*Anacardium occidentale*) and its fruit are widely commercialized. The various species of this family are valued for their quality timbers and for their resins which are used extensively in industry and in medicine. These species release characteristic odors when their resin canals are exposed by injury (Souza and Lorenzi 2005). In Brazil, Anacardiaceae is represented by 55 species distributed among 14 genera, with *Schinus* L. and *Anacardium* L. being the most diverse (BFG 2015).

Variations in the distributions of the secretory canals in the Anacardiaceae and in the chemical compositions of their secretions have been well reported. Secretory canals can be found in the primary, secondary, and pith phloem (Metcalfe and Chalk 1950) and are able to produce resins (Paula and Alves 1973; Gibson 1981; Sawidis et al. 2000), gum resins (Fahn and Evert 1974; Joel and Fahn 1980a, b; Nair et al. 1983; Bhatt and Ram 1992; Vassilyev 2000), gums (Venkaiah 1992), and latex (Venning 1948). Despite the importance of the resin canals in Anacardiaceae, cytological studies have been restricted to a single organ—the stem (Fahn and Evert 1974; Fahn 1979; Joel and Fahn 1980a, b, c; Nair et al. 1983; Venkaiah 1992; Carmello et al. 1995; Machado and Carmello-Guerreiro 2001). The single exception is the study by Lacchia and Carmello-Guerreiro (2009), who analyzed the secretory canals in the flowers and fruits of *Anacardium humile*. According to these authors, in flowers, these canals present epithelial cells with peripheral cytoplasm, while in fruits, the cells have a central vacuole and peripheral cytoplasm, while others have a dense cytoplasm, rich in vesicles, vacuoles, and numerous rounded plastids. This range of cell microstructure may be due to the peculiarities of the organ in which the canal is located, or it may be associated with the functional stage of the secretory cells at the time of the study because, in the same epithelium, not all cells are at the same stage in their secretory cycles (Machado et al. 2017).

This study combines a range of light and electron microscope methods to undertake a comparative analysis of the chemical compositions of the secretions and the cytology of the secretory canals in the above- and belowground stems of *Anacardium humile* A.St.-Hil.—using this species as a model system to explore the effects of environment on these organs.

Anacardium humile, which has various common names in Brazil, including cajuzinho-do-cerrado, cajuí, and cajuzinho-do-campo, is a subshrub native of the Brazilian Cerrado, and very frequent in burned environments (Agostini-Costa et al. 2016). It is characterized by having several erect, aboveground stems reaching about 80 cm in height and with a very extensive woody underground stem and deep roots which penetrates into the soil (to a depth of up to 16 m) to reach the water table (Cota et al. 2017). The aboveground organs are commonly destroyed by fire but the underground stem system is persistent, unaffected by the passage of a fire (Coutinho 1982; Eiten 1982).

Such studies are urgent, especially when considering the importance of *A. humile* in the cerrado, a biodiverse environment of high importance in maintaining the life of the local human and animal populations that very much depend on it both directly and indirectly. In the Cerrado, this species has the ecological functions of providing food for the endemic fauna, as its fruits and seeds are highly sought after by animals, especially by birds and also mammals such as the fox (*Lycalopex vetulus*). Both these animals act as important seed dispersal agents. As a subshrub species, *A. humile* is susceptible to the effects of both man and fire, and finds itself competing with other plant species for the title of most endangered species. The small fruits, when fermented, provide a kind of brandy known by the indigenous people as cauim (Carvalho 2020). The nuts are rich in vitamins B1 and B2, proteins, lipids, niacin, phosphorous, and iron. All organs of *A. humile* are used in folk medicine. The infusion of its leaves and of the bark of the underground stem is used to cure diarrhea. The oil found in the fruits has antiseptic and healing effects, and is also used in industry in the production of plastics, coatings, and insulating materials. The aboveground stem of *A. humile* is rich in vitamin C, fiber, and antioxidants. This biological composition is associated with the prevention of chronic degenerative diseases such as cardiovascular diseases, cancer, and diabetes. The infusion of the flowers is used to fight coughs and to lower glucose level in diabetics (Carvalho 2020).

Our study analyzes the distribution, histochemistry, and cytology of the secretory canals in the above- and belowground stems of *A. humile*, to identify any variation in the morphology and functioning of the secretory canals between above- and belowground stem of the same plant. The results obtained contribute to a better understanding of the aboveground-belowground interactions and implications on plant secretions.

Material and methods

The studies were carried out on specimens of *A. humile* occurring in a natural population in fragments of cerrado in the municipalities of Botucatu and Pratânia, state of São Paulo, Brazil. In this region, individual plants present as subshrubs, about 20 cm high and with extensive belowground stem systems.

Vouchers were deposited at the Herbarium "Irina Delanova de Gemtchujnicov" (BOTU) of the Department of Biostatistics, Plant Biology, Parasitology and Zoology, Institute of Biosciences of Botucatu (IBB), São Paulo State University (UNESP), Botucatu, SP, Brazil.

Samples were taken from the aboveground stems with both primary (0.5 cm from the apex) and secondary (10 cm from the apex) growth and from the proximal region of the belowground stem system at a depth of about 20 cm. Samples were collected from at least five plants, and in such a way as to cause minimal damage to the plants. The collected material was immediately fixed and processed for examination under light and transmission electron microscopes.

Light microscopy

For histological characterization, the material was fixed in FAA 50 (formaldehyde, acetic acid, and 50% ethanol) (Johansen 1940) for 24 h. Then, the material was dehydrated in a graded ethanol series, and embedded in Leica Historesin (Leica Microsystems Inc., Heidelberger, Germany). Sections (5 µm thick) were obtained using a rotary microtome, and stained with toluidine blue pH 4.3 (O'Brien et al. 1964). Permanent slides were mounted with Entellan® and analyzed under a Leica DMR microscope with a Leica DFC 425 digital camera attached.

For in situ histolocalization, hand-cut sections (about 10–12 µm thick) were treated with Sudan IV for detection of total lipids (Johansen 1940); NADI reagent for essential oils and oleoresin (David and Carde 1964); 10% aqueous ferric chloride solution for labeling phenolic compounds (Johansen 1940); 0.02% aqueous solution of ruthenium red for identification of various polysaccharides and pectins (Jensen 1962); periodic acid/Schiff reagent (PAS) for neutral polysaccharides (McManus 1948); Lugol's solution for detection of starch grains and alkaloids (Johansen 1940); bromophenol mercury blue solution for protein detection (Mazia et al. 1953); and tannic acid/iron III chloride for mucilage detection (Pizzolato and Lillie 1973). For each histochemical test, we carried out the standard control procedures suggested by the author of the respective technique.

Transmission electron microscopy (TEM)

To characterize the subcellular organization of the secretory canals, samples were fixed in 2.5% glutaraldehyde in 0.1 mol L^{-1} phosphate buffer (pH = 7.2), and left overnight at 4 °C. The material was then post-fixed in 1% osmium tetroxide (OsO_4) solution in the same buffer for 2 h at room temperature. Afterwards, they were stained in 0.5% uranyl acetate, dehydrated in acetone solution, soaked in acetone solution, and embedded in Araldite® resin. Ultrathin sections were stained with uranyl acetate and lead citrate (Reynolds 1963). The material was examined in a Tecnai Spirit transmission electron microscope (FEI Company) at 80 kV.

To better visualize the population of organelles and changes in the endomembrane system associated with the secretory process, the ZIO method was used (zinc iodide-osmium tetroxide—Reinecke and Walther 1978). For this, the samples were fixed as in the conventional method, washed in phosphate buffer with 8.5% sucrose in TRIS-aminomethane buffer (1.13 M NaCl; 0.11 M $CaCl_2$; 0.03 M $MgCl_2$; 0.01 M TRIS-aminomethane) pH 4.5, and incubated in ZIO in the dark for 19 h. This was followed by dehydration in acetone series, standard embedding, and TEM staining.

To detect acid phosphatase activity, we used the method of Pino et al. (1981). This method has previously been used to study the activity of lytic enzymes present in different compartments of the plant secretory cell, including in the cell walls (Machado and Rodrigues 2019). Preliminary

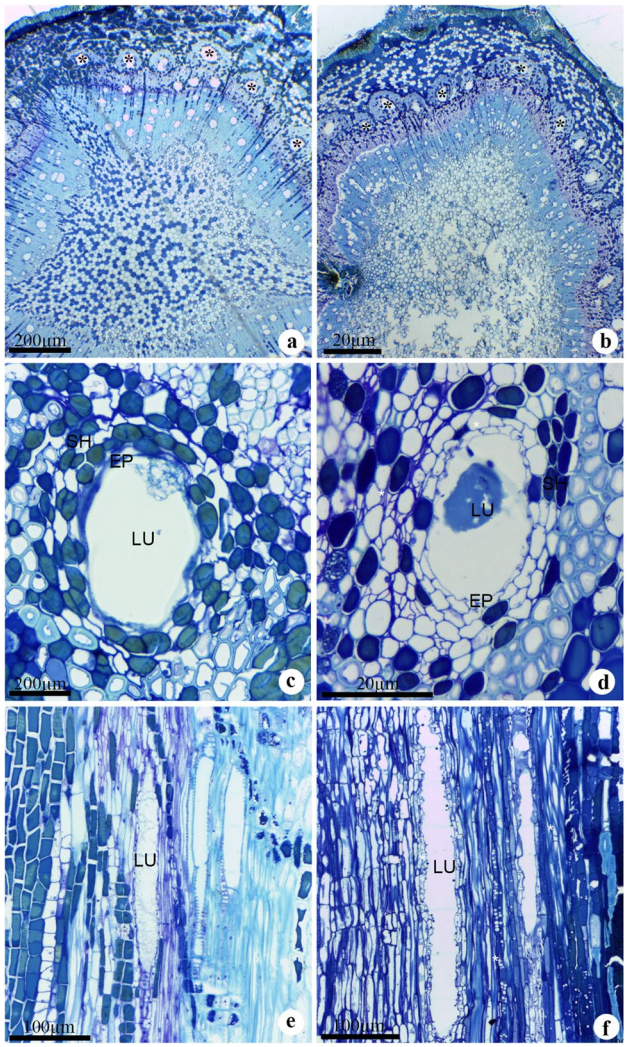

Fig. 1 Secretory canals of aboveground (**a**, **c**, **e**) and belowground stems (**b**, **d**, **f**) of *Anacardium humile*. **a**, **b** Cross-sections showing secretory canals (asterisks) in the primary phloem. **c**, **d** Mature canal with wide lumen (LU) and secretory epithelium (EP) surrounded by a parenchymal sheath (SH). **e**, **f** Longitudinal sections showing secretory canals with elongated lumens (LU)

studies described the participation of the epithelial cell wall in the secretion elimination process (Barreiro and Machado 2007), which suggested the use of this method in the present study. For this, thin sections of the samples were fixed in 2.5% glutaraldehyde in sodium cacodylate buffer for 60 min; washed in 0.1 M cacodylate buffer, pH 7.2, with 8.5% sucrose (4 × 15 min); washed in 0.05 M sodium acetate buffer, pH 5.0, with 5% sucrose (2 × 10 min); and incubated in an appropriate medium (25 mg of cytidine 5′monophosphate; 12 ml of distilled water; 10 ml of 0.05 M sodium acetate buffer, pH 5.0; 3 ml of 1% lead nitrate in distilled water) at 37 °C with constant stirring for 60 min. Then, the sections were washed (1 × 10 min) in 0.05 M sodium acetate buffer, pH 5.0, with 5% sucrose; washed (1 × 10 min) in 0.1 M cacodylate buffer, pH

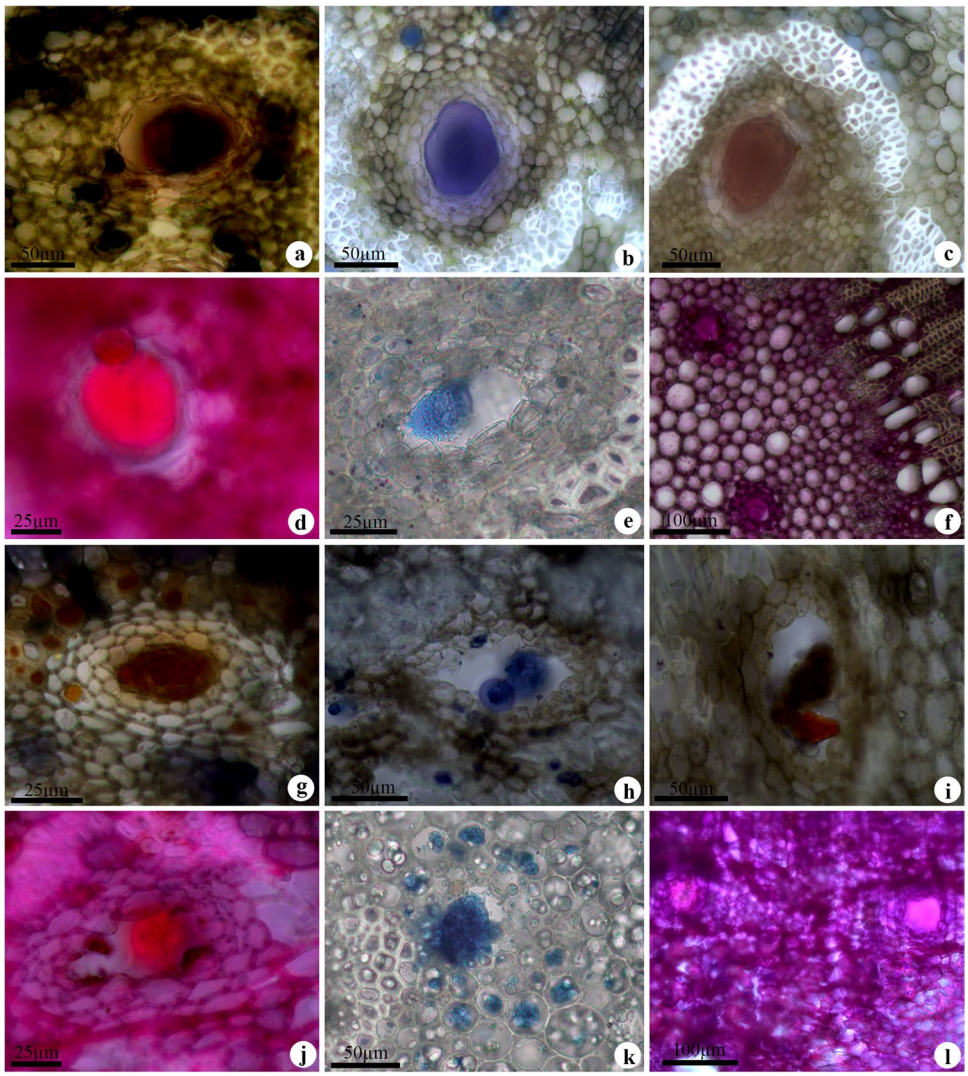

Fig. 2 Histochemical tests of secretory canals in aboveground (**a**–**f**) and belowground stems (**g**–**l**) of *Anacardium humile*. **a**–**e**, **g**–**j** Phloem canals. **f**, **k**, **l** Medullary canals. **a**, **g** Phenolic substances. **b**, **c**, **h**, **i** Terpenoids. **d**, **j** Polysaccharides. **e**, **k** Proteins. **f**, **l** Neutral polysaccharides

Table 1 Histochemistry of the secretory canals of above- and belowground stems of *Anacardium humile*

Reagent	Target compound	Phloem canals		Medullary canals	
		Epithelium	Lumen	Epithelium	Lumen
Ferric chloride	Phenolic compounds	−	+	−	−
NADI reagent	Terpenoids	−	+	−	−
Schiff (PAS)	Neutral polysaccharides	−	−	+	+
Bromophenol mercury blue	Proteins	−	+	−	+
Ruthenium red	Total polysaccharides	+	+	−	−

− no reaction, + positive reaction

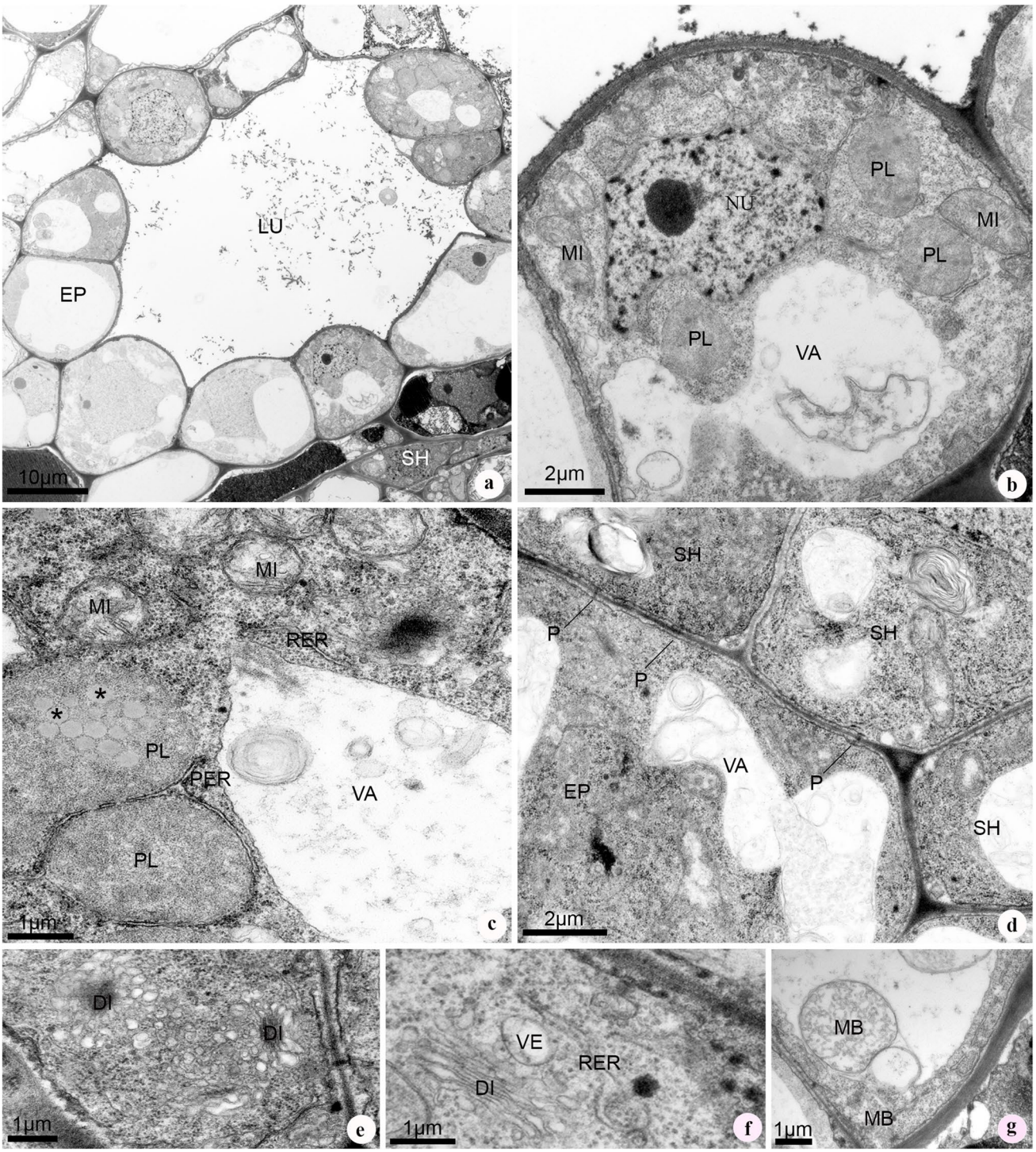

Fig. 3 Electron micrographs of the secretory canals of the aboveground stem of *Anacardium humile*. **a** Mature canal with wide lumen (LU) and secretory epithelium (EP) surrounded by a parenchymal sheath (SH). **b** Epithelial cell with dense cytoplasm, large nucleus (NU), evident nucleolus, large vacuole (VA), plastids (PL), and mitochondria (MI). **c** Part of an epithelial cell showing mitochondria (MI), rough endoplasmic reticulum (RER), polyribosomes, and ellipsoid plastids (PL) with electron-opaque droplets (asterisks) surrounded by periplastid reticulum (PER). **d** Plasmodesmata (P) connecting epithelial cells (EP) to sheath cells (SH). Note the vacuole (VA) with membranous content. **e** Part of the epithelial cell with developed dictyosomes (DI). **f** Rough endoplasmic reticulum (RER), dictyosomes (DI) with dilated cisternae, and vesicles (VE) in the peripheral cytoplasm. **g** Multivesicular bodies (MB) juxtaposed to the plasma membrane and within the vacuoles

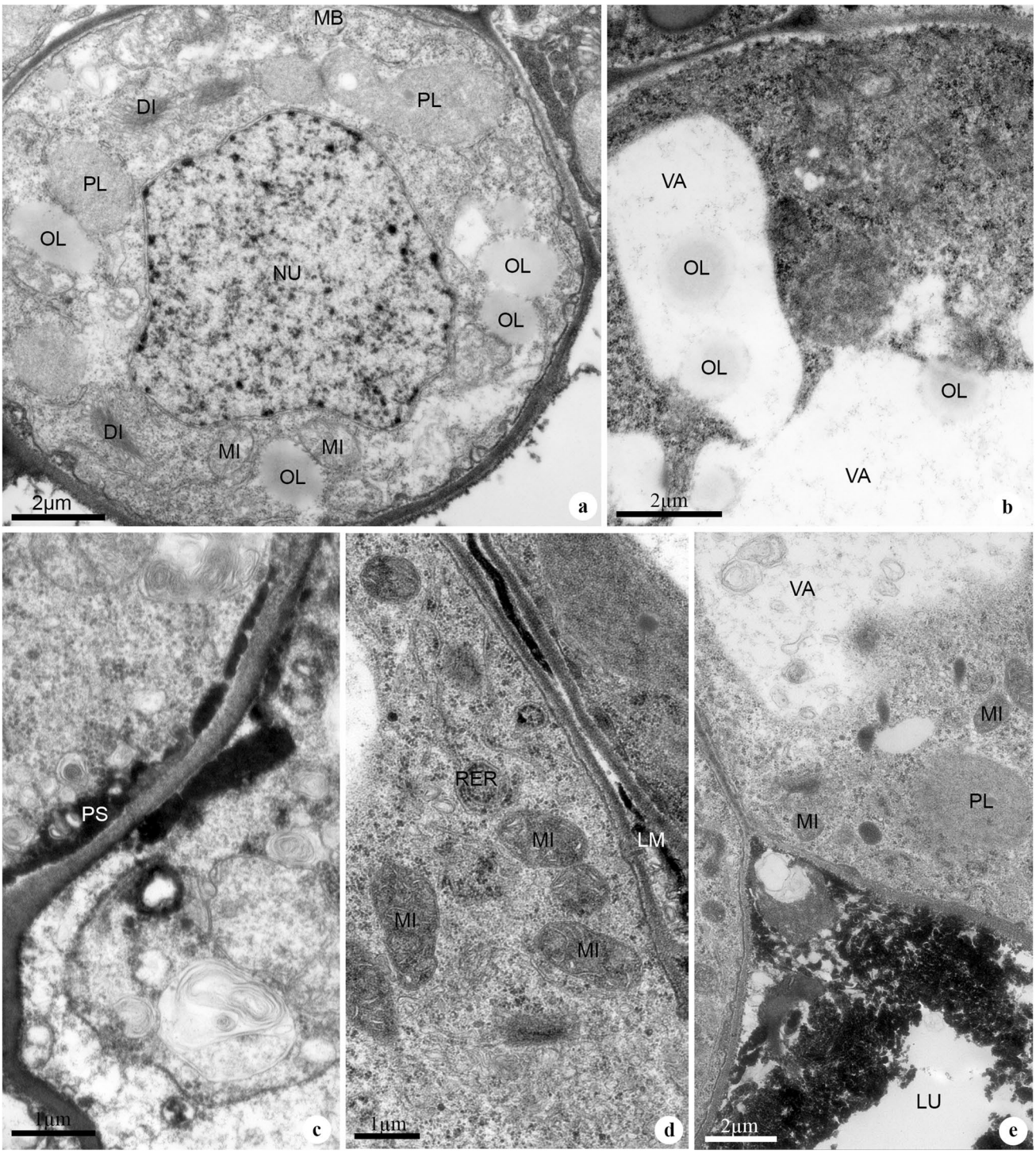

Fig. 4 Electron micrographs of epithelial cells from secretory canals of the aboveground stem of *Anacardium humile*. **a** Epithelial cell with conspicuous nucleus (NU) and dense cytoplasm showing mitochondria (MI), dictyosomes (DI), plastids (PL), and oil droplets (OL). **b** Cytoplasm detail showing oil droplets (OL) inside vacuoles (VA). **c** Neighboring epithelial cells with dark material and electron-dense inclusions in the periplasmic space (PS). **d** Neighboring epithelial cells with dark material and electron-dense inclusions in the middle lamella. Note the occurrence of developed mitochondria (MI) and cisternae of rough endoplasmic reticulum (RER) in the cytoplasm. **e** Electron-dense flocculated material in the canal lumen (LU)

7.2, with 8.5% sucrose; and refixed in glutaraldehyde 2.5% in sodium cacodylate buffer for 30 min. This was followed by post-fixation with osmium tetroxide, dehydration in acetone, and conventional inclusion in TEM.

Results

We compared the secretory canals in the aboveground and in the belowground stems of *A. humile*.

Distribution, histology, and histochemistry of the secretory canals

Secretory canals occurred both in the above- and belowground stems (Fig. 1). The canals were associated with the phloem (Fig. 1a, b) and embedded in the pith. Phloem canals were most abundant and dense and occurred in all samples analyzed, while medullary canals were rarer, sparsely distributed, and often were not observed at all.

Histological analyses showed differentiated secretory canals regardless of the stem growth stage—primary or secondary. For this reason, the descriptions will refer to the characteristics of the secretory epithelium cells without considering the growth stage of the above- and belowground stems. Structurally, in all samples analyzed, the canals were constituted by a uni-stratified secretory epithelium around a wide lumen, where the secretion accumulated (Fig. 1c, d). In all organs investigated, the canals were circular in cross-section (Fig. 1c, d) and elongated in longitudinal section (Fig. 1e, f). In all samples analyzed, the secretory canals were surrounded by a sheath, consisting of one to four layers of oval to tangentially elongated parenchyma cells, with meristematic characteristics. Some parenchymal sheath cells presented cytoplasm with dense contents, histochemically identified as phenolic substances (Fig. 1c, d).

In all samples analyzed from both aboveground (Fig. 2a–f) and belowground (Fig. 2g–l) stems, phenolic compounds (Fig. 2a, g), terpenoids (Fig. 2b, c, h, i), polysaccharides (Fig. 2d, j), and proteins (Fig. 2e) were

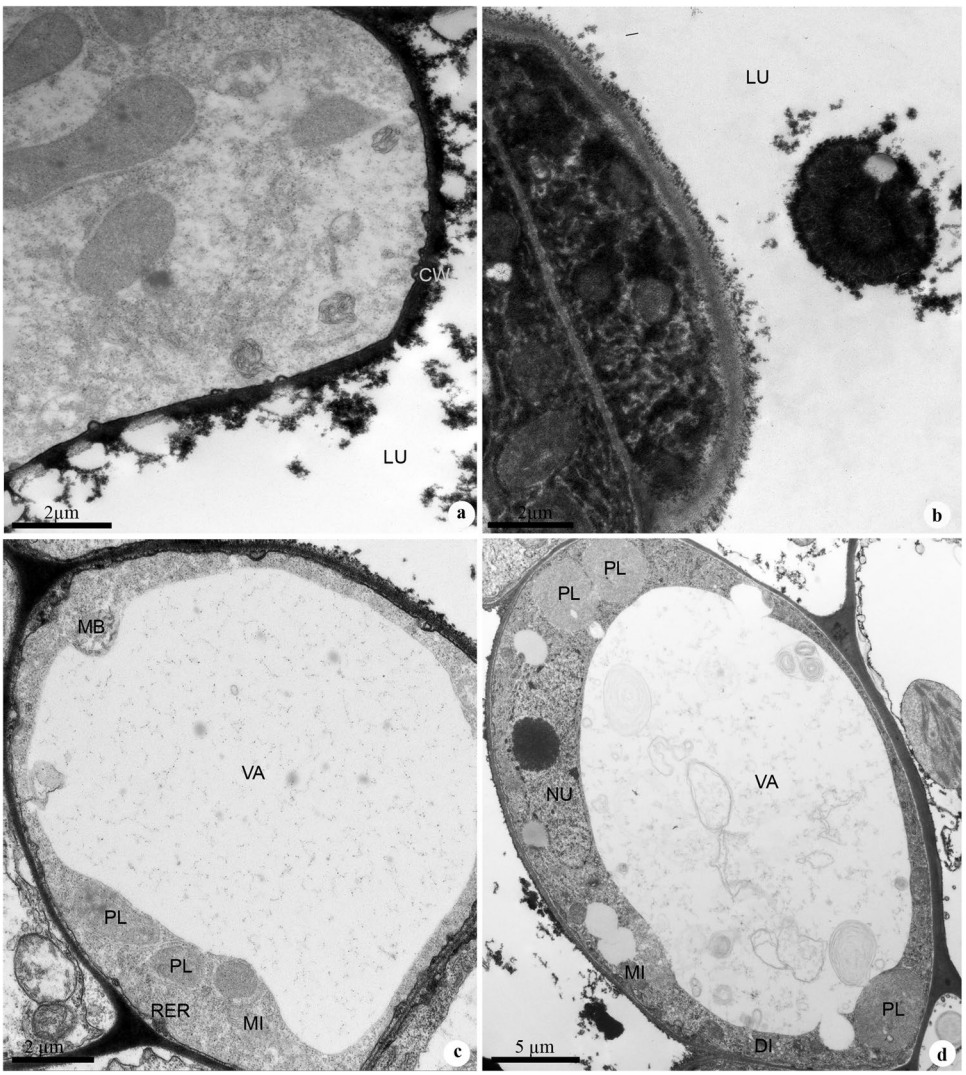

Fig. 5 Electron micrographs of epithelial cells from secretory canals of the aboveground stem of *Anacardium humile*. **a** Secretion-active cell showing dense material adhered to the surface of the tangential wall facing the lumen (LU) and in the lumen. Note the shedding of the cell wall. **b** Cell debris in the lumen of the secretory canal. **c** Senescent cell showing large central vacuole (VA) and peripheral cytoplasm with reduced population of organelles: mitochondria (MI), plastids (PL), and rough endoplasmic reticulum (RER). Note the presence of multivesicular bodies near the vacuole. **d** Senescent cell showing large central vacuole (VA) and peripheral cytoplasm with reduced population of organelles: mitochondria (MI), plastids (PL), and dictyosomes (DI). Note the presence of membrane debris in the vacuole

histochemically identified in the secretion accumulated in the lumen of the phloem-associated canals, while neutral polysaccharides (Fig. 2f, l) and proteins (Fig. 2k) were present in the secretions of the medullary canals (Table 1).

Ultrastructure of the secretory canals

In each secretory canal, there were cells at all stages of the secretory cycle—"pre-secretory," "secretory," and "post-secretory." We will describe the subcellular organizations of the epithelial cells of these stages individually.

The secretory canals of the aboveground stems showed significant ultrastructural differences from the canals of the belowground stems. In the aboveground stems, the epithelial cells presented different sizes and shapes, mostly rounded, some more oval to tangentially elongated (Fig. 3a). The epithelial cells revealed a heterogeneous subcellular organization. Some cells had ultrastructures typical of active secretory cells, while others exhibited the characteristics of senescent cells (Fig. 3a).

Cells active in secretion presented convex faces towards the lumen, thin primary walls, plasma membranes with irregular contours, voluminous nuclei with evident nucleoli, and very dense cytoplasm (Fig. 3b). These cells contained free ribosomes, polyribosomes, mitochondria with developed cristae, and ellipsoid plastids in the cytoplasm with electron-opaque droplets and surrounded by a periplastid reticulum (Fig. 3c). The vacuoles were of different sizes and often had membranous contents. Plasmodesmata were present on the anticlinal walls, connecting with adjacent epithelial cells, and on the inner periclinal walls adjacent to the sheath (Fig. 3d). Well-developed dictyosomes with dilated cisternae, rough endoplasmic reticulum, and numerous vesicles were scattered throughout the cytoplasm, clearly characterizing the trans-Golgi network (Fig. 3e, f). Multivesicular bodies and vesicles were common in the peripheral cytoplasm close to the plasma membrane and close to, or within, the vacuoles (Fig. 3g). Electron-opaque droplets (saturated lipids), histochemically identified as oil droplets, occurred inside vacuoles and

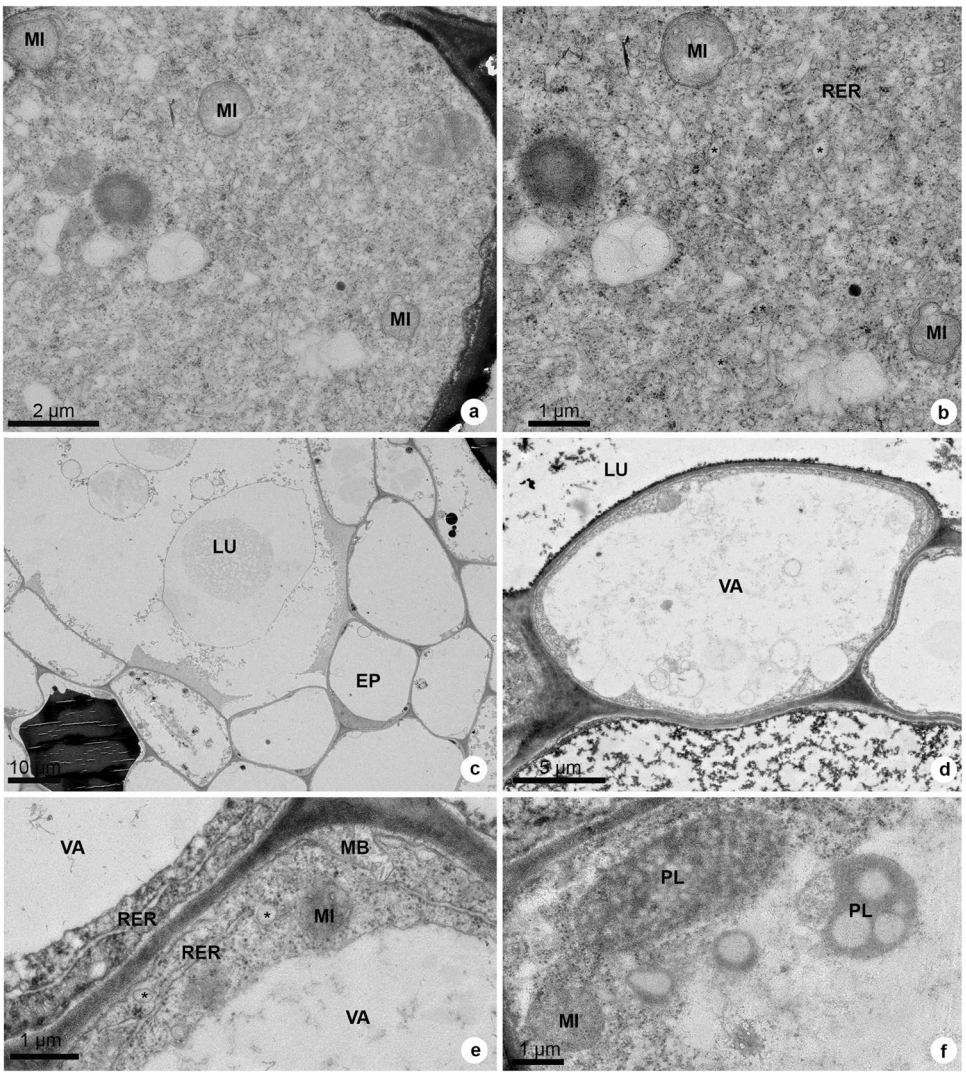

Fig. 6 Electron micrographs of epithelial cells from secretory canals of the belowground stem of *Anacardium humile*. **a** Secretion-active epithelial cell with organelle-poor cytoplasm. Mitochondria, MI. **b** Detail of the cytoplasm of an active epithelial cell in secretion with few organelles. Mitochondria, MI; rough endoplasmic reticulum (RER). **c** Mature canal with wide lumen (LU) and senescent secretory epithelium (EP) surrounded by a parenchymal sheath (SH). Note the elongated epithelial cells with large central vacuole. **d** Senescent epithelial cell with a large vacuole (VA) and cytoplasm reduced to a thin layer at the periphery of the cell. LU, lumen; SH, sheath. **e** Rounded epithelial cell with large vacuole (VA) and cytoplasm reduced to a thin layer at the periphery of the cell with mitochondria (MI). LU, lumen; SH, sheath. **f** Neighboring senescent epithelial cells showing mitochondria (MI) and cisternae of rough endoplasmic reticulum (RER). **g** Part of a senescent epithelial cell showing polymorphic plastids (PL) with electron-opaque droplets

dispersed in the peripheral cytoplasm (Fig. 4a, b). Strongly osmiophilic flocculated materials localized in the periplasmic space (Fig. 4c), in the middle lamella (Fig. 4d), and in the canal lumen (Fig. 4e) were common in these cells. The outer cell wall, tangential to the lumen of the secretory epithelium cells, appeared to be detached from the protoplast and with signs of progressive desquamation (Fig. 5a). Cell debris was observed in the lumens of the canals (Fig. 5b).

The senescent epithelial cells had large central vacuoles and peripheral cytoplasm. There was a decrease in the population of organelles. A few mitochondria, plastids, dictyosomes, and rough endoplasmic reticulum were observed (Fig. 5c). Multivesicular bodies were observed close to the vacuole (Fig. 5c), and there were remnants of membranes inside the vacuoles (Fig. 5d).

The active epithelial cells of the secretory canals of the belowground stem (Fig. 6a, b) presented a cytoplasm low in the numbers of organelles, with some mitochondria, rough endoplasmic reticulum, free ribosomes, and polyribosomes. Many vesicles were present (Fig. 6b).

In all samples analyzed, the vast majority of epithelial cells of the belowground stem secretory canals were senescent (Fig. 6c). The primary walls were thin, the central vacuoles were voluminous, and the cytoplasm was reduced to a thin layer at the periphery of the cell (Fig. 6d). Free ribosomes, rough endoplasmic reticulum, mitochondria (Fig. 6e), and polymorphic plastids with electron-opaque droplets (Fig. 6f) were present in the cytoplasm. Large numbers of multivesicular bodies were associated with the plasma membrane or inside the vacuole (Fig. 7a, b). Electron-opaque inclusions (histochemically identified as lipids) were present in the cytoplasm close to the plasma membrane and in the middle lamella (Fig. 7c). Strongly osmiophilic flocculated material in the canal lumen was common (Fig. 7b–d).

In the secretory canals of both the above- and the belowground stems, the parenchymal sheath cells (Fig. 8) were flattened, juxtaposed and with thin walls, with highly developed central vacuoles, and the cytoplasm greatly reduced with the chloroplasts and mitochondria. Some of

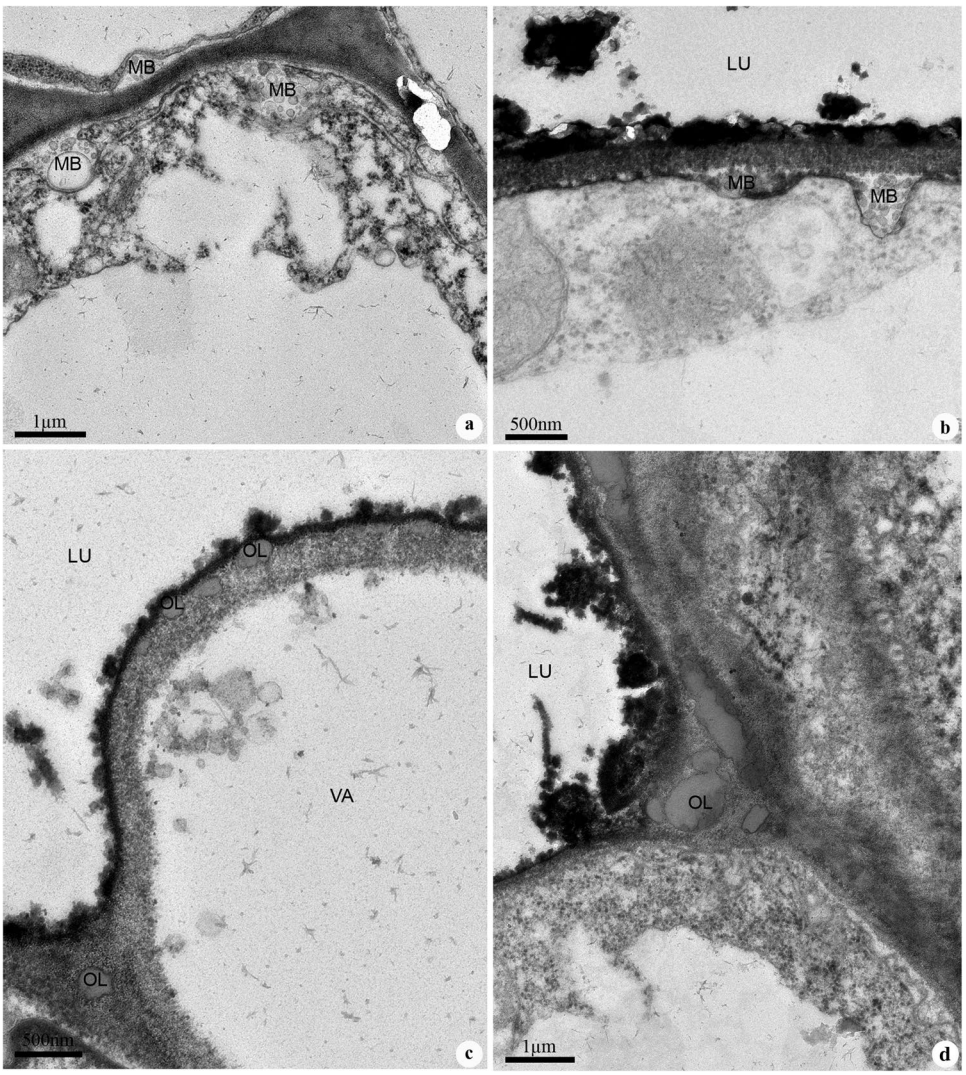

Fig. 7 Electron micrographs of epithelial cells from secretory canals of the belowground stem of *Anacardium humile*. **a** Neighboring epithelial cells showing multivesicular bodies (MB) juxtaposed to the plasma membrane. **b** Part of an epithelial cell showing multivesicular bodies (MB) juxtaposed to the plasma membrane. Note the dense material adhering to the lumen-facing tangential wall surface (LU). **c** Epithelial cell showing oil droplets (OL) close to the plasma membrane and in the middle lamella. **d** Epithelial cell detail showing oil droplets (OL) in the middle lamella and electron-dense flocculated material in the canal lumen (LU)

these cells had homogeneous and dense contents filling the entire vacuole, confirmed by histochemical tests as a phenolic substance (Fig. 8a–c).

In both the above- and belowground stems, acid phosphatase (AcPase) activity was detected in the cell walls of the epithelial cells (Fig. 9). Coarser deposits were present in the walls of the active secretory cells of both the above- (Fig. 9a) and belowground stems (Fig. 9b), while fine granular material was found in the walls of active cells of the belowground stems (Fig. 9b) and in senescent cells in both the above- (Fig. 9c) and belowground stems (Fig. 9d).

In the secretory canals of the aboveground stems (Fig. 10a–f), the ZIO method marked tubular portions of the rough endoplasmic reticulum (Fig. 10a) and the cisternae of the dictyosomes (Fig. 10a–d) in the epithelial cells. Dictyosomes consisted of five to seven stacked, flattened cisternae with dilated ends and associated vesicles (Fig. 10b, d). The reaction products were seen as electron-dense deposits in the lumen of the rough endoplasmic reticulum and cisternae of dictyosomes and in the vesicles that sprout from the dilated ends. Some dictyosomes were fully stained and in others only a few cisternae were stained (Fig. 10b). Cristae of some mitochondria were also stained (Fig. 10e). Vesicles with electron-dense material inside were scattered throughout the cytoplasm (Fig. 10f).

In the secretory canals of the belowground stem (Fig. 10g, h), the ZIO method evidenced the cisternae of dictyosomes and vesicles with osmiophilic content in the epithelial cells (Fig. 10g). The dictyosomes consisted of about five, well-flattened cisternae and had very reduced lumens (Fig. 10h). In the parenchymal sheath cells (Fig. 10i–l) of secretory canals of the above- and belowground stems, the ZIO method marked plastid thylakoids (Fig. 10i), dictyosomes (Fig. 10j), mitochondrial cristae (Fig. 10k), and vesicles with electron-dense material inside (Fig. 10l).

Discussion

Our study confirms that the secretory canals are present in both the above- and the belowground stems of *A. humile* and, moreover, that they share the same histological pattern and

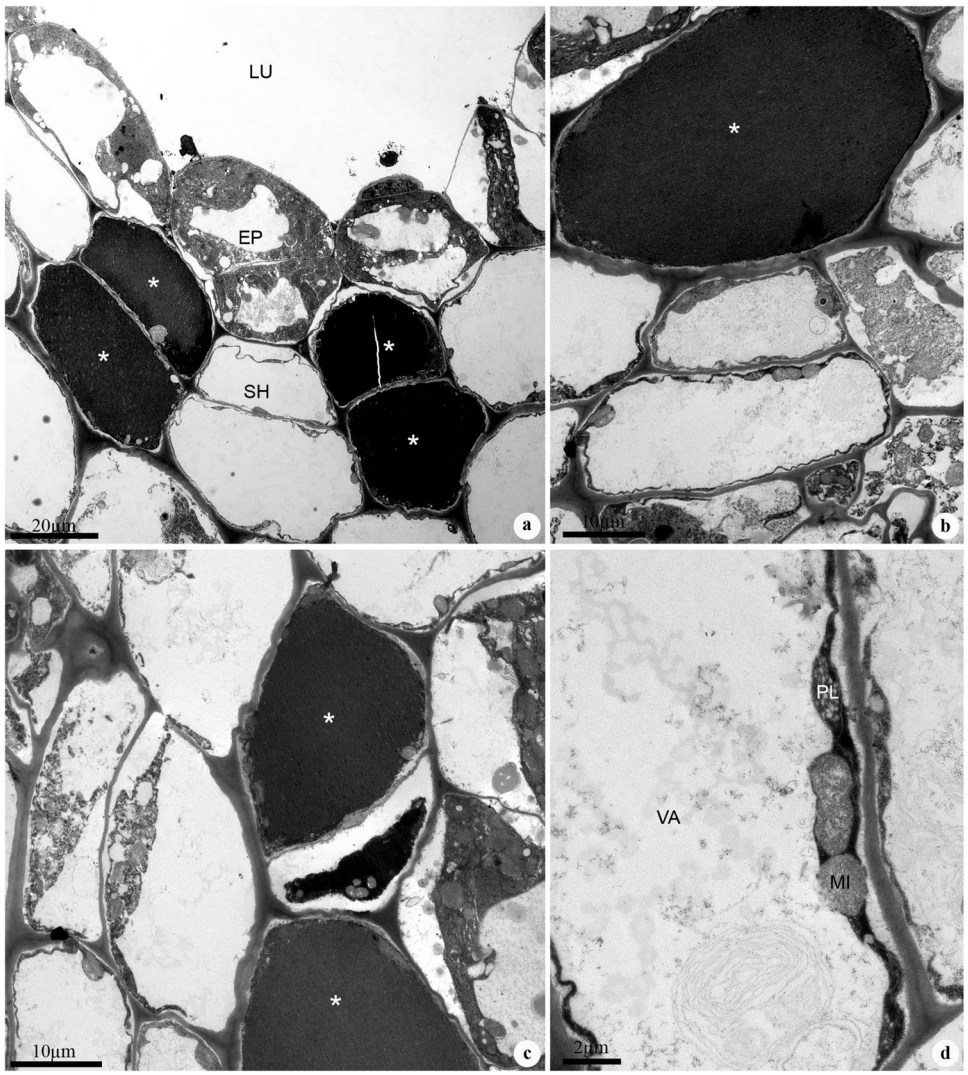

Fig. 8 Electron micrographs of parenchymal sheath cells of secretory canals of *Anacardium humile*. **a** Mature canal with wide lumen (LU) and secretory epithelium (EP) surrounded by a parenchymal sheath (SH). Note that some cells had homogeneous and dense content filling the entire vacuole (asterisks). **b** Detail of sheath cells showing flat, juxtaposed, thin-walled cells with a highly developed central vacuole and greatly reduced cytoplasm. Note that some cells had homogeneous and dense content filling the entire vacuole (asterisks). **c** Detail of sheath cells showing flat, juxtaposed, thin-walled cells with a highly developed central vacuole and greatly reduced cytoplasm. Note that some cells had homogeneous and dense content filling the entire vacuole (asterisks). **d** Part of a sheath cell showing a highly developed vacuole and peripheral cytoplasm with plastids (PL) and mitochondria (MI)

distribution. The occurrence of secretory canals associated with the phloem of the stem is a universal feature of the Anacardiaceae family (Metcalfe and Chalk 1950). Medullary canals are present in only a few genera of the Anacardiaceae such as in *Anacardium*, *Mangifera*, and *Schinus* (Venning 1948; Paviani 1965; Szabó 1971; Paula and Alves 1973; Carmello et al. 1995; Torres and Jauregui 1999; Sawidis et al. 2000; Tolke et al. 2021). Canals associated with the phloem originate from the procambium and appear early in the development of the shoot axis, while the medullary canals arise from the ground meristem and develop only after the formation of the phloem canals (Tolke et al. 2021). Thus, the absence of medullary canals at the shoot apex is associated with the ontogenetic origin of these structures in the medulla.

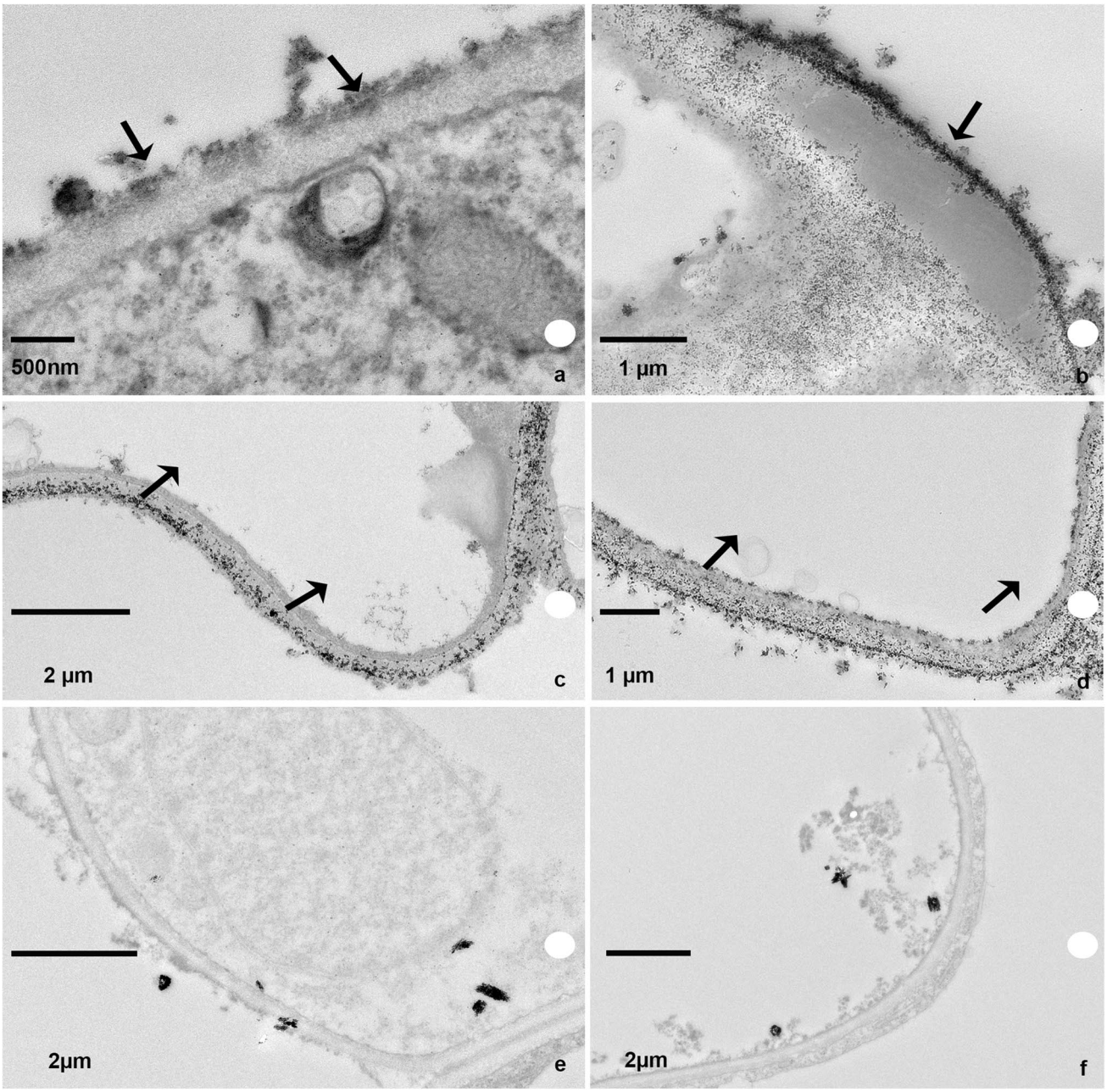

Fig. 9 Ultrastructural cytochemistry for acid phosphatase enzyme (arrows) in the cell wall (CW) of secreting active cells in the epithelium of above- (**a**) and belowground (**b**) stem canals of *Anacardium humile*. Also, senescent cells in the epithelium of above- (**c**) and belowground (**d**) stem canals and negative control (**e**, **f**). **a** Coarser deposits on the walls of active secretory cells. **b** Coarser deposits on the walls of active secretory cells. **c** Fine granular material on the walls of senescent cells. **d** Fine granular material on the walls of senescent cells. **e** Negative control in active cells. **f** Negative control in senescent cells

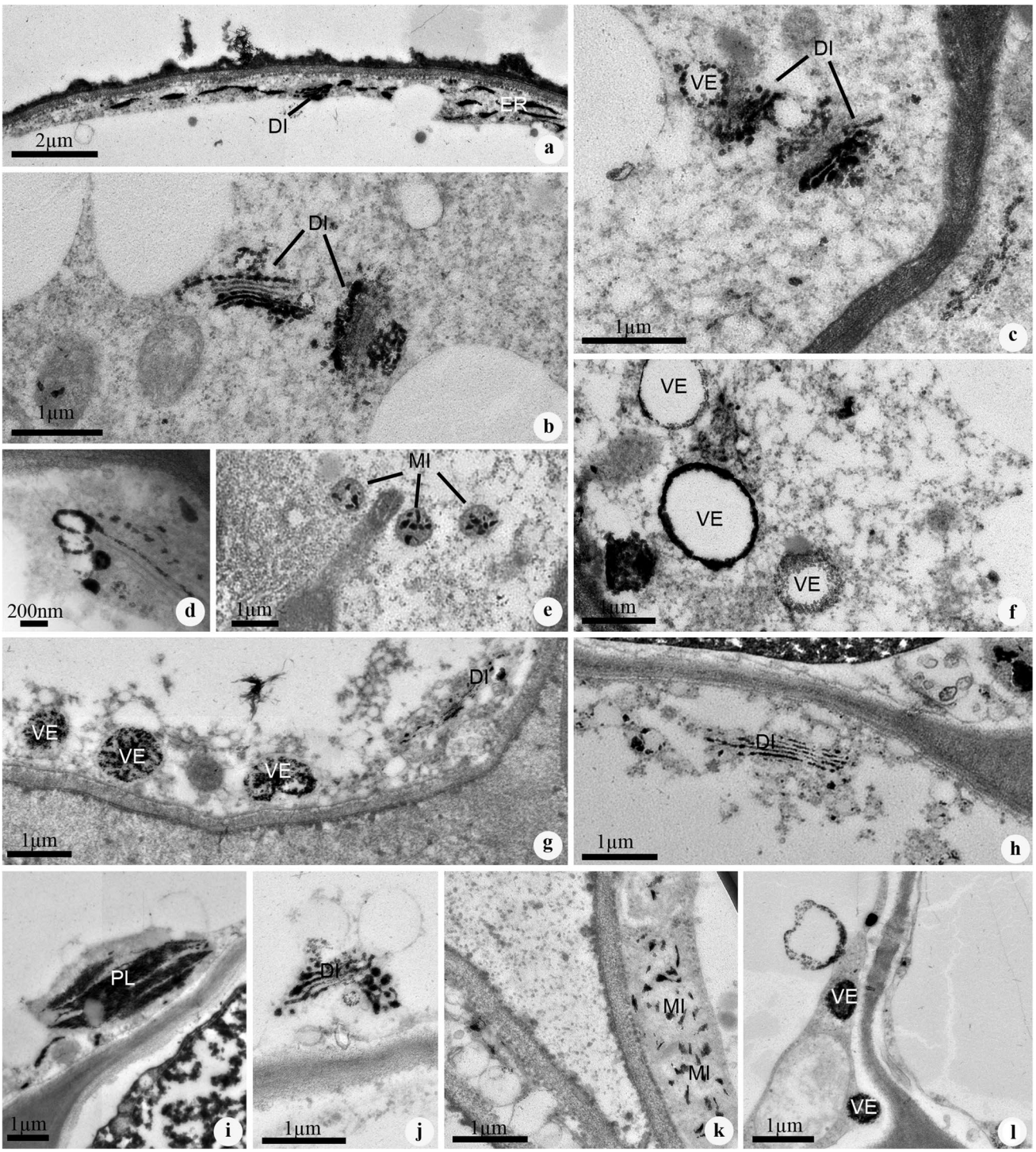

This comparative study of above- and belowground stems reveals that the secretory canals in the aboveground stem present epithelial cells with ultrastructural characteristics typical of cells active in secretion, while in the belowground stem, the subcellular characteristics of the epithelial cells are typical of those with low metabolic rates. These differences in epithelial cell characteristics are probably associated with the distinct above- and belowground environments, since the production of specialized metabolites is directly associated with aspects of radiation and temperature, both of which strongly affect photosynthesis by altering carbon fixation and carbon allocation for the synthesis of different macromolecules (Roshchina and Roshchina 1993; Juneja et al. 2013; Tresmondi et al. 2015, 2017). Rodrigues et al. (2014) observed the influences of light and temperature on the density of canals and secretory cavities in *Pterodon pubescens*

◂**Fig. 10** Electron micrographs (TEM) of epithelial cells of secretory canals of *Anacardium humile* aboveground stem (**a**–**f**) and belowground stem (g–h) and parenchymal sheath cells (**i**–**l**) processed according to the ZIO technique. **a** Detail of an epithelial cell, showing endoplasmic reticulum (ER) and dictyosomes (DI) impregnated with reaction product. **b** Detail of an epithelial cell showing deposits of reaction products in the external cisternae of the dictyosome (DI). **c** Detail of an epithelial cell showing deposits of reaction products in the external cisternae of the dictyosome (DI) and the vesicle (VE) attached to these cisternae. **d** Detail of a dictyosome in an epithelial cell showing deposits of reaction products in the flattened cisternae with enlarged ends. **e** Detail of an epithelial cell showing marked mitochondrial cristae. MI, mitochondria. **f** Vesicles with electron-dense material (VE) dispersed in the cytoplasm of epithelial cells. **g** Cisternae of dictyosomes (DI) and vesicles with osmiophilic content (VE) in epithelial cells. **h** Detail of a dictyosome (DI) in an epithelial cell showing deposits of reaction products in the flattened cisternae. **i** Detail of a sheath cell, showing plastid thylakoids impregnated with reaction products. **j** Detail of a dictyosome (DI) in cell sheath showing deposits of reaction products in the flattened cisternae. **k** Detail of a sheath cell showing marked mitochondrial cristae. MI, mitochondria. **l** Vesicles with osmiophilic content (VE) in the peripheral cytoplasm of the sheath cell

and on the ultrastructure of its epithelial cells. Tresmondi et al. (2015, 2017) also observed differences in ultrastructural characteristics and secretion in colleters of Rubiaceae exposed to different environmental conditions.

The presence of secretory cells of different sizes, shapes, and ultrastructural organizations in the same epithelium of canals of the aboveground stems of *A. humile* contrasts with the uniformity of these characteristics in the secretory canals of the belowground stems. Differences in the characteristics of the secretory cells in the same epithelium have been related to the functional stages of these cells, as already reported in the secretory canals of a number of species of Anacardiaceae (Machado and Carmello-Guerreiro 2001; Lacchia and Carmello-Guerreiro 2009; Tolke et al. 2021).

The results of our histochemical tests reveal that the chemical compositions of the secretions stored in the lumens of the secretory canals of the above- and belowground stems do not differ. In the phloem canals, the secretions are heterogeneous, being constituted by both hydrophilic components (phenolic substances, proteins, and polysaccharides) and lipophilic components (total lipids and terpenoids). However, the secretions of the medullary canals are homogeneous, being composed only of hydrophilic substances (polysaccharides and proteins). The compartmentalization of the secretions observed in the stems of *A. humile* (i.e., with resin production only in the phloem canals) indicates a high degree of specialization of these secretory canals. Differential compositions of secretions produced in secretory canals and cavities have been reported in the vegetative axes of *Copaifera langsdorffii* (Leguminosae) (Rodrigues et al. 2011a, b). However, our results differ from this study, since in *A. humile*, secretory canals occur only in the stem phloem and pith. Factors related to gene regulation of synthesis, metabolism, and terpene compartmentalization should be considered (Zhao et al. 2018; Huang and Osbourn 2019), in addition to the location of these secretory structures adjacent to the phloem, which is the tissue responsible for the transport of the precursors that will form part of the secretion. The subcellular apparatus of the epithelial cells of the phloem secretory canals of the aboveground stem of *A. humile* in the secretory stage is consistent with the production of the polysaccharides and proteins in addition to the lipid substances that we confirmed through histochemical testing. It suggests the secretion of gum resins, as already reported in a number of Anacardiaceae species (Nair et al. 1983; Bhatt and Ram 1992; Tolke et al. 2021). The occurrence of dictyosomes with abundant vesicles, rough endoplasmic reticulum, and ribosomes indicates the production of hydrophilic substances such as polysaccharides and proteins, while the presence of oil droplets dispersed in the cytoplasm and in the matrix of modified plastids is consistent with the synthesis of lipophilic substances (Fahn 1979; Evert 2006). Our results show plastids devoid of inner membranes, with lipid droplets in the matrix, surrounded by periplastid endoplasmic reticulum. According to Cheniclet and Carde (1985), the structure of plastids is directly related to the synthesis of monoterpenes. Cells with typical leucoplasts characterized as plastids lacking ribosomes, thylakoids, and an internal membrane system produce significant amounts of monoterpenes (Cheniclet and Carde 1985). The occurrence of periplastid endoplasmic reticulum may be associated with the transport of oil droplets from the plastid to the peripheral cytoplasm and to lumen of the canal (Bhatt and Ram 1992; Rodrigues et al. 2011a, b).

The presence of dictyosomes, ribosomes, and polyribosomes is also related to the synthesis and elimination of enzymes (Machado and Carmello-Guerreiro 2001; Paiva and Machado 2007; Rodrigues et al. 2011a, b). These enzymes may be involved in the degradation of the cell wall and its desquamation on the side facing the lumen (Rodrigues and Machado 2012). A considerable number of enzymes are associated with the cell walls in plants, performing important biological functions related to the synthesis and modification of wall components, the transport of various metabolites, and defense mechanisms (Hasegawa et al. 1976; Bozzo et al. 2002; Kaida et al. 2008). Some cytochemical studies consider the observation of electron-dense insoluble reaction products is a reliable indicator of localization of acid phosphatase activity (Machado and Rodrigues 2019). Acid phosphatase (AcPase) activity in the cell wall was confirmed by ultrastructural cytochemistry. Acid phosphatase (AcPase) is a lysosomal enzyme found widely in animals and plants, capable of hydrolyzing organic phosphate esters in a wide range of substrates at an acidic pH (Han et al. 2020).

The presence of mitochondria with developed cristae is a result of the high rate of ATP synthesis required for the production of gum resin (Bhatt and Ram 1992).

As observed for the cavities of *Pterodon pubescens* (Rodrigues and Machado 2012), our results suggest secretion release into the canal lumens of *A. humile* involves holocrine,

eccrine, and granulocrine mechanisms. Cellular debris was observed in the canal lumens, indicating that epithelial cells separate from the adjacent ones (desquamation) and are released into the lumen, culminating in the secretion of holocrine substances. Bhatt and Ram (1992) observed free cells in the lumens of *Semecarpus anacardium* secretory canals and associated these cells with holocrine secretion. Machado and Carmello-Guerreiro (2001) also observed epithelial cells being released into the lumens of secretory canals in *Schinus terebinthifolius* fruits and associated them with the addition of materials to the secretion and also with the enlargement of the cavity. Turner et al. (1998) also observed cellular debris in the lumen of the duct but interpreted this as an artifact. Lipid drops close to the plasma membrane suggest an eccrine secretion process (Rodrigues and Machado 2012). Vesicles and multivesicular bodies in the peripheral cytoplasm or juxtaposed to the plasma membrane are evidence of a granulocrine process of secretion (Fahn 1979). The presence of membranous material in the vacuole, observed in the epithelial cells of the secretory canals of the aboveground stems, suggests organelle degradation has characteristics of microautophagy, as discussed in van Doorn and Papini (2013).

In all the belowground stem canal samples, the vacuoles of most epithelial cells become very developed, while their cytoplasm is reduced to a peripheral film, poor in organelles, and with signs of low secretory activity (Rodrigues et al. 2014). The cisternae of the dictyosomes are much reduced compared with those in the epithelial cells of the aboveground stem canals, in which the cisternae are well developed with dilated ends from which vesicles sprout.

The presence of a sheath of cells with meristematic characteristics, surrounding the secretory canals of the above- and the belowground stems of *A. humile*, has been interpreted as responsible for the renewal of the secretory epithelium. This process maintains secretory activity during stem development, suggesting these canals remain active in secretion for a long time (Rodrigues et al. 2014). The presence of a sheath with meristematic characteristics in secretory canals has been described in secretory canals and cavities of a number of other plant species (Machado and Carmello-Guerreiro 2001; Lacchia and Carmello-Guerreiro (2009); Rodrigues et al. 2011a,b; Machado et al. 2017; Palermo et al. 2018; Tolke et al. 2021).

The results discussed above stress the usefulness of combining both light and transmission electron microscopy, along with a range of techniques of ultrastructural cytochemistry in elucidating the functions of secretory canals under differing environmental conditions. Transmission electron microscopy, in combination with cytochemical methods (Fakan 2004), represents an important tool for analysis of the structure–function relationships of secretory systems in plants.

Our results show that particularities in above- and belowground environment have significant implications for ultrastructural morphology and functioning of secretory canals in the stems of *A. humile*. This study opens new perspectives to explore all possible combinations of above- and belowground interactions and their implications for the development of the secretory system of plants that have complex stem systems.

Acknowledgements We thank the technical team of the Electron Microscopy Center (CME), Institute of Biosciences of Botucatu (IBB), São Paulo State University (UNESP), for their assistance in preparing the samples.

Author contribution The study was conceived and designed by SFC and SRM. The experiments were performed by SFC and ELS. The data were analyzed by SFC, ELS, DCS, and SRM. The article was designed and written by SFC and SRM. All authors read and approved the final version of the manuscript.

Funding This work was supported by the Fundação de Amparo à Pesquisa do Estado de São Paulo (FAPESP 2019/19916–1). SR Machado receives a research grant from the National Council for Development and Research (CNPq), process 308982/2020–7.

Data availability The authors made the data transparently available to readers.

Code availability Not used in this work.

Declarations

Ethics approval This work is exempt from ethical approval.

Consent to participate The authors declared that they freely consented to participate in this work.

Consent for publication The authors declared that they freely consented to publish this work.

Conflict of interest The authors declare no competing interests.

References

Agostini-Costa TS, Faria JP, Naves RV, Vieira RF (2016) *Anacardium* spp. In: Vieira RF, Camilo J, Coradin L (ed) Espécies nativas da flora brasileira de valor econômico atual ou potencial; Plantas para o Futuro: Região Centro-Oeste. Ministério da Agricultura, Brasília/DF, pp 138–149

Bardgett RD, van der Putten WH (2014) Belowground biodiversity and ecosystem functioning. Nature 515:505–511. https://doi.org/10.1038/nature13855

Barreiro DP, Machado SR (2007) Coléteres dendróides em *Alibertia sessilis* (Vell.) K. Schum., uma espécie não-nodulada de Rubiaceae. Rev Bras Bot 30:387–399

BFG (2015) Growing knowledge: an overview of seed plant diversity in Brazil. Rodriguésia 66:1085–1113. https://doi.org/10.1590/2175-7860201566411

Bhatt JR, Ram H (1992) Development and ultrastructure of primary secretory ducts in the stem of *Semecarpus anacardium* (Anacardiaceae). IAWA J 13:173–185

Bozzo GG, Raghothama GK, Plaxton WC (2002) Purification and characterization of two secreted purple acid phosphatase isozymes from phosphate-starved tomato (*Lycopersicon esculentum*) cell cultures. Eur J Biochem 269:6278–6286. https://doi.org/10.1046/j.1432-1033.2002.03347.x

Carmello SM, Machado SR, Gregório EA (1995) Ultrastructural aspects of the secretory duct development in *Lithraea molleoides* (Vell.) Engl. (Anacardiaceae). Rev Bras Bot 18:95–103

Carvalho JM (2020) Cauim, slow food. Disponível em https://www.slowfood.com. Acesso em 05 de maio de 2022.

Cheniclet C, Carde JP (1985) Presence of leucoplasts in secretory cells and of monoterpenes in the essential oil: a correlative study. Isr J Plant Sci 34:219–238

Cota LG, Moreira PA, Brandão MM, Royo VA, Melo Junior AF, Menezes EV, Oliveira DA (2017) Structure and genetic diversity of *Anacardium humile* (Anacardiaceae): a tropical shrub. Genet Mol Res (Online) 16(3):gmr16039778

Coutinho LM (1982) Ecological effect of fire in Brazilian cerrado. In: Huntley BJ, Walker BH (eds) Ecology of tropical savannas. Springer-Verlag, Berlin

David R, Carde JP (1964) Coloration differentielle dês inclusions lipidique et terpeniques des pseudophylles du pine maritime au moyen du reactif Nadi. C R Acad Sci Paris, Série D 257:1338–1340

Del Valle JC, Buidea ML, Whittal JB, Narbona E (2018) Phenotypic plasticity in light-induced flavonoids varies among tissues in *Silene littorea* (Caryophyllaceae). Environ Exp Bot 153:100–107

Dickison WC (2000) Integrative plant anatomy. Academic, San Diego

Eiten G (1982) Brazilian "savannas." In: Huntley BJ, Walker BH (eds) Ecology of tropical savannas. Springer-Verlag, Berlin

Evert RF (2006) Esau's plant anatomy; meristems, cells and tissues of the plant body their structure, function and development. Wiley-Interscience, New York

Fahn A (1979) Secretory tissues in plants. Academic Press, London

Fahn A, Evert RF (1974) Ultrastructure of secretory ducts of *Rhus glabra* L. Am J Bot 61:1–14

Fakan S (2004) Ultrastructural cytochemical analyses of nuclear functional architecture. Eur J Histochem 48:5–14

Gibson AC (1981) Vegetative anatomy of *Pachycormus* (Anacardiaceae). Bot J Linn Soc 83:273–284

Han Y, Quan K, Chen J, Qiu H (2020) Advances and prospects on acid phosphatase biosensor. Biosens Bioelectron 170:112671. https://doi.org/10.1016/j.bios.2020.112671

Hasegawa Y, Lynn KR, Brockba WJ (1976) Isolation and partial characterization of cytoplasmic and wall-bound acid phosphatases from wheat roots. Can J Bot 54.https://doi.org/10.1139/b76-125

Huang AC, Osbourn A (2019) Plant terpenes that mediate belowground interactions: prospects for bioengineering terpenoids for plant protection. Pest Manag Sci 75:2368–2377

Jensen WA (1962) Botanical histochemistry: principles and practice. W. H, Freeman, San Francisco

Joel DM, Fahn A (1980a) Ultrastructure of the resin ducts of *Mangifera indica* L. (Anacardiaceae). 1. Differentiation and senescence of the shoot ducts. Ann Bot 46:225–233

Joel DM, Fahn A (1980b) Ultrastructure of the resin ducts of *Mangifera indica* L. (Anacardiaceae). 2. Resin secretion in the primary stem ducts. Ann Bot 46:779–783

Joel DM, Fahn A (1980c) Ultrastructure of resin ducts of *Mangifera indica* L. (Anacardiaceae). III. Secretion of protein-polysaccharide mucilage in fruit. Ann Bot 46:785–790

Johansen DA (1940) Plant microtechnique. McGraw-Hill, New York

Judd WS, Campbell CS, Kellogg EA, Stevens PF, Donoghue MJ (2007) Plant systematics: a phylogenetic approach. Sinauer associates Inc, Massachussets

Juneja A, Ceballos RM, Murthy GS (2013) Effects of environmental factors and nutrient availability on the biochemical composition of algae for biofuels production: a review. Energies 6:4607–4638. https://doi.org/10.3390/en6094607

Kaida R, Hayashi T, Kaneko TS (2008) Purple acid phosphatase in the walls of tobacco cells. Phytochemistry 69:2546–2551. https://doi.org/10.1016/j.phytochem.2008.07.008

Lacchia APS, Carmello-Guerreiro SM (2009) Aspectos ultra-estruturais dos canais secretores em órgãos vegetativos e reprodutivos de Anacardiaceae. Acta Bot Bras 23:376–388

Machado SR, Carmello-Guerreiro SM (2001) Estrutura e desenvolvimento de canais secretores em frutos de *Schinus terebinthifolius* Raddi (Anacardiaceae). Acta Bot Bras 15:189–195

Machado SR, Rodrigues TM (2019) Autophagy and vacuolar biogenesis during the nectary development. Planta 250:519–533. https://doi.org/10.1007/s00425-019-03190-7

Machado SR, Canaveze Y, Rodrigues TM (2017) Structure and functioning of oil cavities in the shoot apex of *Metrodorea nigra* A. St.-Hil. (Rutaceae). Protoplasma 254:1661–1674

Mazia D, Brewer PA, Alfert M (1953) The cytochemistry staning and measurement of protein with mercuric bromofenol blue. Bio Bull 104:57–67

Mcmanus JFA (1948) Histological and histochemical uses of periodic acid. Stain Technol 23:99–108

Metcalfe CR, Chalk L (1950) Anatomy of the dicotyledons: leaves, stem, and wood in relation to taxonomy, vol II. Claredon, Oxford

Nair GM, Venkaiah K, Shah JJ (1983) Ultrastructure of gumresin ducts in cashew (*Anacardium occidentale*). Ann Bot 51:297–305

O'Brien T, Feder N, Mccully M (1964) Polychromatic staining of plant cell walls by toluidine blue. Protoplasma 59:368–373

Paiva EAS, Machado SR (2007) Structural and ultrastructural aspects of ontogenesis and differentiation of resin secretory cavities in *Hymenaea stigonocarpa* (Fabaceae -Caesalpinioideae) leaves. Nord J Bot 24:423–431

Palermo FH, Rodrigues MIA, De Nicolai J, Machado SR, Rodrigues TM (2018) Resin secretory canals in *Protium heptaphyllum* (Aubl.) Marchand. (Burseraceae): a tridimensional branched and anastomosed system. Protoplasma 255:899–910

Paula JE, Alves JLH (1973) Anatomia de *Anacardium spruceanum* Benth. ex Engl. (Anacardiaceae da Amazônia). Acta Amaz 3:39–53

Paviani TI (1965) Contribuição ao conhecimento do gênero *Schinus* L. Anatomia de quatro espécies e uma variedade. Rev Fac Farm Bioquim St Maria 11:91–110

Pell SK, Mitchell JD, Miller AJ, Lobova TA (2011) Anacardiaceae. In: Kubitzki K (ed) The families and genera of vascular plants. Flowering plants. Eudicots. Sapindales, Curcubitales, Myrtales. Springer, Berlin, vol X

Pino RM, Pino LC, Bankston PW (1981) The relationships between the Golgi apparatus, GERL, and lysosomes of fetal rat liver Kupffer cells examined by ultrastructural phosphatase cytochemistry. J Histochem Cytochem 29:1061–1070

Pizzolato TD, Lillie RD (1973) Mayer's tannic acid ferric chloride stain for mucins. J Histochem Cytochem 21:56–64

Reinecke M, Walther C (1978) Aspects of turnover and biogenesis of synaptic vesicles at locust neuromuscular junctions as reveled by iodide-osmium tetroxide (ZIO) reacting with intravesicular sh-groups. J Cell Biol 21:839–855

Reynolds ES (1963) The use of lead citrate at high pH as an electron-opaque stain in electron microscopy. J Cell Biol 17:208–212

Rodrigues TM, Machado SR (2012) Oil glands in *Pterodon pubescens* Benth. (Leguminosae-Papilionoideae): distribution, structure, and secretion mechanisms. Int J Plant Sci 173:984–992

Rodrigues TM, Teixeira SP, Machado SR (2011) The oleoresin secretory system in seedlings and adult plants of copaíba (*Copaifera langsdorffii* Desf., Leguminosae-Caesalpinioideae). Flora 206:585–594

Rodrigues TM, Santos DC, Machado SR (2011) The role of the parenchyma sheath and PCD during the development of oil cavities in *Pterodon pubescens* (Leguminosae-Papilionoideae). C R Biol 334:535–543

Rodrigues, TM, Buarque, PFSM, Coneglian AG, Reis DC (2014) Light and temperature induce variations in the density and ultrastructure of the secretory spaces in the diesel-tree (*Copaifera langsdorffii* Desf.-Leguminosae) Trees 28:613–623. https://doi.org/10.1007/s00468-013-0976-8

Roshchina VV, Roshchina VD (1993) The excretory function of higher plants. Springer, Berlin

Royo VA, Mercadante-Simões MO, Ribeiro LM, Oliveira DA, Aguiar MMR, Costa ER, Ferreira PRB (2015) Anatomy, histochemistry, and antifungal activity of *Anacardium humile* (Anacardiaceae) leaf. Microsc Microanal Microstruct 21:1549–1561

Sawidis T, Dafnis S, Weryzko-Chmielewska E (2000) Distribution, development and structure of resin ducts in *Pistacia lentiscus* var. chia Duhamel. Flora 195:83–94

Souza VC, Lorenzi H (2005) Botânica sistemática: guia ilustrado para identificação das famílias de angiospermas da flora brasileira, baseado em APG II. Instituto Plantarum, Nova Odessa/SP, pp 432–434

Szabó L (1971) Development of balsam canals and the localization of tannin in some organs of Sumac (*Cotinus coggygria* Scop.). Agrobotanika 11:219–233

Tolke ED, Lacchia APS, Lima EA, Demarco D, Ascensão L, Carmello-Guerreiro SM (2021) Secretory ducts in Anacardiaceae revisited: updated concepts and new findings based on histochemical evidence. S Afr J Bot 138:394–405

Torres M, Jauregui D (1999) Caracterizacion anatomica foliar de cuatro especies de arboles frutales: *Anacardium occidentale* L. (merey), *Mangifera indica* L. (mango), *Spondias purpurea* L. (ciruela de huesito) y *Psidium guajava* L. (guayaba). Ernstia 9:155–173

Tresmondi F, Nogueira A, Guimarães E, Machado SR (2015) Morphology, secretion composition, and ecological aspects of stipular colleters in Rubiaceae species from tropical forest and savanna. Naturwissenschaften 102(11–12):73. https://doi.org/10.1007/s00114-015-1320-5

Tresmondi F, Canaveze Y, Guimarães E, Machado SR (2017) Colleters in Rubiaceae from forest and savanna: the link between secretion and environment. Sci Nat 104:17. https://doi.org/10.1007/s00114-017-1444-x

Turner GW, Lange BM, Gifford EM (1998) Schizogenous secretory cavities of *Citrus union* (L.) Burm. F. and a re-evaluation of the lysigenous gland concept. Int J Plant Sci 159:75–88

van der Putten WH et al (2009) Empirical and theoretical challenges in aboveground–belowground ecology. Oecologia 161:11–14. https://doi.org/10.1007/s00442-009-1351-8

van Doorn WG, Papini A (2013) Ultrastructure of autophagy in plant cells: a review. Autophagy 9:1922–1936

Vassilyev AE (2000) Quantitative ultrastructural data of secretory duct epithelial cells in *Rhus toxicodendron*. Int J Plant Sci 161:615–630

Venkaiah K (1992) Development, ultrastructure and secretion of gum ducts in *Lannea coromandelica* (Houtt.) Merrill (Anacardiaceae). Ann Bot 69:449–457

Venning FD (1948) The ontogeny of the laticiferous canals in the Anacardiaceae. Am J Bot 35:637–644

Zhao R, Lu L, Shi Q, Chen J, He Y (2018) Volatile terpenes and terpenoids from workers and queens of *Monomorium chinense* (Hymenoptera: Formicidae). Molecules 23:2838

Identification and characterization of autophagy in resin secretory canals

Shelly F. de Carvalho [1,2*], Elton L. Scudeler[3], Daniela C. dos Santos[1,4] and Silvia R. Machado [1,2*]

1 Electron Microscopy Center (CME), Institute of Biosciences of Botucatu (IBB), São Paulo State University (UNESP), Botucatu, SP, Brazil; shelly.favorito@unesp.br
2 Department of Biostatistics, Plant Biology, Parasitology and Zoology, Institute of Biosciences of Botucatu (IBB), São Paulo State University (UNESP), Botucatu, SP, Brazil; silvia.machado@unesp.br
3 Department of General and Applied Biology, Institute of Biosciences, São Paulo State University (UNESP), Rio Claro, SP, Brazil; elton.scudeler@unesp.br
4 Department of Structural and Functional Biology, Botucatu Institute of Biosciences (IBB), São Paulo State University (UNESP), Botucatu, SP, Brazil; daniela.santos@unesp.br

* Corresponding author: Electron Microscopy Center (CME), Institute of Biosciences of Botucatu (IBB), São Paulo State University (UNESP), CEP: 18618-689, Brazil. Tel.: + 55 14 38800715. E-mail: silvia.machado@unesp.br

Abstract

Autophagy is a highly conserved cellular process for the degradation of cytoplasmic organelles and proteins in eukaryotes. In plants, autophagy can be classified into macroautophagy and microautophagy, as well as into several less-studied types such as selective autophagy and mega-autophagy. Recent studies show that autophagy is involved in a number of processes of plant development and to plant stress responses, being essential for the maintenance of cellular homeostasis. The occurrence and types of autophagy in the development of secretory structures have not been much studied. In this study, to better understand the implications of autophagy in the development and functioning of resin-secreting canals, we investigated the occurrence and characterized the types of autophagy in the secretion canals using *Anacardium humile* A.-St. Hil as a model. Our results show the occurrence of macroautophagy and microautophagy in epithelial cells of the resin-secreting canals in *A. humile*. Using immunolocalization methods for autophagosomes in confocal microscopy associated with ultrastructural cytochemistry, we clearly identified the autophagic process. We also describe in detail the structures related to autophagy at an ultrastructural level. This study highlights the role of autophagy in the development of resin-secreting canals under normal developmental conditions.

Keywords: autophagy, immunohistochemistry, macroautophagy, microautophagy, secretory canals, ultrastructure.

Abbreviations:

AcPase: acid phosphatase activity

ATG: proteins related to autophagy

AVi: initial autophagic vacuole

MVB: multivesicular bodies

PBS: phosphate buffered saline

PCD: programmed cell death

RER: rough endoplasmic reticulum

SER: smooth endoplasmic reticulum

ZIO: method zinc iodide - osmium tetroxide

Introduction

The recycling of cellular components is essential for the survival and growth of many organisms (Wang et al. 2020). Plants have developed sophisticated recycling mechanisms for their cellular constituents (Marshall and Vierstra 2018) and these include autophagy. In this catabolic process, cytoplasmic constituents are degraded in lytic organelles (lysosomes in animals and fungi, or vacuoles in plants) and the products of this degradation are returned to the cytoplasm to be reused (Contento et al. 2005; Bassham 2007; Avin-Wittenberg et al. 2012; Bozhkov 2018; Soto-Burgos et al. 2018). Autophagy is essential for maintaining cellular homeostasis, contributing to various plant developmental processes and stress responses such as to nutrient restriction and infection (Sienko et al. 2020; Mahood 2021; Magen et al. 2022).

In plants, autophagy is often divided into two main types: microautophagy and macroautophagy (Mitou et al. 2009; Van Doorn and Papini 2013). In microautophagy, a small, single-membrane vesicle is formed through the invagination of the vacuolar membrane enclosing cytosolic components. Microautophagy is involved in the accumulation and storage of proteins and lipids, the degradation of starch grains, leaf senescence, the accumulation of anthocyanins, the development and germination of seeds and in pre-secretory stage of nectaries in epidermal cells (Bassham et al. 2006; Chanoca et al. 2015; Soto-Burgos et al. 2018; Wang et al. 2018; Machado and Rodrigues 2019). Macroautophagy, is simply referred to as autophagy and is the most-studied form in plants. Although what occurs is similar to that in animal cells, it has its own characteristics (Papini et al. 2014). It is characterised by the engulfment of cytoplasmic contents and organelles in double-membrane vesicles called autophagosomes or autophagic vesicles (Yoshimoto et al. 2014; Soto-Burgos et al. 2018; Zhang et al. 2018). Macroautophagy involves several steps, including the formation and expansion of phagophores and their closure directed towards autophagosome formation and, finally, their fusion with the vacuole (Wojciechowska et al. 2021). During this process, the autophagosome engulfs and transports material to the vacuole. Then, the outer membrane of the autophagosome fuses with the tonoplast and the inner membrane and the material it contains are released into the lumen of the vacuole where degradation by resident hydrolases takes place (Yoshimoto et al. 2009; Zhuang et al. 2013). Degraded products are transported back to the cytoplasm, where they are reused (Yang and Bassham 2015). Alternatively, autophagosomes can transform into acidic and lytic lysosome-like structures, and the fusion with the vacuole occurs as a secondary event (Wang et al. 2018). Autophagosomes

undergo a progressive maturation process by interacting with multivesicular bodies (MVBs) and/or late endosomes to generate intermediate/hybrid compartments called amphisomes, which are at the intersection of autophagous and endocytic pathways (Ganesan and Cai 2021). In plants, recent work suggests the endoplasmic reticulum is the source of membranes and signalling for autophagosomal biogenesis (Zhuang et al. 2018). Additional types of autophagy have been described in plants (Van Doorn and Papini 2013): selective autophagy, when partial degradation of the cytoplasm and/or specific organelles (plastids, mitochondria) occurs while still in the cytoplasm, and mega-autophagy, when the membrane of the vacuole ruptures and releases hydrolases into the cytoplasm, completely degrading it and, hence, resulting in cell death. This is commonly interpreted as a type of programmed cell death (PCD). These two types of autophagy remain little studied, especially in respect to the molecular mechanisms associated with each (Yoshimoto and Ohsumi 2018).

Advances in research into autophagy in plants have been made possible through the use of multiple techniques including transmission electron microscopy (Van Doorn and Papini 2013), ultrastructural cytochemistry (Cai et al. 2009; Machado and Rodrigues 2019) and fluorescence microscopy using specific markers (Yoshimoto and Ohsumi 2018; Zhang et al. 2018).

Transmission electron microscopy was one of the first tools used to characterize autophagy, and it is still one of the most reliable methods for monitoring autophagy in cells and tissues in nanoscale (Mitou et al. 2009; Zheng et al. 2018; Zhang et al. 2018; Machado and Rodrigues 2019). In addition, the use of ultrastructural cytochemistry for membrane impregnation and acid phosphatase localization brings a more objective and reliable interpretation of this process (Machado and Rodrigues 2019).

More than 40 proteins related to autophagy (ATG) are known, among these is ATG8 (Magen et al. 2022). This is a useful marker protein for the study of autophagy, since it is located both in the inner and outer membranes of autophagosomes. Furthermore, ATG8 plays a unique role during selective autophagy, in which cargo recognition is performed by receptors that also recognise ATG8 on the autophagosomal membrane (Magen et al. 2022). ATG8 is an important marker of the autophagic process and the use of immunolocalization techniques in confocal microscopy is complementary technique for detecting autophagy (Mitou et al. 2009).

The participation of autophagy in normal plant development processes, such as the differentiation of tracheal elements, in leaf senescence (Kwon et al. 2010) and in the

differentiation of reproductive structures (Haddad et al. 2019) is well known. On the other hand, little is known of the occurrence of autophagy and its implications for the development of secretory structures (Zhang et al. 2018; Machado and Rodrigues 2019). Zhang et al. (2018) identified and described in detail the autophagic process during the development of non-articulated laticifers of *Euphorbia kansui*, also confirming the presence of autophagosomes, autolysosomes and lysosome-like structures. Machado and Rodrigues (2019) reported three types of autophagy during the development of the extrafloral nectary of *Citharexylum myrianthum*, two of these - macroautophagy and microautophagy – are associated with the biogenesis of vacuoles in the pre-secretory stage, whereas mega-autophagy is associated with cell death and is restricted to the post-secretory stage.

The occurrence of resin-secreting canals is a striking feature in Anacardiaceae (Pell et al. 2011; Royo et al. 2015), and constitutes a resin production site of great commercial importance in this family (Pickel 2008). Microscope studies over recent decades have contributed considerably to our knowledge of the formation, development and functioning of the resin-bearing canals/cavities in Anacardiaceae and other families (Fahn and Evert 1974; Nair et al. 1983; Machado and Carmello-Guerreiro 2001; Lacchia and Carmello-Guerreiro 2009). Although morphological evidence of autophagy can be detected, such aspects were not adequately explored or even mentioned in these studies. Precise knowledge of when, in which tissues and under what conditions autophagy is activated is important to our understanding of the physiological functions of autophagy in plants (Yoshimoto and Ohsumi 2018).

To better understand the implications of autophagy in the development and functioning of these resin-secreting canals, this study investigates the occurrence and characterises the types of autophagy in the secretion canals of *Anacardium humile* A.-St. Hil., a species of Anacardiaceae native to the Cerrado.

Material and methods

The studies were carried out on specimens of *Anacardium humile* vegetating in a native population existing in the Cerrado in the municipalities of Botucatu (22°57'17”S, 48°26'6”W) and Pratânia (22°49'14”S, 48° 44'56”W), state of São Paulo, Brazil. Vouchers were deposited at the Herbarium “Irina Delanova de Gemtchujnicov” (BOTU) of the Botany Department of the Botucatu Institute of Biosciences, UNESP, Botucatu, SP, under registration number BOTU 34536.

Samples from the stem apex (including leaf primordia and young leaves), without mechanical damage and injuries, were collected from at least five adult individuals.

Transmission electron microscope studies

For conventional ultrastructural analyses in transmission electron microscopy (TEM), the samples were fixed in Karnovsky's solution (Karnovsky 1965) for 24 h, washed three times for 5 min each in 0.1M phosphate buffer (pH 7.3), post-fixed in 1% osmium tetroxide in the same buffer for 2 h at room temperature. Afterwards, they were washed three times for 10 min each in distilled water, contrasted in block in 0.5% uranyl acetate for 2 h at room temperature; dehydrated in increasing acetone solutions, soaked in acetone solution and Araldite® resin for 24 h and embedded in Araldite®. Ultrathin sections were counterstained with uranyl acetate and lead citrate (Reynolds 1963). The material was examined in a Tecnai Spirit Transmission Electron Microscope (FEI Company) at 80 kV.

For better visualisation of the population of organelles and changes in the endomembrane system associated with the secretory process, the ZIO method (zinc iodide - osmium tetroxide - Reinecke and Walther 1978) was used. For this, the samples were fixed as in the conventional method for TEM, washed in phosphate buffer with 8.5% sucrose, washed in TRIS-aminomethane buffer, pH 4.5 and incubated in ZIO in the dark for 19 h. This was followed by dehydration in acetone, conventional embedding and staining.

To detect hydrolases residing in vacuoles and autophagic vesicles (acid phosphatase activity) (Pino et al. 1981), samples were fixed in 2.5% glutaraldehyde in sodium cacodylate buffer, washed in 0.1 M cacodylate buffer, pH 7, 2, with 8.5% sucrose, washed in 0.05 M sodium acetate buffer, pH 5.0 with 5% sucrose and incubated in an appropriate medium at 37°C with constant stirring for 60 min. Then, the sections were washed in 0.05 M sodium acetate buffer, pH 5.0 with 5% sucrose, washed in 0.1 M cacodylate buffer, pH 7.2, with 8.5% sucrose and fixed in glutaraldehyde 2 .5% in sodium cacodylate buffer for 30 min. This was followed by post-fixation with osmium tetroxide, dehydration in acetone and conventional inclusion in TEM.

Fluorescence microscope studies

For detection of autophagic vesicles by immunofluorescence, we used an adaptation of the protocol described in Zhang et al. (2018). Samples (n=5) of newly collected material were placed in methanol for 5 min at room temperature and subsequently fixed in 4%

paraformaldehyde for 20 min at room temperature. Next, they were washed in PBS with 0.5% Triton X-100 for 30 min and blocked with 3% BSA in PBS with 0.5% Triton X-100 for 30 min with stirring. Sections were then incubated with anti-ATG8a antibody (ab77003; Abcam, 1:500 in PBS with 1% BSA) and washed with PBS containing 0.5% Triton X-100. Subsequently, the sections were incubated with goat anti-rabbit IgG conjugated with fluorescein isothiocyanate (Alexa Fluor 488; Invitrogen, 1:750 in PBS with 1% BSA for 1 h. After washing in PBS for 30 min, the slides were mounted in Fluoroshield (Sigma) and observed under a confocal microscope (Leica – TCS SP5) (excitation laser 488nm). Images were acquired using LAS AF software. Negative controls with the omission of the primary antibody were performed. Some sections which were not subjected to any either treatment or incubation, were checked and did not exhibit autofluorescence (data not shown).

Results

Conventional TEM analyses revealed that in all samples analysed, the secretory canals were associated with the phloem and were constituted by a uni-stratified secretory epithelium around a wide lumen. The epithelial cells presented different sizes and shapes and exhibited distinct subcellular organisation according to the stage of the secretory cycle in which they were found (Fig. 1a). In the secretory stage, epithelial cells were more voluminous, spherical to wedge-shaped and characterised by dense and abundant cytoplasm rich in free ribosomes and polyribosomes, rough (RER) and smooth (SER) endoplasmic reticulum, well-developed Golgi bodies with many cisternae and vesicles adjacent mitochondria and globular plastids containing electron-opaque inclusions (Fig. 1b-f). Periplastid endoplasmic reticulum was commonly seen (Fig. 1b-e).

In cells active in secretion, endoplasmic reticulum profiles were in a semi-arc shape (Fig. 1f-i, Fig. 2a), characterising the formation of the phagophore or initial autophagic vacuole (AVi), considered the initial phase of macroautophagy. In many of these cells, the cytoplasm was strongly electron-dense with a large proliferation of smooth endoplasmic reticulum (SER). Mitochondria contained degraded cristae and accumulated membrane debris (Fig. 2b). Membranes from the SER appeared as dense tubes scattered throughout the cytoplasm and around organelles (Fig. 2a,b,e). The dictyosomes were highly developed with many associated vesicles (Fig. 2c-f), which appeared distributed in a network around portions of cytoplasm (Fig. 2g). These vesicles fused to form small autophagic vacuoles, which later also fused to form larger vacuoles (Fig. 2h-i). Electron-

lucent structures with cytoplasmic contents were present, evidencing the formation of autophagosomes (Fig. 3a-f). Multilamellar bodies within these structures were also present (Fig. 3g-i).

As secretion progressed, the cells became less voluminous, tangentially elongated, with an irregular cell wall and exhibited reduced cytoplasm, a single central vacuole was formed (Fig. 4). Multivesicular bodies were observed inside the vacuoles (Fig. 4a-c). At this stage, the vacuoles were electron-lucent and contained membrane debris (Fig. 4d-f); the tonoplast showed invaginations and protrusions encompassing cytoplasmic material (Fig. 4e-f), characteristics of microautophagy.

At the end of the secretory stage, the epithelial cells presented thin walls, cytoplasm reduced to a thin parietal layer, a wide central vacuole with intact tonoplast, the cytoplasm was restricted to the periphery of the cell and the organelles were reduced in number (Fig. 4g-i). In none of the samples analysed was there any sign of rupture of the tonoplast, therefore, no sign of mega-autophagy.

Products of the ZIO reaction are seen as electron-dense deposits in the lumen of the rough endoplasmic reticulum (Fig. 5a-c), in the cisternae of dictyosomes (Fig. 5c-g), and in the vesicles that bud from their dilated ends (Fig. 5g-h). Some dictyosomes were fully stained by ZIO while, in others, the median cisternae were not stained (Fig. 5g).

The product of the AcPase reaction appeared as clumps of electron-dense material in the lumen of the endoplasmic reticulum (Fig. 6a) and in the cisternae of dictyosomes (Fig. 6b-d), mainly in the dilated ends. AcPase was evident in vesicles budding from the endoplasmic reticulum and dictyosomes (Fig. 6b-e). Dense bodies in juxtaposition to the tonoplast of autophagic vacuoles were observed (Fig. 6f). The reaction products were present in multivesicular bodies close to the cell wall (Fig. 6g). Coarser deposits were present on the walls of secretory cells active in secretion (Fig. 6g), while fine granular material was found on the walls of senescent cells (Fig. 6h), which was not observed in the negative control (Fig. 6i).

In the detection of autophagic vesicles by immunofluorescence (Fig. 7), green-fluorescent signal dots were distributed in epithelial cells and the parenchyma sheath of secretory canals compared to controls without anti-ATG8a antibody. This confirms that the autophagy occurs in the resin canals.

Discussion

Here, through analysis in transmission electron microscopy and confocal microscopy, we have identified two types of autophagy are involved in the resin secretory cycle in *A. humile* - macroautophagy and microautophagy. Although the questions about how the components degraded in the vacuoles will be part of the secretion have not yet been answered, we show that in the cells of the resin-secreting canals autophagy is responsible for the vesicular transport and degradation of cytoplasmic components and also actively participates in the biogenesis of vacuoles, playing a fundamental role in the secretion metabolism. Often associated with cell death, we have also seen that autophagy is associated with the metabolic maintenance processes under normal development conditions.

The cells of the resin secretory canals had different shapes and ultrastructural characteristics, and these are associated with the functional stage during the secretory cycle (Machado and Carmello-Guerreiro 2001; Lacchia and Carmello-Guerreiro 2009; Tolke et al. 2021). Bulky, spherical cells, with convex walls facing the lumen, conspicuous nucleus, dense cytoplasm rich in organelles and poorly developed vacuoles, are usually observed at the peak of secretion, while oval cells in the tangential direction, with a thin cell wall, bulky central vacuole and peripheral cytoplasm with few organelles are observed at the end of secretion.

The epithelial cells of the secretory canals in the secretory stage showed pre-autophagosomal structures (or initial autophagic vacuoles) and autophagosomes clearly identified by the different techniques used. These confirmed the occurrence of macroautophagy in the development of the secretory canals. It is currently believed that plant autophagosomes originate from multiple sites. In this sense their origins are similar to those in mammals (Kim et al. 2020). We suggest that in these resin-secreting canals they originate from the endoplasmic reticulum and dictyosomes. Enlarged tubules emerging from the smooth endoplasmic reticulum unite with vesicles emerging from dictyosomes. As they do so, they encompass a part of the cytoplasm so as to form small autophagic vacuoles, similar to those observed previously (Papini et al. 2014; Zhang et al. 2018, Machado and Rodrigues 2019). Multilamellar bodies sequestered by autophagosomes along with the cytoplasmic portion were also observed. Again, these were as previously described (Papini et al. 2014; Machado and Rodrigues 2019).

The detection of AcPase activity in the endoplasmic reticulum, in the cisternae of dictyosomes, in vesicles originating from both, and in autophagic vacuoles is associated with the biogenesis of autophagic vacuoles from these organelles during the resin

secretory process (Machado and Rodrigues 2019). Acid phosphatase (AcPase) is a lysosomal enzyme found widely in animals and plants. It is able to hydrolyse organic phosphate esters in a wide range of substrates at an acidic pH (Han et al. 2020). Cytochemical studies consider the observation of an electron-dense insoluble reaction product to be a reliable indicator of the location of acid phosphatase activity (Machado and Rodrigues 2019). The presence of AcPase can be considered a reliable marker of autophagy, since it is present in the cytoplasmic degradation processes (Cai et al. 2009). The distribution of AcPase inside the tonoplast, and inside the autophagic vacuoles suggests its participation in the cytoplasmic degradation in these resin secretory canals. In contrast, in the reserve vacuoles, AcPase was not detected, highlighting the presence of vacuoles with different functions. The detection of AcPase in the cell wall indicates the participation of enzymes in its degradation, and the products of this reaction become part of the secretion produced by the canal.

The ZIO method clearly reveals the morphology of the dictyosomes and the polarisation of their cisternae, in addition to the origin of lytic vesicles. The contribution of dictyosomes and the vesicles that connect dictyosomes and endoplasmic reticulum in the origin of lytic vacuoles was observed here and found to be similar to that described in nectaries (Machado and Rodrigues 2019).

The fluorescent stains on cells of the epithelium of the secretory canals in confocal microscopy with the use of ATG8, clearly demonstrate the presence of autophagosomes in these cells. The formation of autophagosomes is mainly regulated by a range of proteins related to autophagy (ATG) (Kim et al. 2022). ATG8 is a central component in the autophagic machinery related to autophagosome formation and is present in both the inner and outer membranes at the beginning of autophagosome formation (when it is still considered a phagophore) and remains in the inner membrane until degradation in the vacuole (Magen et al. 2022). Due to these characteristics, ATG8 is a good marker for tracking autophagy from the initial stages to degradation in the vacuole (Bassham 2015), and it can be used in immunocytochemical or immunohistochemical studies. Zhang et al. (2018) used the ATG8 antibody in confocal microscopy and observed structures related to autophagy in laticifers.

In this study, when the resin canal epithelium cells were in an advanced stage of secretion, they showed portions of cytoplasm being encompassed by the tonoplast. They also showed many membranous structures (similar to multilamellar bodies) inside these vacuoles. Such features are typical of microautophagy (Van Door and Papini 2013).

Previous studies have described plant microautophagy involved in the accumulation of anthocyanin in the vacuole, the elimination of chloroplasts and cellular components during stress (Chanoca et al. 2015, Goto-Yamada et al. 2019, Nakamura and Izumi 2019, Sienko et al. 2020). The vacuolar invaginations that occur during microautophagy serve as membrane reservoirs enabling rapid changes in vacuolar volume (Chanoca et al. 2015). We clearly observed an increase in vacuole volume with advance in the secretory process. Unlike our observations, Machado and Rodrigues (2019) observed microautophagy in vacuole biogenesis and protein and membrane recycling in the early stages of nectary development.

The end of the secretory cycle of a secretary gland generally involves the rupture of the tonoplast and the consequent degradation of the cellular components by mega-autophagy (Machado and Rodrigues 2019). Our results reveal for *A. humile* that at the end of the secretory process, the vacuole becomes single, central and voluminous, and the cytoplasm restricted to a thin layer on the periphery of the cell. However, there is no rupture of the tonoplast and, therefore, there is no evidence of mega-autophagy.

This study demonstrates that ultrastructural characterisation under the TEM in association with ultrastructural cytochemistry and immunolocalization techniques using specific antibodies are very effective tools for monitoring autophagy in plants (Bassham 2015), detecting autophagic structures (Van Door and Papini 2013; Yoshii and Mizushima 2017) and correctly confirming the types of autophagy in play (Klionsky et al. 2021, Wojciechowska et al. 2021).

Acknowledgement

We thank the technical team of the Electron Microscopy Center (CME), Institute of Biosciences of Botucatu (IBB), São Paulo State University (UNESP) for their assistance in preparing of the samples. This work was supported by the Fundação de Amparo à Pesquisa do Estado de São Paulo. (FAPESP 2019/19916-1; 2021/13392-0). SR Machado receives a research grant from the National Council for Development and Research (CNPq) process 308982/2020-7.

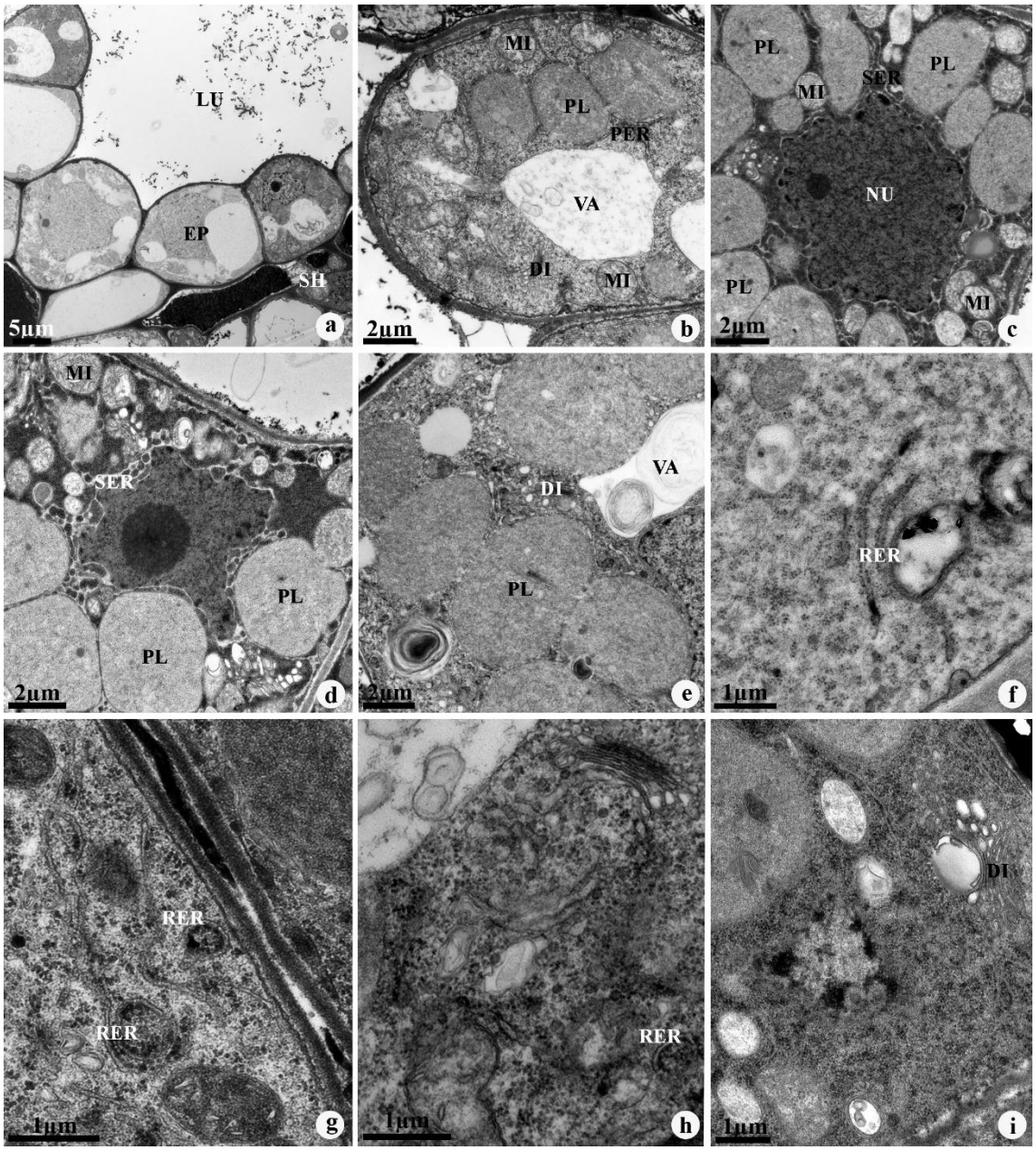

Fig. 1 Electron micrographs of the secretory canals of the stem of *Anacardium humile*. (a) Mature canal with wide lumen (LU) and secretory epithelium (EP) surrounded by a parenchymal sheath (SH). Note that epithelial cells have different ultrastructural characteristics. (b) Epithelial cell with dense cytoplasm, evident vacuole (VA), ellipsoid plastids (PL) with electro-opaque droplets surrounded by periplastid endoplasmic reticulum (PER), mitochondria (MI) and dictyosomes (DI). (c) Part of an epithelial cell showing evident nucleus (NU), mitochondria (MI), smooth endoplasmic reticulum (SER) and numerous plastids (PL). (d) Part of an epithelial cell showing highly proliferated smooth endoplasmic reticulum (SER), mitochondria (MI) and numerous plastids (PL). (e) Part of the epithelial cell with dictyosomes (DI), plastids (PL) and vacuole (VA) with

membranous content. (f-h) Parts of an epithelial cell showing rough endoplasmic reticulum (RER) in a semi-arc shape. (i) Parts of an epithelial cell showing rough dictyosomes (DI) in a semi-arc shape

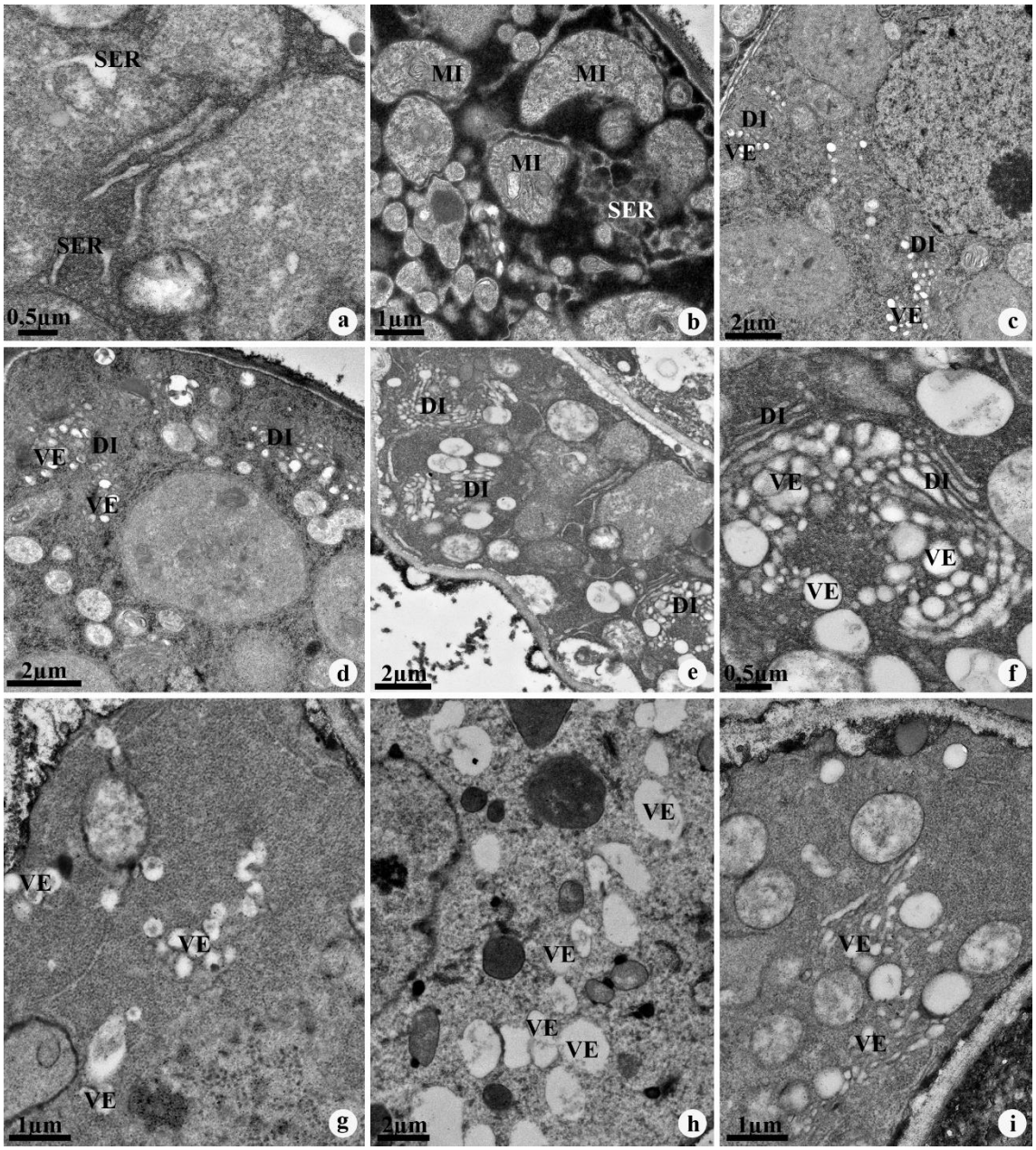

Fig. 2 Electron micrograph of epithelial cells from the stem secretory canals of *Anacardium humile*. (a) Smooth endoplasmic reticulum (SER) in a semi-arc shape, enclosing part of the cytoplasm. (b) Part of an epithelial cell with dense cytoplasm with highly proliferated smooth endoplasmic reticulum (SER) and mitochondria (MI) with degraded cristae and membrane remnants inside. (c-d) Parts of an epithelial cell showing dictyosomes (DI) with many vesicles (VE). (e) Part of an epithelial cell with highly developed dictyosomes (DI) with many associated vesicles. (f) Detail of a dictyosome (DI) showing vesicles (VE) distributed in a network around portions of cytoplasm. (g) Part of an epithelial cell with vesicles (VE) scattered in the cytoplasm. (h) Part of an epithelial cell with vesicles (VE) scattered in the cytoplasm. Note that smaller vesicles fuse. (i) Part of an epithelial cell with vesicles (VE) scattered in the cytoplasm

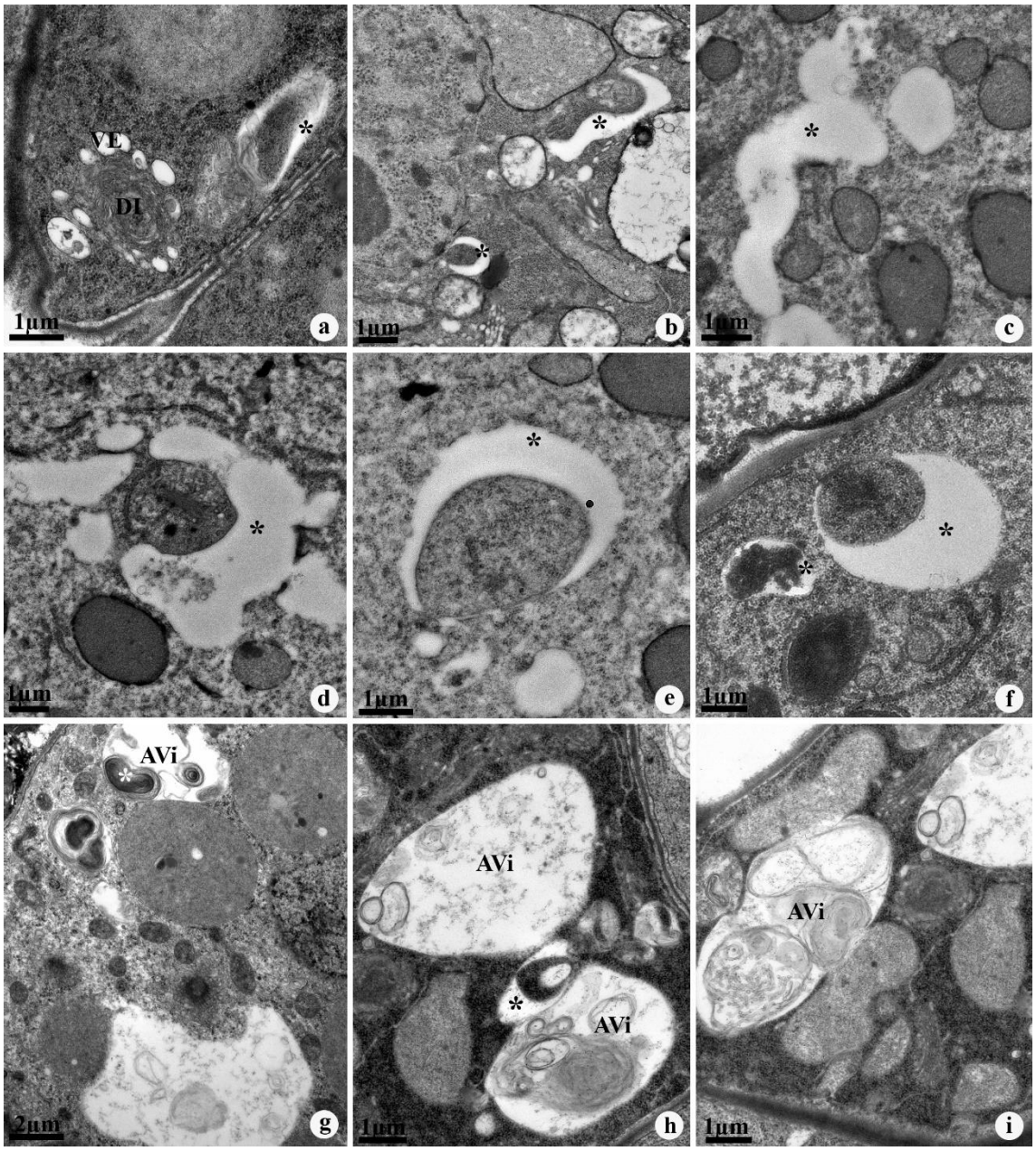

Fig. 3 Electron micrograph of epithelial cells from the stem secretory canals of *Anacardium humile.* (a-f) Part of an epithelial cell showing vesicles (VE) from dictyosomes (DI) surrounding portions of cytoplasm. Parts of the cytoplasm are surrounded by an electron-lucent double-membrane structure (arrow) (autophagosomes). (g-i) Part of an epithelial cell showing autophagic vacuoles (AVi) with multilamellar bodies (asterisk) inside

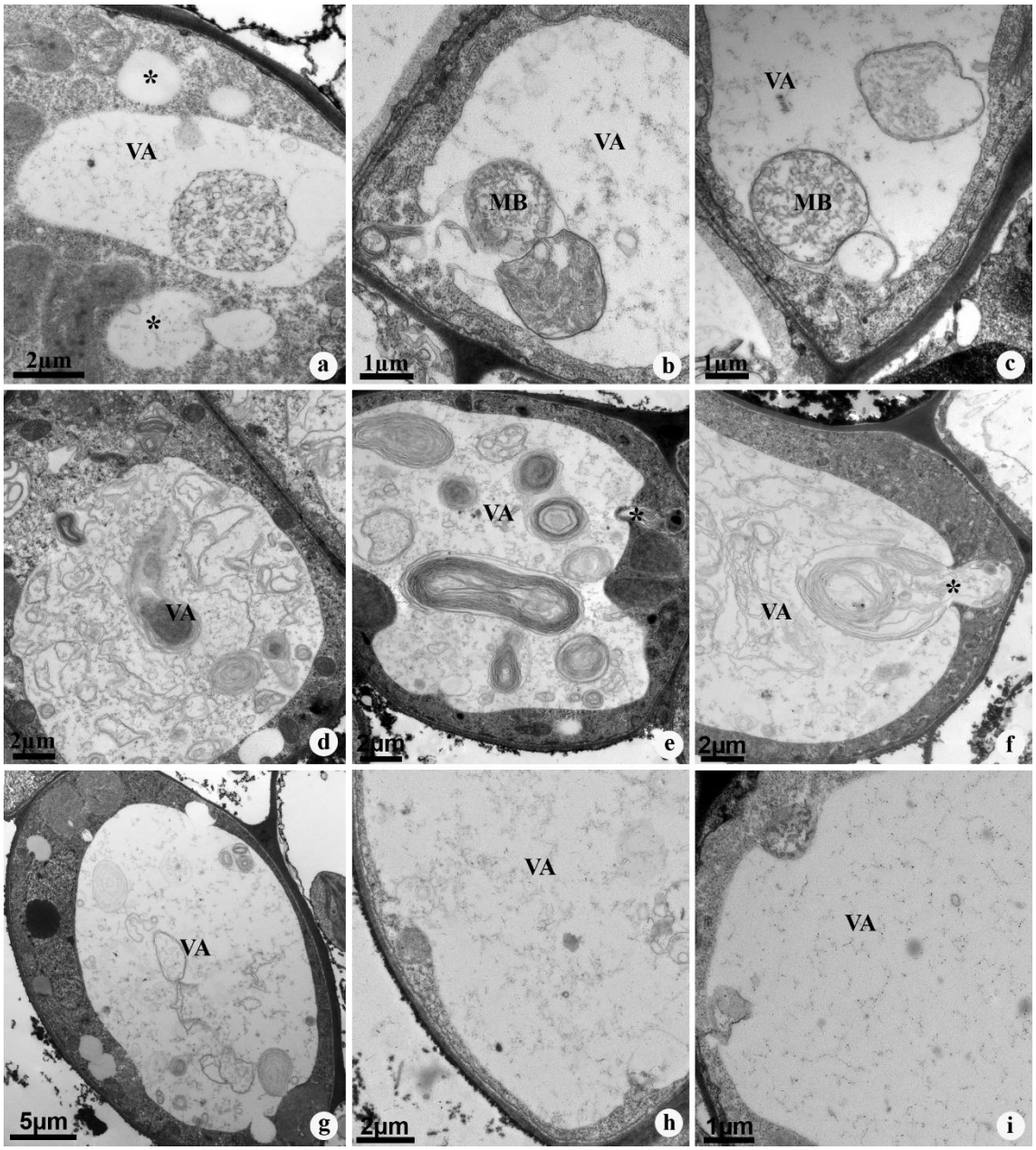

Fig. 4 Electron micrograph of epithelial cells of the secretory ducts of the stem of *Anacardium humile*. (a) Part of an epithelial cell showing fusion of smaller vacuoles (asterisk) and formation of a single vacuole (VA). (b-c) Parts of epithelial cells showing large vacuole (VA) with multivesicular bodies (MB) inside. (d-f) Parts of epithelial cells showing single, large, central vacuole (VA) with much membrane debris. Note the tonoplast invaginations (asterisks) which are responsible for engulfing cytoplasmic material. (g-i) Parts of tangentially elongated epithelial cells showing large central vacuole (VA), reduced and peripheral cytoplasm with few organelles

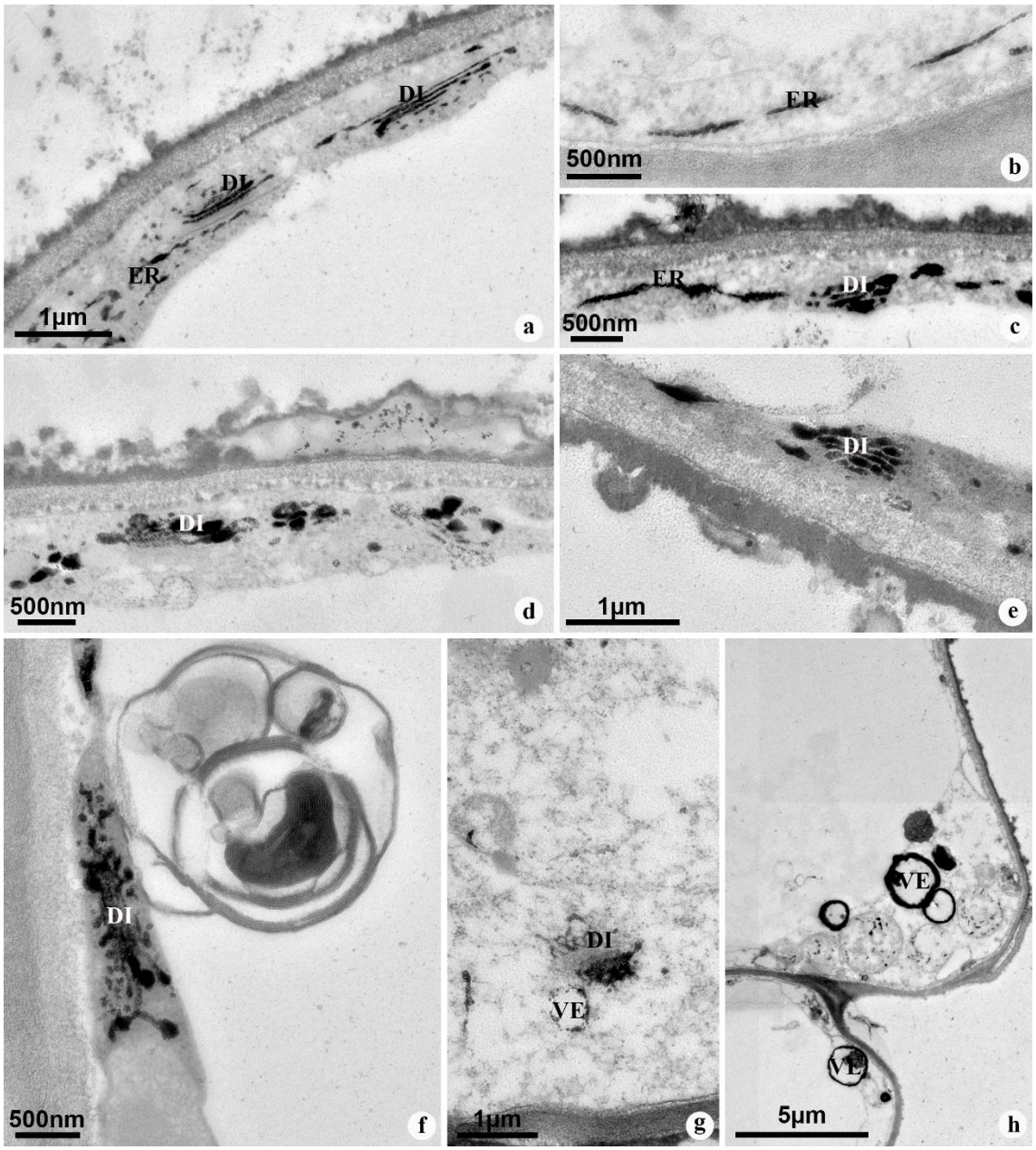

Fig. 5 Electron micrograph of epithelial cells of the secretory canals of the stem of *Anacardium humile* processed using the ZIO technique. (a) Detail of an epithelial cell, showing endoplasmic reticulum (ER) and dictyosomes (DI) impregnated with reaction product. (b) Detail of an epithelial cell showing deposits of reaction products in the lumen of the endoplasmic reticulum (ER). (c) Detail of an epithelial cell showing deposits of reaction products in the cisternae of the dictyosome (DI) and endoplasmic reticulum (ER). (d-f) Details of dictyosomes (DI) showing deposits of reaction products in flattened cisternae and flared ends. (g) Detail of an epithelial cell showing dictyosome cisternae (DI) and vesicles with osmiophile content (VE) in epithelial cells. Note that the median cisterns are not marked. (h) Detail of an epithelial cell showing vesicles with osmiophilic (VE) content

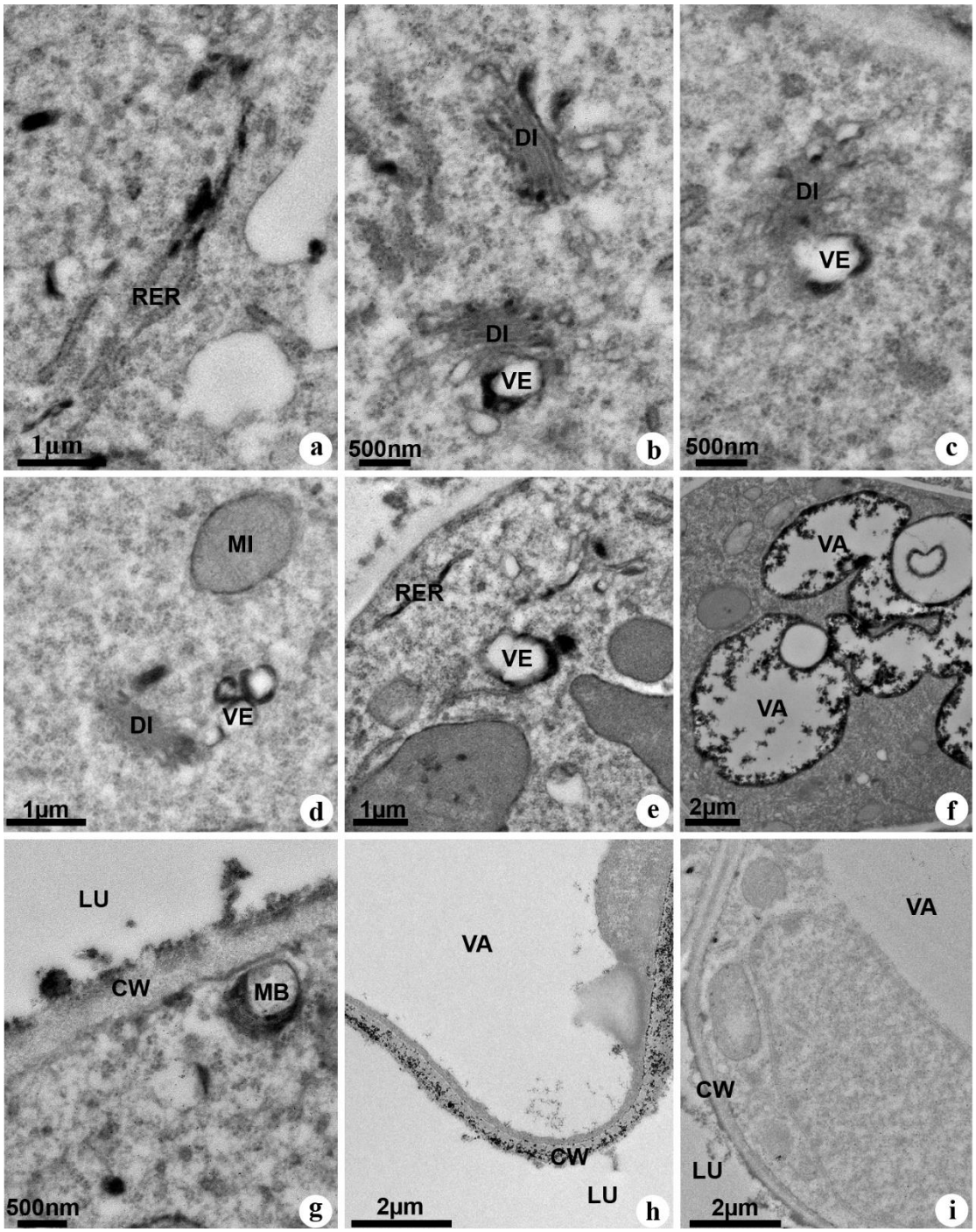

Fig. 6 Ultrastructural cytochemistry for acid phosphatase enzyme in the cell epithelium of stem canals (a-h) and negative control (i). (a) Dense reaction product inside RER. (b-d) Dense deposits inside Golgi body cisternae and vesicles. (e) Dense bodies filled with AcPase reaction product near and within the vesicles and inside RER. (f) Reaction product along the tonoplast inner surface. (g) Coarser deposits on the walls of active secretory cells and inside the multivesicular body. (h) Fine granular material on the walls of senescent cells. (i) Negative control in active cells. RER: rough endoplasmic reticulum,

DI: dictyosome, VE: vesicle, MI: mitochondria, VA: vacuole, CW: cell wall, MB: LU: lumen

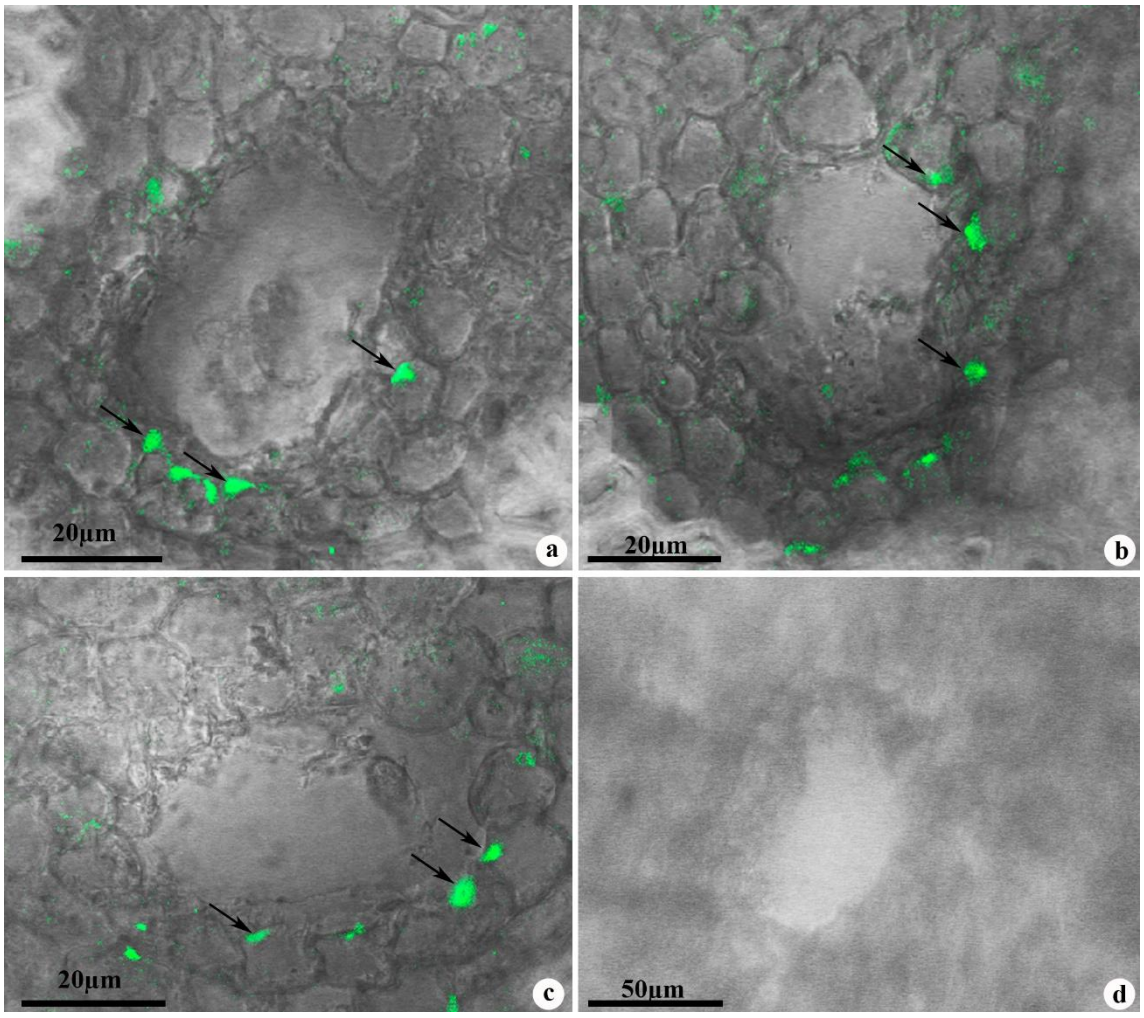

Fig. 7 Expression of anti-ATG8a-Alexa Fluor 488 in cross-sections of resin-secreting ducts of *Anacardium humile* stem observed under a confocal microscope. (a-c) Stems treated with anti-ATG8a-Alexa Fluor 488 antibody. The green colour signals (arrows) indicate the presence of autophagosomes in the cells of the secretory epithelium and parenchymal sheath. (d) Stem without treatment with anti-ATG8a-Alexa Fluor 488 (control)

References

Avin-Wittenberg T, Honig A, Galili G (2012) Variations on a theme: plant autophagy in comparison to yeast and mammals. *Protoplasma*, 249, 285–299 https://doi.org/10.1007/s00709-011-0296-z.

Bassham DC (2007) Plant autophagy - more than a starvation response. *Curr. Opin,* 10, 1–7.

Bassham DC (2015) Methods for analysis of autophagy in plants. *Methods*, 75, 181–188.

Bassham DC, Laporte M, Marty F, Moriyasu Y, Ohsumi Y, Olsen LJ, Yoshimoto K (2006) Autophagy in development and stress responses of plants. *Autophagy*, 2, 2–11.

Bozhkov PV (2018) Plant autophagy: Mechanisms and functions. *J. Exp. Bot*, 69, 1281–1285. https://doi.org/10.1093/jxb/ery070.

Cai X, Li W, Yin L (2009) Ultrastructure and cytochemical localization of acid phosphatase of laticifers in *Euphorbia kansui* Liou. *Protoplasma*, https://doi.org/10.1007/s00709-009-0065-4.

Chanoca A, Kovinich N, Burkel B, Stecha S, Bohorquez-Restrepo A, Ueda T, Eliceiri KW, Grotewold E, Otegui MS (2015) Anthocyanin Vacuolar Inclusions Form by a Microautophagy Mechanism. *The Plant Cell*, 27, 2545–2559. https://doi.org/10.1105/tpc.15.00589.

Contento AL, Xiong Y, Bassham DC (2005) Visualization of autophagy in *Arabidopsis* using the fluorescent dye monodansylcadaverine and a GFP-AtATG8e fusion protein. *Plant Journal*, 42, 598–608.

Fahn A, Evert RF (1974) Ultrastructure of secretory ducts of *Rhus glabra* L. *Am. J. Bot*, 61, 1–14.

Ganesan D, Cai Q (2021) Understanding amphisomes. *Biochem*, 478, 1959–1976. https://doi.org/10.1042/BCJ20200917.

Goto-Yamada S, Oikawa K, Bizan J, Shigenobu S, Yamaguchi K, Mano S, Hayashi M, Ueda H, Hara-Nishimura I, Nishimura M, Yamada K (2019) Sucrose starvation induces microautophagy in plant root cells. *Front. Plant Sci.*, 10, 1-16. https://doi.org/10.3389/fpls.2019.01604.

Haddad IVN, Sá-Haiad B, Santiago-Fernandes LDR, Machado SR (2019) Pollen grain development and male sterility in the perfect Flowers of *Maytenus obtusifolia* Mart. (Celastraceae). *Protoplasma*, 256, 745–761. https://doi.org/10.1007/s00709-018-01336-0.

Han Y, Quan K, Chen J, Qiu H (2020) Advances and prospects on acid phosphatase biosensor. *Biosens*, 170, 1-9. https://doi.org/10.1016/j.bios.2020.112671.

Karnovsky MJ (1965) A formaldehyde-glutaraldehyde fixative of high osmolality for use in electron microscopy. *J. Cell Biol,* 27, 1A-149A.

Kim JH, Jung H, Chung T (2020) Birth, Growth, Maturation, and Demise of Plant Autophagic Vesicles. *J. Plant Biol.*, 63, 155–164. https://doi.org/10.1007/s12374-020-09252-8.

Kim JH, Jung H, Choi YE, Chung T (2022) Autophagy inducers lead to transient accumulation of autophagosomes in *Arabidopsis* roots. *Plant Cell Rep.*, 41, 463–471. https://doi.org/10.1007/s00299-021-02821-2.

Klionsky DJ, Abdel-Aziz AK, Abdelfatah S et al. (2021) Guidelines for the use and interpretation of assays for monitoring autophagy (4th edition). *Autophagy,* 17, 1-1382. https://doi.org/10.1080/15548627.2020.1797280.

Kwon SI, Cho HJ, Jung JH, Yoshimoto K, Shirasu K, Park OK (2010) The Rab GTPase RabG3b functions in autophagy and contributes to tracheary element differentiation in *Arabidopsis*. *Plant J.*, 64, 151–164. https://doi.org/10.1111/j.1365-313X.2010.04315.x.

Lacchia APS, Carmello-Guerreiro SM (2009) Aspectos ultra-estruturais dos canais secretores em órgãos vegetativos e reprodutivos de Anacardiaceae. *Acta Bot Brasilica*, 23, 376–388.

Machado SR, Carmello-Guerreiro SM (2001) Estrutura e desenvolvimento de canais secretores em frutos de *Schinus terebinthifolius* Raddi (Anacardiaceae). *Acta Bot Brasilica,* 15, 189–195.

Machado SR, Rodrigues TM (2019) Autophagy and vacuolar biogenesis during the nectary development. *Planta*, 250, 519–533. https://doi.org/10.1007/s00425-019-03190-7.

Magen S, Seybold H, Laloum D, Avin-Wittenberg T (2022) Metabolism and autophagy in plants - a perfect match. *FEBS Letters*, 1-19. https://doi.org/10.1002/1873-3468.14359.

Mahood HE (2021) Autophagy in Plants during Nutrient Starvation, Osmotic and Heat Stresses. *Annals of R.S.C.B,* 25(3), 7933 – 7944.

Marshall RS, Vierstra RD (2018) The master of bulk and selective recycling. *Annu Rev Plant Biol.*, 69, 173–208. https://doi.org/10.1146/annurev-arplant-042817-040606.

Mitou G, Budak H, Gozuacik D (2009) Techniques to study autophagy in plants. *Int J Plant Genomics*, 1-14. https://doi.org/10.1155/2009/451357.

Nair GM, Venkaiah K, Shah JJ (1983) Ultrastructure of gumresin ducts in cashew (*Anacardium occidentale*). *Ann Bot.*, 51, 297–305.

Nakamura S, Izumi M (2019) Chlorophagy is ATG gene-dependent microautophagy process, *Plant Signal*, 14(1). https://doi.org/10.1080/15592324.2018.1558679.

Papini A, Mosti S, van Doorn WG (2014) Classical macroautophagy in *Lobivia rauschii* (Cactaceae) and possible plastidial autophagy in *Tillandsia albida* (Bromeliaceae) tapetum cells. *Protoplasma,* 251, 719–725. https://doi.org/10.1007/s00709-013-0567-y.

Pell SK, Mitchell JD, Miller AJ, Lobova TA (2001) Anacardiaceae. In: Kubitzki, K, eds. The Families and Genera of Vascular Plants: Flowering Plants. Eudicots: Sapindales, Cucurbitales, Myrtales: Vol. 10. Springer, Berlin/Heidelberg, 7–50.

Pickel DBJ (2008) Flora do Nordeste do Brasil segundo Piso e Marcgrave: no século XVII. Recife: EDUFRPE.

Pino RM, Pino LC, Bankston PW (1981) The relationships between the Golgi apparatus, GERL, and lysosomes of fetal rat liver kupffer cells examined by ultrastructural phosphatase cytochemistry. *J. Histochem. Cytochem.*, 29, 1061–1070.

Reinecke M, Walther C (1978) Aspects of turnover and biogenesis of synaptic vesicles at locust neuromuscular junctions as reveled by iodide-osmium tetroxide (ZIO) reacting with intravesicular shgroups. *J. Cell Biol.,* 21, 839–855.

Reynolds ES (1963) The use of lead citrate at high pH as an elestron-opaque stain in electron microscopy. *J. Cell Biol.,* 17, 208–212.

Royo VA, Mercadante-Simões MO, Ribeiro LM, Oliveira DA, Aguiar MMR, Costa ER, Ferreira PRB (2015) Anatomy, histochemistry, and antifungal activity of *Anacardium humile* (Anacardiaceae) leaf. *Microsc*. 21, 1549–1561. https://doi.org/10.1017/S1431927615015457.

Siénko K, Poormassalehgoo A, Yamada K, Goto-Yamada S (2020) Microautophagy in Plants: Consideration of Its Molecular Mechanism. *Cells,* 9, 887. https://doi.org/10.3390/cells9040887.

Soto-Burgos J, Zhuang X, Jiang L, Bassham DC (2018) Dynamics of autophagosome formation. *Plant Physiol.*, 176, 219–229. https://doi.org/10.1104/pp.17.01236.

Tolke ED, Lacchia APS, Lima EA, Demarco D, Ascensão L, Carmello-Guerreiro SM (2021) Secretory ducts in Anacardiaceae revisited: Updated concepts and new findings based on histochemical evidence. *S. Afr. J. Bot.,* 138, 394-405. https://doi.org/10.1016/j.sajb.2021.01.012.

Van Doorn WG, Papini A (2013) Ultrastructure of autophagy in plant cells: A review. *Autophagy*, 9, 1922–1936. https://dx.doi.org/104161/auto.26275.

Wang P, Mugume Y, Bassham DC (2018) New advances in autophagy in plants: Regulation, selectivity and function. *Semin. Cell Dev. Biol.*, 80, 113–122. https://doi.org/10.1016/j.semcdb.2017.07.018

Wang M, Li X, Luo S, Fan B, Zhu C, Chen Z (2020) Coordination and Crosstalk between Autophagosome and Multivesicular Body Pathways in Plant Stress Responses. *Cells*, 9, 119. http://dx.doi.org/10.3390/cells9010119.

Wojciechowska N, Michalak KM, Bagniewska-Zadworna A (2021) Autophagy—an underestimated coordinator of construction and destruction during plant root ontogeny. *Planta,* 254, 15. https://doi.org/10.1007/s00425-021-03668-3.

Yang X, Bassham DC (2015) New Insight into the Mechanism and Function of Autophagy in Plant Cells. *Int Rev Cell Mol Biol.,* 320, 1–40.

Yoshii SR, Mizushima N (2017) Monitoring and Measuring Autophagy. *Int. J. Mol. Sci.,* 18, 1865. http://dx.doi.org/10.3390/ijms18091865.

Yoshimoto K, Ohsumi Y (2018) Unveiling the Molecular Mechanisms of Plant Autophagy—From Autophagosomes to Vacuoles in Plants. *Plant Cell Physiol.,* 59(7), 1337–1344. https://doi.org/10.1093/pcp/pcy112.

Yoshimoto K, Jikumaru Y, Kamiya Y, Kusano M, Consonni C, Panstruga R, Ohsumi Y, Shirasu K (2009) Autophagy Negatively Regulates Cell Death by Controlling NPR1-Dependent Salicylic Acid Signaling during Senescence and the Innate Immune Response in *Arabidopsis*. *The Plant Cell Online,* 21, 2914–2927.

Yoshimoto K, Shibata M, Kondo M, Oikawa K, Sato M, Toyooka K, Shirasu K, Nishimura M, Ohsumi Y (2014) Organ-specific quality control of plant peroxisomes is mediated by autophagy. *J. Cell. Sci.,* 127, 1161–1168. https://doi.org/10.1242/jcs.139709.

Zhang Q, Wang D, Zhang H, Wang M, Li P, Fang X, Cai X (2018) Detection of autophagy processes during the development of nonarticulated laticifers in *Euphorbia kansui* Liou. *Planta,* 247, 845– 861. https://doi.org/10.1007/s00425-017-2835-0.

Zhuang X, Wang H, Lam SK, Gao C, Wang X, Cai Y, Jiang L (2013) A BAR-Domain Protein SH3P2, Which Binds to Phosphatidylinositol 3-Phosphate and ATG8, Regulates Autophagosome Formation in *Arabidopsis*. *The Plant Cell*, 25, 4596–4615. http://www.plantcell.org/cgi/doi/10.1105/tpc.113.118307.

Zhuang X, Chung KP, Luo M Jiang L (2018) Autophagosome Biogenesis and the Endoplasmic Reticulum: A Plant Perspective. *Trends Plant Sci.,* 23(8), 677-692. https://doi.org/10.1016/j.tplants.2018.05.002.

Evidências ultraestruturais e imunohistoquímicas de autocitotoxicidade em canais secretores de resina

Introdução

Resinas são misturas de substâncias incluindo terpenos (voláteis e não voláteis), flavonoides e lipídeos que podem ser produzidas em tricomas ou ductos secretores (Roshchina e Roshchina 1993).

Os terpenos são caracterizados como compostos com estruturas de hidrocarbonetos simples enquanto terpenóides (hidrocarbonetos contendo oxigênio) são definidos como classe de terpenos modificados com diferentes grupos funcionais e grupos metil movidos ou removidos em várias posições (Perveen 2018). Terpenos e terpenóides têm comprovada atividade antimicrobiana contra bactérias e fungos, principalmente através de suas habilidades para promover a ruptura celular e inibição de proteínas e síntese de DNA (Alvarez-Martínez et al. 2021). Os terpenos apresentam conhecida atividade citotóxica e alterações severas na topografia e morfologia das organelas têm sido frequentemente reportadas em diferentes organismos expostos a essas substâncias (Scudeler et al. 2016; 2019).

Nas glândulas vegetais, os terpenos/terpenoides podem danificar irreversivelmente o citoplasma da célula vegetal culminando com a sua autólise (Roshchina e Roshchina 1993; Aziz et al. 2005; Besser et al. 2009; Zhao et al. 2018; Isah 2019). O isolamento das substâncias tóxicas em compartimentos intracelulares específicos ou a sua modificação química em substâncias inativas tem sido considerados mecanismos que protegem o citoplasma dos efeitos tóxicos das secreções (Roshchina e Roshchina 1993; Huang e Osbourn 2019). No entanto, os danos celulares e reações de sinalização ligada às próprias secreções dessas células são ainda pouco conhecidos (Canaveze et al. 2021).

Em uma análise detalhada das células de óleo de nim (*Azadirachta indica* A. Juss (Meliaceae) durante o ciclo secretor, Canaveze et al. (2021) observaram acentuada hipertrofia celular, aumento da vesiculação das membranas celulares, dilatação das cisternas do retículo endoplasmático, hipertrofia mitocondrial em processo de cristólise, vacúolos autolíticos e degeneração vacuolar culminando na autólise do protoplasto, além de depósitos citoplasmáticos de cálcio e expressão da HSP70 (*heat shock protein 70*). Tais alterações morfológicas seguiram um padrão semelhante ao reportado em tecidos

animais expostos ao óleo de nim, um dos biopesticidas mais amplamente utilizados na atualidade (Scudeler et al. 2016).

Ao examinar os estudos ultraestruturais realizados com estruturas secretoras de terpenos disponíveis em literatura, geralmente observamos alterações morfológicas ao longo do processo secretor similares às reportadas por Scudeler et al. (2016) e Canaveze et al. (2021). No entanto, essas alterações têm sido negligenciadas ou associadas com senescência ou de morte celular programada. A combinação de métodos em imunohistoquímica e ultraestrutura celular convencional e citoquímica tem sido fundamental para compreender as repostas das células secretoras às próprias secreções que produzem.

No estudo realizado por Canaveze et al. (2021), foi utilizado como modelo célula secretora isolada (idioblasto) especializada na síntese de terpenos, onde as substâncias produzidas permanecem em compartimentos dentro da célula, isto é, secreção intracelular (Fahn 1979). Assim, é necessário testar a ocorrência de autotoxicidade e mecanismos citoprotetores em estruturas secretoras multicelulares mais complexas com secreção extracelular, como por exemplo, espaços secretores. Canais e cavidades secretores são glândulas compostas por um epitélio de células secretoras que delimitam um lúmen amplo (espaço intercelular), onde as substâncias produzidas são descarregadas e ficam armazenadas (Fahn 1979). No presente trabalho, por meio da aplicação de métodos de imunohistoquimicos e ultraestrutura investigamos a ocorrência de indícios de autotoxicidade e mecanismos de citoproteção em canais secretores de resina.

Usamos como modelo de estudo, exemplares de *Anacardium humile* A. St.-Hil., um subarbusto nativo do Cerrado brasileiro, pertencente à família Anacardiaceae (Almeida et al. 1998) e portadora de canais secretores de resina (Carvalho et al. 2022). Conhecido popularmente como cajuzinho-do-cerrado, cajuí e cajuzinho-do-campo, pode atingir cerca de 80cm de altura e se caracteriza por apresentar vários ramos aéreos eretos e um caule subterrâneo muito desenvolvido (Cota et al. 2017). Tanto o caule aéreo como o caule subterrâneo apresentam canais secretores corticais associados ao floema e canais medulares. Canais associados ao floema secretam predominantemente lipídeos, terpenos e fenóis e canais medulares, proteínas e polissacarídeos (Carvalho et al. 2022). Neste estudo, focamos as análises nos canais secretores floemáticos presentes no caule aéreo.

Material e métodos

Os estudos foram realizados em espécimes de *Anacardium humile* crescendo em uma população nativa do cerrado *strictu sensu* localizada nos municípios de Botucatu (22°57'17"S, 48°26'6"W) e Pratânia (22°49' 14"S, 48° 44'56"W), estado de São Paulo, Brasil. Os vouchers foram depositados no Herbário "Irina Delanova de Gemtchujnicov" (BOTU) do Departamento de Botânica do Instituto Botucatu de Biociências, UNESP, Botucatu, SP, sob o registro BOTU 34536.

Amostras do ápice do caule (incluindo primórdios foliares e folhas jovens), sem danos mecânicos e injúrias, foram coletadas de pelo menos cinco indivíduos adultos.

Estudos em microscopia eletrônica de transmissão (TEM)

Para análises ultraestruturais convencionais sob microscopia eletrônica de transmissão (TEM), as amostras foram fixadas em solução de Karnovsky (Karnovsky 1965) por 24 horas, lavadas 3 vezes de 5 minutos em tampão fosfato 0,1M (pH 7,3), pós-fixadas em 1% tetróxido de ósmio no mesmo tampão por 2 horas em temperatura ambiente. Em seguida, são lavadas 3 vezes de 10 minutos em água destilada, contrastadas em bloco em acetato de uranila 0,5% por 2 horas em temperatura ambiente; desidratados em solução crescente de acetona, embebidos em solução de acetona e resina Araldite® por 24 horas e embebidos em Araldite®. Seções ultrafinas foram contrastadas com acetato de uranila e citrato de chumbo (Reynolds 1963). O material foi examinado em Microscópio Eletrônico de Transmissão Tecnai Spirit (FEI Company) a 80kv.

Imunolocalização

Para a detecção de estresse celular e resposta citoprotetora, através da atividade da HSP70 (*heat shock protein* 70) (Scudeler et al. 2019), secções de material recém coletado foram fixadas por 4h em paraformaldeído a 4%, lavados em tampão PBS e incubados em solução de peróxido de hidrogênio 0,6% em PBS por 10 minutos para inativação da peroxidase endógena. Em seguida, as secções foram submetidas ao bloqueio protéico em BSA a 3% e incubados em câmara úmida com o anticorpo primário monoclonal mouse anti-heat shock protein 70 (anti-HSP 70, clone 5A5, ab2787, Abcam®Inc., Cambridge, MA, USA). Após, foi utilizado um sistema de detecção de antígenos imunoenzimáticos (ab236466 – Mouse and Rabbit Specific HRP/DAB IHC Detection Kit - Micropolymer). Controles foram feitos a partir da omissão do anticorpo primário.

Para a detecção de morte celular por apoptose pela atividade da Caspase 3, amostras de material recém coletadas foram fixadas por 4h em paraformaldeído a 4%, lavados em tampão PBS e incubados em solução de peróxido de hidrogênio 0,6% em PBS por 10 minutos para inativação da peroxidase endógena. Em seguida, as secções foram submetidas ao bloqueio protéico em BSA a 3% e incubados em câmara úmida com o anticorpo primário Rabbit Anti-Cleaved Caspase-3 (ab 49822). Posteriormente, foi utilizado um sistema de detecção de antígenos imunoenzimáticos (ab236466 – Mouse and Rabbit Specific HRP/DAB IHC Detection Kit - Micropolymer). Controles foram feitos a partir da omissão do anticorpo primário.

Resultados

As análises ultraestruturais já publicadas em Carvalho et al. (2022) revelaram que os canais secretores floemáticos apresentaram células epiteliais em diferentes estágios do processo secretor ocorrendo lado a lado. As células ativas em secreção apresentam a parede convexa voltada para o lúmen com paredes celulares finas, citoplasma denso com polirribossomos, ribossomos livres, plastídeos modificados, mitocôndrias com cristas evidentes, dictiossomos com muitas vesículas e retículo endoplasmático liso e rugoso desenvolvidos e presença de corpos multivesiculares. Já as células senescentes são alongadas tangencialmente, com paredes celulares finas, apresentam um grande vacúolo central, citoplasma periférico com poucas organelas e muitas vesículas.

Em células metabolicamente ativas, a secreção apresenta-se como inclusões elétron-luscentes no interior de vacúolos, vesículas e no espaço periplasmático (Fig.1). Essas células apresentaram citoplasma fortemente elétron-denso com intensa proliferação do retículo endoplasmático liso e de vesículas provenientes dos dictiossomos (Fig.2). Os elementos do retículo endoplasmático liso apresentaram lúmen dilatado e as mitocôndrias apresentaram cristas degradadas e estrutura multilamelar em seu interior (Fig.2d e Fig.3a,b).

Em algumas células ativas em secreção, estruturas autofágicas como fagóforos (Fig.2c), autofagossomos (Fig.3c) e vacúolos autofágicos com restos de membranas (Fig.2d, Fig.3b,c,d) foram evidentes.

As análises de imunolocalização mostraram reação anti-Hsp70 positiva em algumas células epiteliais (Fig.4a-d) representadas pela coloração acastanhada de grânulos no citoplasma das células. Reações anti-Caspase 3 não foram observadas (Fig. 4e). Os controles negativos não apresentaram reação anti-HSP70 (Fig.4f).

Discussão

Os resultados desse estudo confirmam que os componentes da resina produzida pelos canais secretores floemáticos de *A. humile* é citotóxica para as células que a produz, ao mesmo tempo que as células epiteliais apresentam mecanismos citoprotetores que mantém a célula viva durante o processo secretor. Observamos que as mudanças nas características ultraestruturais das células do epitélio secretor de resina durante a secreção são semelhantes àquelas observadas em células animais expostas a substâncias terpênicas.

Tem sido comprovado que o acúmulo intracelular de certos compostos terpenóides é tóxico para as células que os produzem afetando o seu crescimento e fisiologia (Aziz et al. 2005; Besser et al. 2009; Zhao et al. 2018; Isah 2019). Os terpenos não voláteis (diterpenos, estesterpenos, triterpenos e outros terpenos maiores) são geralmente produzidos e armazenados primeiramente em pequenas quantidades no citoplasma. Mais tarde, essas secreções entram no vacúolo, compartimento onde ficam armazenados enquanto a célula permanecer viva. Com o acúmulo progressivo de terpenóides, o protoplasto eventualmente degenera (Fahn 1979; Buvat 1989; Roshchina e Roshchina 1993; Evert 2006). Assim, a homeostase da célula secretora desses compostos é mantida pelo isolamento das substâncias no interior de vacúolos, espaço periplasmático, espaço subcuticular ou através de sua eliminação para espaços intercelulares (Roshchina e Roshchina 1993). A compartimentalização da secreção em vacúolos, vesículas e espaço periplasmático, conforme observado neste estudo, é uma característica relacionada à toxicidade dos terpenos (Roshchina e Roshchina 1993; Zhao et al. 2018; Canaveze et al. 2021). No caso dos canais secretores, o armazenamento da secreção no lúmen do canal secretor, a qual é externalizada apenas em casos de injúria, também representa um mecanismo de proteção às células epiteliais.

As alterações observadas na morfologia e topografia das organelas durante o ciclo secretor em *A. humile*, tais como proliferação de retículo endoplasmático liso que apresentou cisternas dilatadas, mitocôndrias intumescidas em processo de cristólise e proliferação de vesículas dos dictiossomos são indicações de resposta morfológica à citotoxicidade da secreção, tipicamente terpenos, similares às descritas em células animais expostas a substâncias terpênicas (Cheville 2009; Catae et al. 2014; Scudeler e Santos 2014; Scudeler et al. 2016; 2019) e reportados por Canaveze et al. (2021) em células secretoras de óleo de nim.

A presença da HSP70 e evidências do processo autofágico como a presença de fagóforos, autofagossomos e vacúolos com restos de membranas nas células epiteliais dos

canais secretores são indícios de mecanismos citoprotetores. As proteínas de choque térmico (HSPs) auxiliam no dobramento das proteínas recém-sintetizadas, ou protegem as proteínas que se dobram incorretamente (Haq et al. 2019). Durante a exposição a vários fatores como calor, substâncias tóxicas e poluentes, as plantas reduzem a síntese normal de proteínas e passam a traduzir as HSPs (Vierling 1991; Waters et al. 1996; Ait-Aissa et al. 2000; Haq et al. 2019) criando uma resistência ao estresse. De modo semelhante, a autofagia é um processo que desempenha um papel importante na manutenção da homeostase perante diferentes estresses (Alvin-Wittenberg 2019; Gou et al. 2019), reciclando nutrientes e evitando a morte celular (Magen et al. 2022). A presença de corpos multivesiculares próximos à membrana plasmática também é uma evidência de processo endocítico relacionado à reciclagem de materiais e manutenção da homeostase celular (An et al. 2007; Hanson e Cashikar 2012).

Em nosso estudo, não observamos células em processo de morte celular programada, assim como não identificamos a presença da caspase 3 nas técnicas de imunolocalização, corroborando nossa tese de que existem mecanismos citoproterores que evitam a morte celular e mantém a homeostase celular durante o processo secretor.

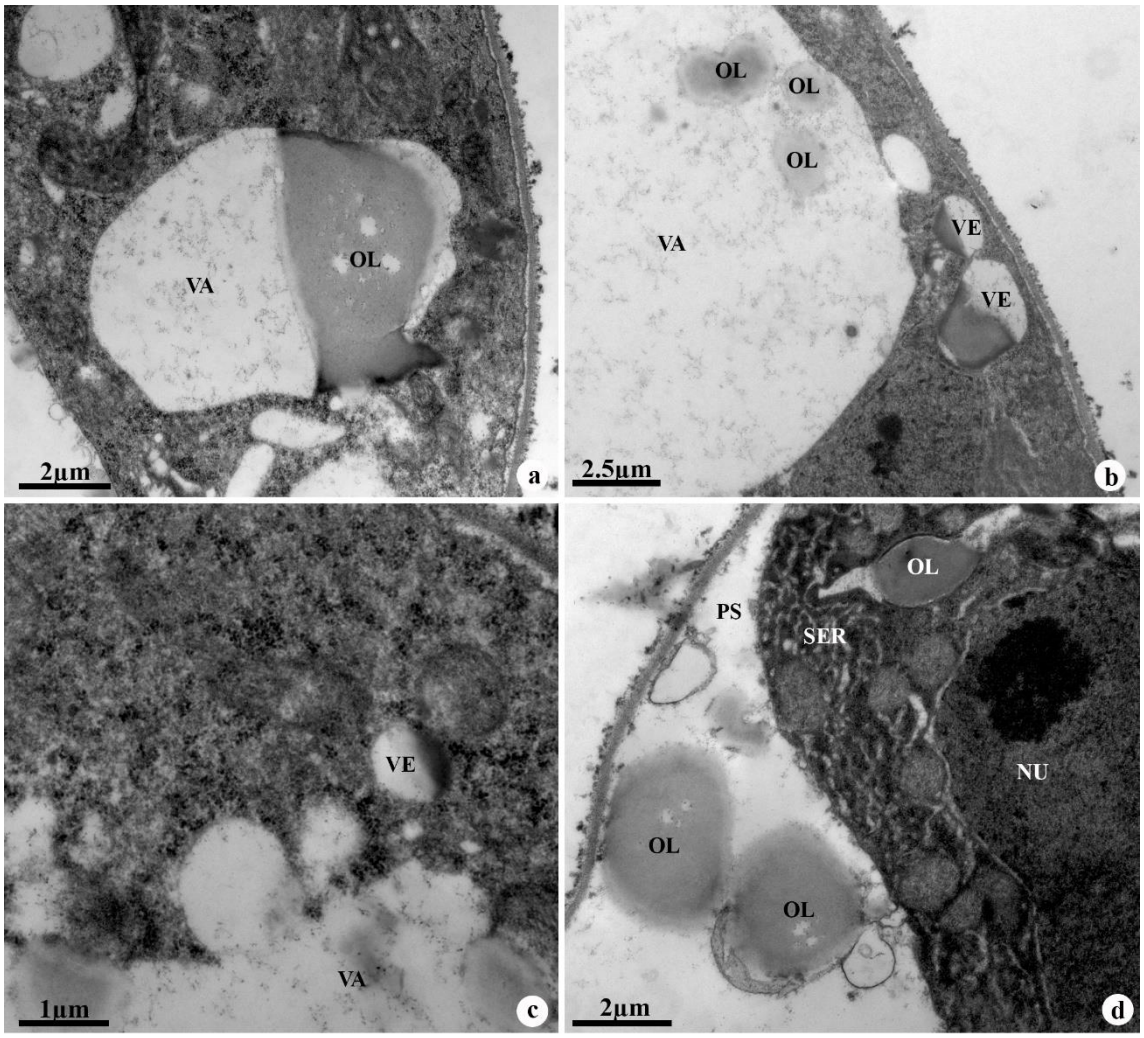

Fig. 1 Células epiteliais metabolicamente ativas dos canais secretores. (a) Detalhe de célula epitelial com citoplasma denso com vacúolo autofágico (VA) com conteúdo lipídico (OL) em seu interior. (b-c) Detalhe de célula epitelial com citoplasma denso com vacúolo autofágico (VA) com conteúdo lipídico (OL) em seu interior. Note esse mesmo conteúdo nas vesículas (VE) adjacentes. (d) Detalhe de célula epitelial com citoplasma denso, núcleo (NU) com nucléolo evidente e intensa proliferação de retículo endoplasmático liso (SER). Note conteúdo lipídico (OL) no interior vacúolo e no espaço periplasmático

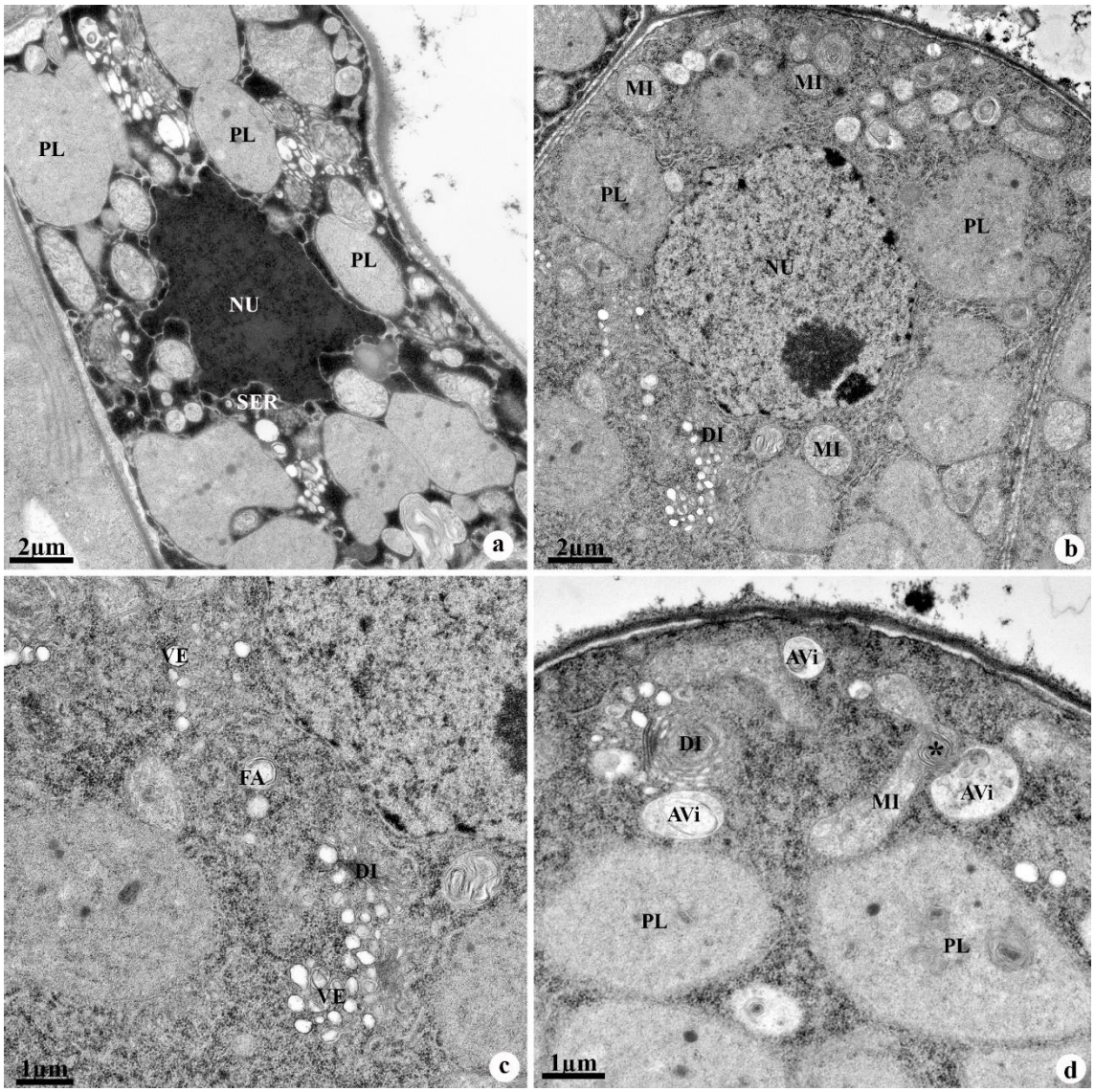

Fig. 2 Células epiteliais metabolicamente ativas dos canais secretores. (a) Célula epitelial com citoplasma fortemente elétrondenso e intensa proliferação do retículo endoplasmático liso (SER), núcleo conspícuo (NU) e plastídeos (PL). (b) Célula epitelial com núcleo conspícuo (NU), plastídeos (PL), mitocôndrias (MI) e dictiossomos (DI) com muitas vesículas. (c) Detalhe de célula epitelial com muitas vesículas (VE) provenientes dos dictiossomos (DI) e fagóforos (FA). (d) Detalhes de célula epitelial mostrando mitocôndrias (MI) com cristas degradadas e estrutura multilamelar em seu interior (asterisco) e vacúolos autofágicos iniciais (AVi) com restos de membranas

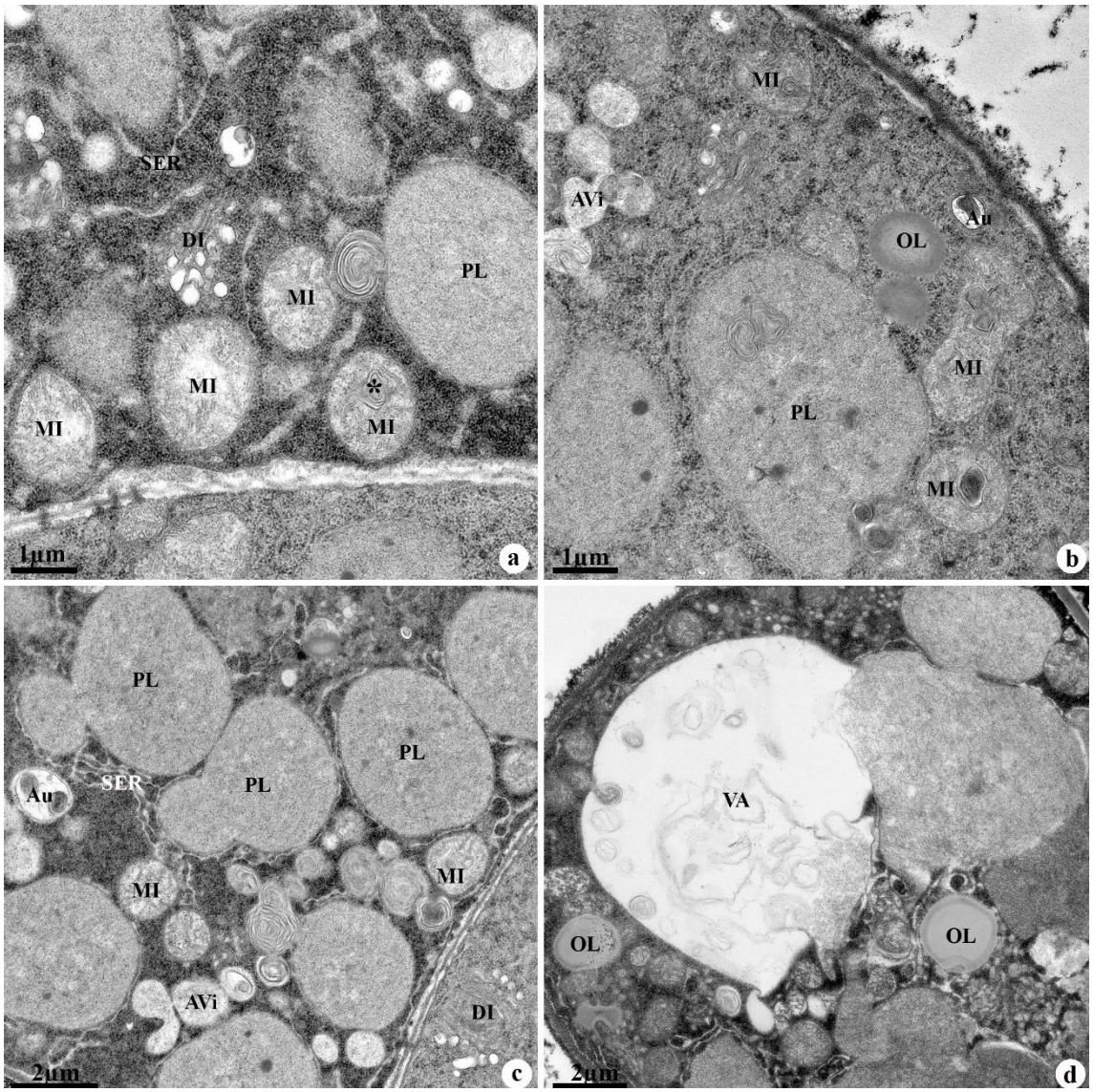

Fig. 3 Células epiteliais metabolicamente ativas dos canais secretores. (a) Detalhe de célula epitelial com citoplasma denso com plastídeos (PL), mitocôndrias (MI) com cristas degradadas e estrutura multilamelar em seu interior (asterisco), dictiossomos (DI) e retículo endoplasmático liso (SER) com lúmen dilatado. (b) Detalhe de célula epitelial com citoplasma denso com plastídeos (PL), mitocôndrias (MI) com cristas degradadas e estrutura multilamelar em seu interior e gotas lipídicas (OL) dispersas no citoplasma. Note a presença de autofagossomos (Au) e vacúolos autofágicos iniciais (AVi). (c) Detalhe de célula epitelial com citoplasma denso com retículo endoplasmático liso (SER) com lúmen dilatado, plastídeos (PL), mitocôndrias (MI) e vacúolos autofágicos iniciais (AVi) e autofagossomos (Au). (d) Detalhe de célula epitelial com citoplasma denso com vacúolo autofágico (VA) bem desenvolvido com conteúdo membranoso e gotas lipídicas (OL) no citoplasma

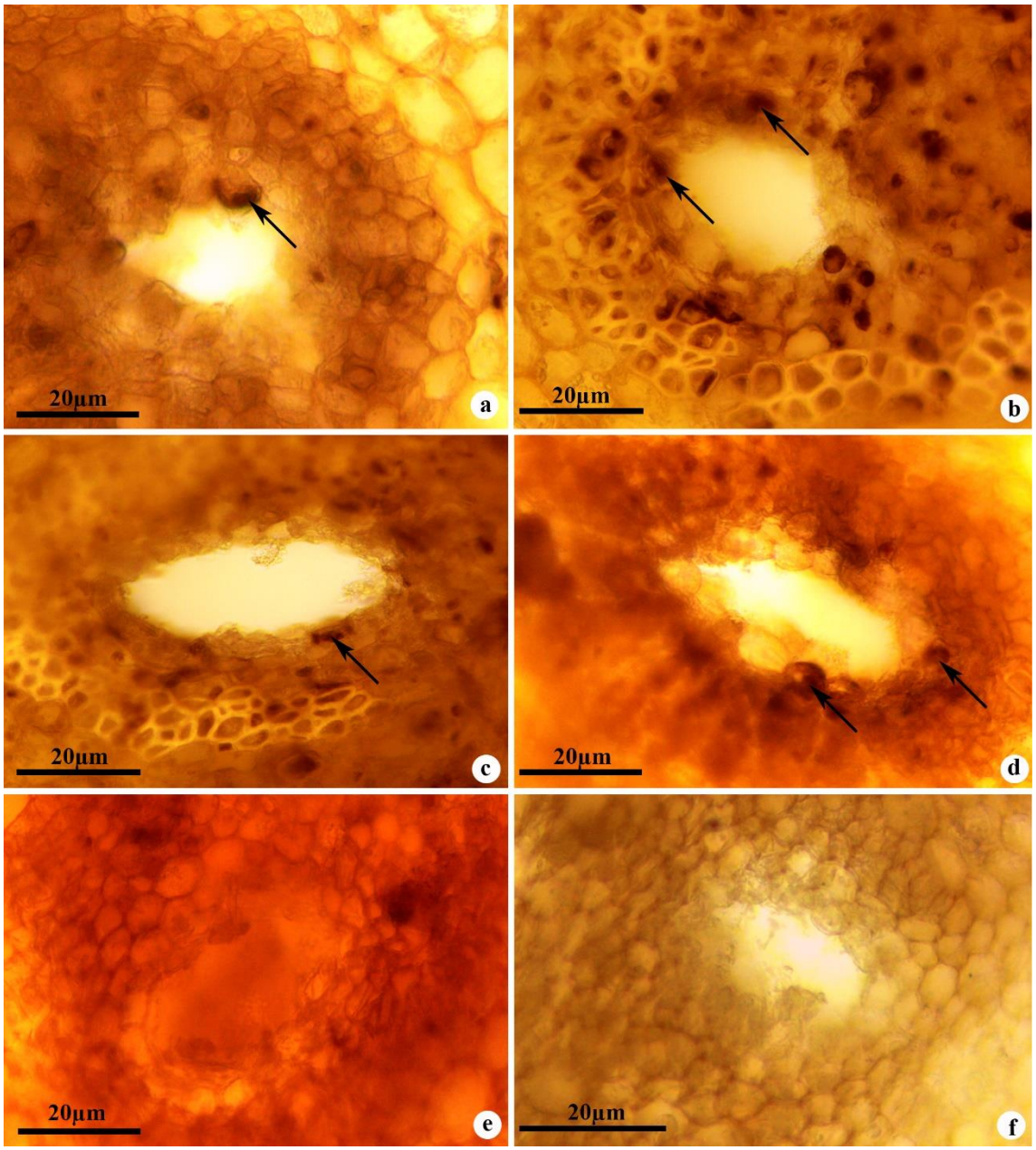

Fig. 4 Marcação imuno-histoquímica com anti-Hsp 70 e anti-Caspase 3 em células do epitélio secretor de *Anacardium humile*. (a-d) Cor acastanhada no citoplasma indicando marcação positiva para HSP70 (setas). (e) Cortes transversais sem marcação para Caspase 3, indicando ausência de morte celular programada. (f) Controle negativo com a omissão dos anticorpos primários

Referências bibliográficas

Aı¨t-Aı¨ssa S, Porcher JM, Arrigo AP,Lambre C. 2000. Activation of the hsp70 promoter by environmental inorganic and organic chemicals: relationships with cytotoxicity and lipophilicity. Toxicology 145: 147 – 157.

Almeida S P, Proença C E B, Sano S M, Ribeiro J F. 1998. Cerrado: espécies vegetais úteis.

Alvarez-Martínez FJ, Barrajon-Catal E, Herranz-Lopez M, Micol V. 2021. Antibacterial plant compounds, extracts and essential oils: An updated review on their effects and putative mechanisms of action. Phytomedicine 90. https://doi.org/10.1016/j.phymed.2021.153626.

Alvin-Wittenberg T. 2019. Autophagy and its role in plant abiotic stress management. Plant Cell Environ. 42:1045–1053.

An Q, van Bel AJE; Hückelhoven R. 2007. Do Plant Cells Secrete Exosomes Derived from Multivesicular Bodies? Plant Signaling & Behavior 2 (1): 4-7.

Aziz N, Paiva NL, May GD, Dixon RA. 2005. Transcriptome analysis of alfalfa glandular trichomes. Planta 221:28–38.

Besser K, Harper A, Welsby N, Schauvinhold I, Slocombe S, Li Y, Dixon RA, Broun P. 2009. Divergent regulation of terpenoid metabolism in the trichomes of wild and cultivated tomato species. Plant Physiol 149:499–514.

Buvat R. 1989. Ontogeny, cell differentiation, and structure of vascular plants. Springer Verlag, Berlin.

Canaveze Y, Scudeler EL, Machado SR. 2021. Neem secretory cells: developmental cytology and indications of cell autotoxicity. Protoplasma. doi: https://doi.org/10.1007/s00709-020-01580-3.

Carmello SM, Machado SR, Gregório EA. 1995 Ultrastructural aspects of the secretory duct development in *Lithraea molleoides* (Vell.) Engl.(Anacardiaceae). Revista Brasileira de Botânica 18(1): 95-103.

Carvalho SF, Scudeler EL, Santos DC, Machado SR. 2022. Intraspecific variation in ultrastructure and secretion of the resin canals in *Anacardium humile* Anacardiaceae). Protoplasma. doi: https://doi.org/10.1007/s00709-022-01823-5.

Catae AF, Roat TC, Oliveira RA, Nocelli RCF, Malaspina O. 2014. Cytotoxic effects of thiamethoxan in the midgut and malpighian tubules of Africanized Apis mellifera (Hymenoptera: Apidae). Microsc Res Tech 77:274–281.

Cheville NF. 2009. Response to cellular injury. In: Cheville NF (ed) Ultrastructural pathology, the comparative cellular basis of disease. Willey-Blackwell, Ames, pp 3–31.

Cota LG, Moreira PA, Brandão MM, Royo VA, Melo Junior AF, Menezes EV, Oliveira DA. 2017. Structure and genetic diversity of *Anacardium humile* (Anacardiaceae): a tropical shrub. Genet. mol. res. (Online) 16 (3): gmr16039778.

Fahn A.1979. Secretory tissues in plants. Academic Press, London.

Gou W, Li X, Guo S, Liu Y, Li F, Xie Q. 2019. Autophagy in Plant: A New Orchestrator in the Regulation of the Phytohormones Homeostasis. Int. J. Mol. Sci. doi:10.3390/ijms20122900.

Hanson PI and Cashikar A. 2012. Multivesicular Body Morphogenesis. Annu. Rev. Cell Dev. Biol. 28:337–62.

Haq S, Khan A, Ali M, Khattak AM, Gai W, Zhang H, Wei A, Gong Z. 2019. Heat Shock Proteins: Dynamic Biomolecules to Counter Plant Biotic and Abiotic stresses. International Journal of Molecular Sciences. doi:10.3390/ijms20215321.

Huang AC, Osbourn A. 2019. Plant terpenes that mediate below-ground interactions: prospects for bioengineering terpenoids for plant protection; a mini-review. Pest Manag Sci 75:2368–2377. doi: DOI 10.1002/ps.5410.

Isah T. 2019. Stress and defense responses in plant secondary metabolites production. Biol Res 52:39. https://doi.org/10.1186/s40659-019- 0246-3.

Junqueira LCU, Junqueira LMMS. 1983. Técnicas básicas de citologia e histologia. Livraria Editora, Santos, São Paulo.

Karnovsky MJ. 1965. A formaldehyde-glutaraldehyde fixative of high osmolality for use in electron microscopy. Journal of Cell Biology 27: 1A-149A.

Langenheim JH. 2003. Plant resins: chemistry, evolution, ecology, and ethnobotany. Oregon, US: Timber Press.

Magen S, Seybold H, Laloum D, Avin-Wittenberg T. 2022. Metabolism and autophagy in plants - a perfect match. FEBS Letters doi:10.1002/1873-3468.14359.

Martínez M, Pinto GL, Sanabria L, Beltrán O, Igartuburu JM, Bahsas A. 2003. Structural features of an arabinogalactan gum exudates from *Spondias dulcis* (Anacardiaceae). Carbohydrate Research 338: 619-624.

Martínez M, Pinto GL, Gonzáles MB, Herrera J, Oulyadic H, Guilhaudis L. 2008. New structural features of *Spondias purpurea* gum exudate. Food Hydrocolloids 22:1310-1314.

Pinto GL, Martínez M, Beltrán O, Rincón F, Igartuburu JM, Luis FR. 2000. Structural investigation of the ploysaccharide of *Spondias mombin* gum. Carbohydrate polymers 43: 105-112.

Perveen S. 2018. Introductory Chapter: Terpenes and Terpenoids. In: Perveen S, Al-Taweel A. Terpens and terpenoids BoD – Books on Demand, 152 páginas.

Prado E, Demarco D. 2018. Laticifers and secretory ducts: similarities and diferences. In: Hufnagel, L. (Ed.), Ecosystem Services and Global Ecology, IntechOpen, London, pp. 103-123.

Reynolds ES. 1963. The use of lead citrate at high pH as an elestron-opaque stain in electron microscopy. Journal of Cell Biology 17: 208–212.

Roshchina VV, RoshchinaVD. 1993. The excretory function of higher plants. Springer, Berlin.

Sant'Anna-Santos BF, Thadeo M, Meira RMSA, Ascensão L. 2006. Anatomia e histoquímica das estruturas secretoras do caule de *Spondias dulcis* Forst.F. (Anacardiaceae). Revista Árvore 30: 481-489.

Scudeler EL, Garcia ASG, Padovani CR, Pinheiro PFF, Santos DC. 2016. Cytotoxic effects of neem oil in the midgut of the predator *Ceraeochrysa claveri*. Micron80:96–111.

Scudeler EL, Garcia ASG, Padovani CR, Santos DC. 2019. Pest and natural enemy: how the fat bodies of both the southern armyworm *Spodoptera eridania* and the predator *Ceraeochrysa claveri* react to azadirachtin exposure. Protoplasma 256:839–856. Doi: https://doi.org/10.1007/s00709-019-01347-5.

Scudeler EL, Santos DC. 2014. Side effects of neem oil on the midgut endocrine cells of the green lacewing *Ceraeochrysa claveri* (Navás) (Neuroptera:Chrysopidae). Neotrop Entomol 43:154–160.

Tolke ED, Lacchia APS, Demarco D, Carmello-Guerreiro SM. 2017. Pericarp ontogeny of *Tapirira guianensis* Aubl. (Anacardiaceae) revals a secretory endocarp in young stage. Acta Botanica Brasilica 31: 319-329.

Tolke ED, Lacchia APS, Lima EA, Demarco D, Ascensão L, Carmello-Guerreiro SM. 2021. Secretory ducts in Anacardiaceae revisited: Updated concepts and new findings based on histochemical evidence. South African Journal of Botany 138: 394-405. https://doi.org/10.1016/j.sajb.2021.01.012

Vierling E. 1991. The roles of heat shock proteins in plants. Annu. Rev. Plant Physiology Plant Mol. Bio. 42:579-620.

Waters ER, Lee GJ, Vierling E. 1996. Evolution, structure and function of the small heat shock proteins in plants. Journal of Experimental Botany, 47 (296): 325-338.

Zhao C, Kim YK, Zeng Y, Wang MLX, Hu C, Gorman C, Dai SY, Ding S-Y, Yuan JS. 2018. Co-compartmentation of terpene biosynthesis and storage via synthetic droplet. ACS Synth Biol 7:774–781.

Considerações finais

Nesse estudo, o uso de métodos imunohistoquímicos combinados com análises convencionais e ultracitoquímicas em microscopia eletrônica de transmissão permitiu acessar variações no aparato celular e na dinâmica de secreção de resina em canais secretores presentes no caule em suas porções aérea e subterrânea de plantas de *Anacardium humile.* A combinação desses métodos foi eficiente para responder as questões apresentadas nos objetivos da tese.

Os resultados obtidos mostraram que há variações intraindividuais nos canais secretores do caule em *A. humile* na porção aérea e subterrânea apresentando diferenças na estrutura subcelular e na dinâmica de secreção de acordo com o ambiente em que se encontravam. Os canais do caule na porção aérea apresentam células epiteliais com características de alta atividade enquanto que os canais do caule na porção subterrânea apresentam características de baixa atividade.

Comprovamos a ocorrência e identificamos dois tipos de autofagia - macroautofagia e microautofagia - durante o ciclo secretor de resina, mostrando que a autofagia em plantas também está associada a processos de manutenção do metabolismo em condições normais de desenvolvimento. Nas células epiteliais dos canais secretores de resina, a autofagia é responsável pela reciclagem de componentes celulares e organelas danificadas, pelo transporte vesicular e biogênese dos vacúolos, desempenhando um papel fundamental no metabolismo da secreção.

Ainda, os resultados desse estudo confirmam que a resina produzida pelos canais secretores corticais de *A. humile* é citotóxica para as células que a produz, ao mesmo tempo que as células epiteliais apresentam mecanismos citoprotetores que mantém a célula viva durante o processo secretor.

Durante o processo de obtenção dos resultados encontramos algumas dificuldades técnicas provavelmente relacionadas aos componentes da secreção. A fixação e a pós-fixação do material para as técnicas de MET e a aplicação das técnicas de imunolocalização requereram um delineamento experimental rigoroso e a adaptação das técnicas usuais em célula animal e plantas modelo para plantas nativas. Nas amostras de imunolocalização em MET, a pós-fixação com tetróxido de ósmio não foi realizada, facilitando os cortes ultrafinos e assim obtendo melhores resultados. As imagens em MET foram feitas em diferentes aumentos, salientando a necessidade de grandes aumentos para se observar claramente os resultados dos testes citoquímicos.

Nosso trabalho gera perspectivas e incentivo para aplicação de diferentes técnicas de microscopia de luz e eletrônica, incluindo imunolocalização e citoquímica ultraestrutural em estudos de célula vegetal em espécies nativas

Como próximo passo, estamos finalizando análises imunohistoquímicas e ultraestruturais de canais secretores medulares produtores de substâncias hidrofílicas (proteínas e polissacarídeos) com o objetivo de compará-los aos canais corticais produtores de substâncias lipofílicas, especialmente terpenos, e avaliar as modificações morfológicas durante o ciclo secretor.